

Characterizing The Indole-3-Acetic Acid Biosynthesis Pathways In *Pseudomonas Putida*
UW4

by

Daiana Duca

A thesis
presented to the University of Waterloo
in fulfillment of the
thesis requirement for the degree of
Master of Science
in Biology

Waterloo, Ontario, Canada, 2013

© Daiana Duca 2013

AUTHOR'S DECLARATION

I hereby declare that I am the sole author of this thesis. This is a true copy of the thesis including any required final revisions, as accepted by my examiners. I understand that my thesis may be made electronically available to the public.

ABSTRACT

Plant growth-promoting bacteria employ a variety of biochemical and genetic strategies to facilitate plant growth. One of the most prominent and important of these mechanisms is the production of the plant hormone indole-3-acetic acid. *Pseudomonas putida* UW4 is a rhizospheric plant-growth-promoting bacterium that has the ability to produce IAA. The sequencing of this bacterium's genome allowed for the identification of seven separate genes that encode enzymes potentially involved in the biosynthesis of IAA. These seven genes appear to be part of at least three different IAA biosynthesis pathways. We sought to better understand the IAA biosynthesis pathways operating in *Pseudomonas putida* UW4 by isolating, purifying and characterizing some of the implicated enzymes. The focus was on two particular enzymes, nitrilase and nitrile hydratase which participate in the indole-3-acetonitrile pathway. Substrate feeding assays revealed the role of each enzyme. The pH and temperature profiles of both enzymes were determined in order to better understand the catalytic activity and give insight into how these enzymes may be regulated. Multiple sequence alignments and phylogenetic trees were constructed to infer the phylogeny of these putative IAA-enzymes.

ACKNOWLEDGEMENTS

Foremost, I would like to express my immense gratitude to my supervisors Dr. Bernie Glick and Dr. David Rose, for their continuous support throughout this project. Thank you both for your patience, motivation, encouragement, and knowledge. I would also like to thank my committee members, Dr. Kirsten Muller and Dr. Trevor Charles for their support and contributions to this thesis. As well, a very big thanks to Dr. Ron Johnson at the University of Guelph for agreeing to let me use your facility and especially to the HPLC technician Yu Gu for all your help and guidance.

To the former lab members Jin Duan and Shimaila Ali, I am so grateful to have had the opportunity to work alongside you. Thank you for mentoring me and for all your help and suggestions. I have learned so much from both of you! To my present lab member, Janet Lorv, thank you for everything, especially all the computer help and for keeping me sane throughout all of our lab mishaps. Thank you to the members of the Rose lab for their help with the FPLC and to the Heikkila lab for being such great lab neighbours. Thanks to all my other fellow grad-students, visiting scholars and exchange students that have lent me their expertise along the way.

A special thanks to all my friends who have been there for me these last two years. Thank you for understanding when I had to sacrifice fun. Kas- I cannot thank you enough, not only for your help intellectually and personally, but for showing me what it means to be a good person. Srdj- we have an understanding that goes beyond words, nevertheless thank you for riding the roller coaster with me.

From the bottom of my heart, I would like to thank my entire family for their love and encouragement. All of you mean the world to me. To my parents who have always supported me in all my pursuits, thank you for giving me strength and for believing in me. To my brother Alex, who inspires me with his unwavering positivity. To my grandparents, although an ocean separates us, I've felt your love and your support every day of this journey.

TABLE OF CONTENTS

AUTHOR'S DECLARATION	ii
ABSTRACT	iii
ACKNOWLEDGEMENTS	iv
LIST OF FIGURES	ix
LIST OF TABLES	xi
INTRODUCTION	1
INDOLE-3-ACETIC ACID AND PLANTS	1
INDOLE-3- ACETIC ACID TRANSPORT IN PLANTS	1
THE PLANT RESPONSE TO INDOLE-3-ACETIC ACID	3
THE BIOSYNTHESIS OF INDOLE-3-ACETIC ACID	5
THE INDOLE-3-ACETIC ACID BIOSYNTHESIS PATHWAYS	7
THE INDOLE-3-PYRUVIC ACID PATHWAY	8
THE INDOLE-3-ACETAMIDE PATHWAY	11
THE INDOLE-3-ACETONITRILE/ INDOLE-3-ACETYLDOXIME PATHWAY	14
INDOLE-3-ACETIC ACID AND PLANT GROWTH PROMOTING BACTERIA	16
INDOLE-3-ACETIC ACID AND PHYTOPATHOGENS	19
FACTORS INVOLVED IN INDOLE-3-ACETIC ACID PRODUCTION IN BACTERIA	23
THE ROLE OF INDOLE-3-ACETIC ACID IN BACTERIA	25
PURPOSE OF THIS RESEARCH	27
MATERIALS AND METHODS	30
BACTERIAL CULTURES	30
IAA PRODUCTION BY <i>P. PUTIDA</i> UW4	32
Salkowski Assay	32
IAA HPLC Assay	34
CLONING	35
Genomic DNA Isolation	35
Primers	35
PCR-Genomic DNA	38
pET30b(+) Plasmid Isolation and Digestion	39
Cloning into pET30b(+)	40
PROTEIN EXPRESSION	43
Transformation into <i>E. coli</i> BL21 (DE3).....	43
Target Protein Expression	43
Determining the Solubility of the Expressed Proteins	44
Culture Preparation for Large-Scale Expression and Purification.....	46
Culture Preparation for Small-Scale Expression and Purification.....	46
PROTEIN PURIFICATION	47
His GraviTrap™ Purification	47
His SpinTrap™ Purification	47
PROTEIN DESALTING /BUFFER EXCHANGE	48
Centrifugal Filter Tubes	48
Dialysis	48
DENSITOMETRY	49

FAST PERFORMANCE LIQUID CHROMATOGRAPHY (FPLC)	49
Purification by Anion Exchange FPLC	49
Native Size Determination by Size Exclusion Chromatography (SEC) FPLC	50
ENZYME CHARACTERIZATION	50
Activity Assays	50
Temperature Optima	51
pH Optima.....	51
Time Curve	52
Optimizing NthAB Activity.....	52
CONTROLS	53
HPLC ANALYSIS	54
MULTIPLE SEQUENCE ALINGMENTS & PHYLOGENETIC ANALYSIS	55
GENERAL PROTOCOLS	57
PREPARATION AND TRANSFORMATION OF COMPETENET <i>E. COLI</i>	57
DETERMINATION OF PROTEIN CONCENTRATION	57
SODIUM DODECYL SULFATE POLYACRYLAMIDE GEL ELECTROPHORESIS (SDS-PAGE)	57
DIALYSIS	58
RESULTS	59
CLONING IAA GENES	59
DETERMINING IF THE PUTATIVE IAA PROTEINS ARE EXPRESSED AND SOLUBLE	62
PROTEIN PURIFICATION	68
DETERMINING THE NATIVE SIZE OF PROTEINS	71
CONTROLS	75
ENZYME CHARACTERIZATION	79
OPTIMIZING NthAB ACTIVITY	86
IAA QUANTIFICATION	89
NITRILASE MOTIFS	93
PHYSICOCHEMICAL PROPERTIES OF NITRILASE	95
MULTIPLE SEQUENCE ALIGNMENTS	98
PHYLOGENETIC TREES	101
DISCUSSION	110
NITRILASE	111
Nitrilase Enzyme Activity	112
Nitrilase Temperature and pH Optima.....	116
Native Size of Nitrilase	117
Amide Production by Nitrilase	118
NITRILE HYDRATASE	119
Nitrile Hydratase Enzyme Activity.....	120
Nitrile Hydratase Temperature & pH Optima	123
Native Size of Nitrile Hydratase	124
Nitrile Hydratase Activator Proteins.....	124
Nitrilase vs. Nitrile Hydratase	126
THE GENES	129
Genetic Organization on the UW4 Chromosome	130
SEQUENCE ALIGNMENTS	136
Nitrilase	136
Nitrile Hydratase	138

P47K Putative Activator Protein.....	140
PHYLOGENETIC TREES	143
Nitrilase Phylogeny.....	143
Nitrile Hydratase Phylogeny.....	147
P47K Putative Activator Protein Phylogeny	149
CONCLUSION	151
REFERENCES.....	152

LIST OF FIGURES

Figure 1. Model of the auxin response at different IAA levels	4
Figure 2. Tryptophan Dependent IAA Biosynthetic Pathways	7
Figure 3. The Indole-3-Pyruvic Acid Pathway	8
Figure 4. The Indole-3-Acetamide Pathway	11
Figure 5. The Indole-3-Acetonitrile/Indole-3-Acetaldoxime Pathway	14
Figure 6. IAA in pathogenic plant/bacterial interactions	22
Figure 7. IAA biosynthetic pathways in <i>Pseudomonas putida</i> UW4	29
Figure 8. The Salkowski Assay of IAA Standards	33
Figure 9. Cloning the <i>nthAB</i> gene into the pET30b(+) vector for expression.	42
Figure 10. KOD-PCR of putative IAA genes from <i>P. putida</i> UW4 genomic DNA.....	60
Figure 11. Confirming the cloning of <i>nit</i> and <i>nthAB</i> into pET30b(+)	61
Figure 12. Examining PheD protein expression with SDS-PAGE	64
Figure 13. Examining IaaM and Aux protein expression with SDS-PAGE.....	65
Figure 14. Examining Nit protein expression with SDS-PAGE.....	66
Figure 15. Examining NthAB protein expression with SDS-PAGE	67
Figure 16. SDS-Page of Nit, NthAB and P47K (putative activator) proteins after His SpinTrap purification	69
Figure 17. SDS-PAGE of Nit protein after anion exchange FPLC purification.....	70
Figure 18. SDS-PAGE of Nit protein after SEC FPLC	72
Figure 19. SDS-PAGE Protein Molecular Weight Calibration Curve	73
Figure 20. Size Exclusion Gel Chromatography Protein Standard Curve	74
Figure 21. Nit activity over time	80
Figure 22. Temperature rate profile of Nit from <i>P. putida</i> UW4.	81
Figure 23. pH – rate profile of Nit from <i>P. putida</i> UW4.....	82
Figure 24. Temperature rate profile of NthAB from <i>P. putida</i> UW4.....	83
Figure 25. pH – rate profile of NthAB from <i>P. putida</i> UW4.	84

Figure 26. HPLC separation of NthAB assay products at room temperature.....	85
Figure 27. HPLC separation of a mixture of four standards.....	90
Figure 28. HPLC separation of an IAA fraction from an ethyl acetate extract of <i>P. putida</i> UW4 culture solution	92
Figure 29. Multiple sequence alignment of nitrilase proteins.....	99
Figure 30. Multiple sequence alignment of nitrile hydratase α - subunit protein	100
Figure 31. Nitrilase phylogeny inferred using Maximum-likelihood method	102
Figure 32. Nitrile hydratase α -subunit phylogeny inferred using ML method..	104
Figure 33. Nitrile hydratase β -subunit phylogeny inferred using ML method.....	106
Figure 34. P47K activator protein phylogeny inferred using the ML method.....	108
Figure 35. Genetic organization of the nitrile hydratase gene cluster of <i>P. putida</i> UW4.	134
Figure 36. Genetic organization of the characterized nitrilase gene of <i>P. putida</i> UW4.	134
Figure 37. Genetic organization of the seven putative nitrilase superfamily genes of <i>P.</i> <i>putida</i>	135

LIST OF TABLES

Table 1. Bacterial strains, plasmids and constructs used in this study.....	31
Table 2. Primers used to amplify the <i>nit</i> , <i>nthA</i> , <i>nthB</i> , <i>P47K</i> , <i>aux</i> and <i>iaaM</i> putative IAA biosynthesis genes.....	37
Table 3. Spontaneous, non-enzymatic conversion of IAN into either IAM or IAA, as well as conversion of IAM into IAA, at different temperatures	76
Table 4. Spontaneous, non-enzymatic conversion of IAN into either IAM or IAA, as well as conversion of IAM into IAA, at different pH values.....	77
Table 5. Testing crude extracts from non-transformed <i>E. coli</i> BL21(DE3) and <i>E. coli</i> BL21(DE3) transformed with the empty pET3-b(+) vector for the ability to convert the IAN substrate into IAM or IAA.....	78
Table 6. Determining whether the Fe co-factor and P47K activator protein are needed for NthAB activity.....	87
Table 7. NthAB activity assay at different concentrations of enzyme (100 or 150 µg/mL) and substrate (0.5 or 1 mM).....	88
Table 8. The amount of IAA present in the ethyl acetate extract of <i>P. putida</i> UW4 culture solution supplemented with 0, 250 or 500 µg/mL.....	91
Table 9. Nitrilase Motif Patterns.....	94
Table 10. Physicochemical properties of aliphatic, aromatic and <i>P. putida</i> UW4 nitrilases	97
Table 11. Characterization of various nitrilase enzymes from different bacteria.....	115
Table 12. Characterization of various nitrile hydratase enzymes from different bacteria	122
Table 13. The specific activity of nitrilase and nitrile hydratase enzymes from various bacteria.....	128

INTRODUCTION

INDOLE-3-ACETIC ACID AND PLANTS

Indole-3-acetic acid is a phytohormone that serves as a key modulator of plant growth and development. This important phytohormone controls nearly every aspect of plant growth and architecture including; cell division, elongation, fruit development, initiation of roots, leaves and flowers, cambial growth, vascular development and senescence (Halliday et al., 2009; Grossmann, 2010; McSteen, 2010; Phillips et al., 2011). Moreover, indole-3-acetic acid acts as a signal within the plant, directing physiological and tropic responses to environmental stimuli. Specifically, indole-3-acetic acid plays a role in a phenomenon known as “shade avoidance syndrome (SAS)” in which the plant stem extends toward the light source, minimizing its exposure to shade (Uggla et al., 1996; Tao et al., 2008; Halliday et al., 2009; Grossmann, 2010; McSteen, 2010; Phillips et al., 2011; Casal, 2013).

INDOLE-3- ACETIC ACID TRANSPORT IN PLANTS

Indole-3-acetic acid directs plant tissue initiation, differentiation and growth by forming concentration gradients. The phytohormone is synthesized and transported throughout the plant, where it concentrates in different local areas. Accumulation in specific tissues disturbs the local indole-3-acetic acid homeostasis and triggers a physiological response. Indole-3-acetic acid is mainly synthesized in young leaves and apical meristems of shoots and is then transported throughout the whole plant via the phloem (Taiz and Zieger, 1991; Teale et al., 2006; Eklund et al., 2010; Tromas & Perrot-

Rechenmann, 2010). In woody trees, the phytohormone is transported through the vascular cambium whereas in leafy plants it is transported through the vascular parenchyma (Teale et al., 2006). This long distance transport is efficient but cannot be finely regulated (Tromas & Perrot-Rechenmann, 2010).

Polar auxin transport between individual cells involves the diffusion of this molecule across cell walls and membranes. The hydrophobic protonated form (IAAH) can diffuse across cell membranes freely, however the hydrophilic anionic form (IAA⁻) cannot (Tromas & Perrot-Rechenmann, 2010). Therefore, the anionic form is actively transported via specific auxin-influx carriers and efflux transporters. Auxin has a pKa of 4.75 and the proportion of the hydrophilic anionic and the hydrophobic protonated forms depends on the pH. In the plant apoplast, the pH is approximately 5.6 so that about 20% of indole-3-acetic acid is in the diffusible protonated form (IAAH), whereas in the cytosol, the pH is 7.4 and most of the indole-3-acetic acid is in the anionic undiffusible form (Teale et al., 2006; Eklund et al., 2010; Tromas & Perrot-Rechenmann, 2010).

Indole-3-acetic acid governs the pattern of plant tissue development in a dose dependent manner. Endogenous concentrations of IAA vary greatly among different organs, tissues or even cells. The amount of active IAA is dependent upon the regulation of its synthesis, transport to or from specific cells or tissues, IAA inactivation and reactivation and degradation (Normanly, 2010). Typically the concentration of IAA is low (5–500 ng/gfw) in leaves and stems and perhaps 10–100 times lower in roots (Maldiney et al., 1986; Blakesley et al., 1990; Reid et al., 2011). However, even at such

low concentrations, IAA is a master regulator of plant development.

THE PLANT RESPONSE TO INDOLE-3-ACETIC ACID

In plants, IAA and AUX/IAA repressor proteins interact with the TRANSPORT INHIBITOR RESPONSE 1/ AUXIN F-BOX PROTEIN (TIR1/AFB) auxin receptors to mediate an auxin response. Both IAA and Aux/IAA repressor protein bind to the same pocket on the surface of TIR1 (Hayashi et al., 2008). TIR1 is a component of the SKP1-CULLIN-F-BOX PROTEIN complex (SCF_{TIR1}). This complex ubiquitinates the auxin repressor proteins (AUX/IAA) and thereby designates them for 26S proteasome degradation (Hayashi et al., 2008).

Auxin response factors (ARF) are transcription factors that regulate the expression of auxin response genes by binding to auxin response elements (AuxRE) in promoters of these genes (Guilfoyle & Hagen, 2007). ARFs function together with Aux/IAA repressors in an auxin-regulated manner. For example, at low IAA concentrations, the repressor proteins (AUX/IAA) form dimers with ARF transcription activators, thereby blocking expression of auxin response genes (Figure 1). At high IAA concentrations, both IAA and the AUX/IAA repressor proteins bind to the TIR1 receptor, AUX/IAA repressor is then ubiquitinated and designated for proteosomal degradation, and the ARF transcription factors are freed. As a result there is an activation of auxin response genes (Figure 1) (Guilfoyle & Hagen, 2007; Hayashi et al., 2008).

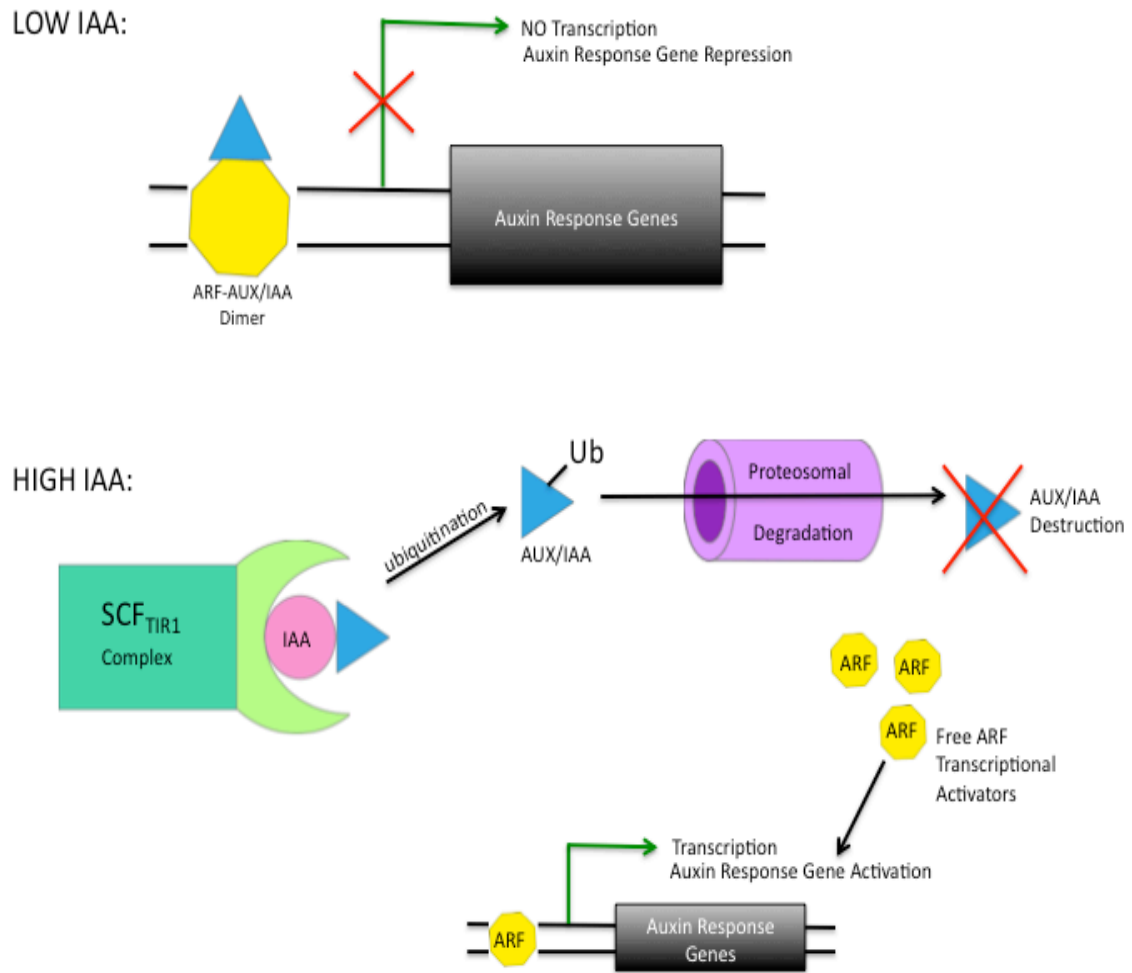


Figure 1. Model of the auxin response at different IAA levels

THE BIOSYNTHESIS OF INDOLE-3-ACETIC ACID

Indole-3-acetic acid (IAA) was first discovered in plants at the end of the 19th century and this discovery initiated the field of “auxinology”. Over the last few decades, several pathways of indole-3-acetic acid biosynthesis have been proposed. These pathways were determined by identifying the enzymes that catalyze each reaction and the intermediates involved at each step of the pathway (Tromas & Perrot-Rechenmann, 2010; Lehmann et al., 2010). The presence of multiple parallel and redundant pathways within a single organism creates a robust IAA biosynthetic network. Different pathways may intersect with one another, which poses difficulties when trying to characterize them. This multi-route system compensates for the loss of any particular pathway, as IAA production can be fluxed through an alternate route. Due to the intricate nature of IAA biosynthesis, there is no plant IAA auxotrophic mutant that is completely devoid of its ability to produce IAA, emphasizing the importance of having a functioning IAA biosynthetic mechanism (Lehmann et al., 2010).

The characterization of a given pathway may involve either the development of IAA-deficient mutants or the biochemical characterization of the enzymes or intermediates in the pathway. Genetic approaches can determine whether a proposed pathway is important for IAA biosynthesis and the contribution of each pathway to the overall pool of IAA. If a particular gene plays a crucial role in IAA biosynthesis, the inactivation of that gene is expected to disrupt the pathway, leading to a decrease in IAA production. The resultant plant phenotype would reveal dramatic developmental defects (Zhao et al., 2002; Soeno et al., 2010). Biochemical approaches aim to isolate and purify the enzymes that catalyze IAA biosynthesis. Substrate feeding assays may reveal the role

and specificity of each enzyme. Determining the structure and function of proteins involved in IAA biosynthetic pathways is a cornerstone in understanding how these pathways work.

THE INDOLE-3-ACETIC ACID BIOSYNTHESIS PATHWAYS

IAA biosynthesis may be tryptophan-dependent or independent of tryptophan. In tryptophan-dependent IAA biosynthesis, the following pathways have been postulated to exist in plants and bacteria utilizing tryptophan as a precursor:

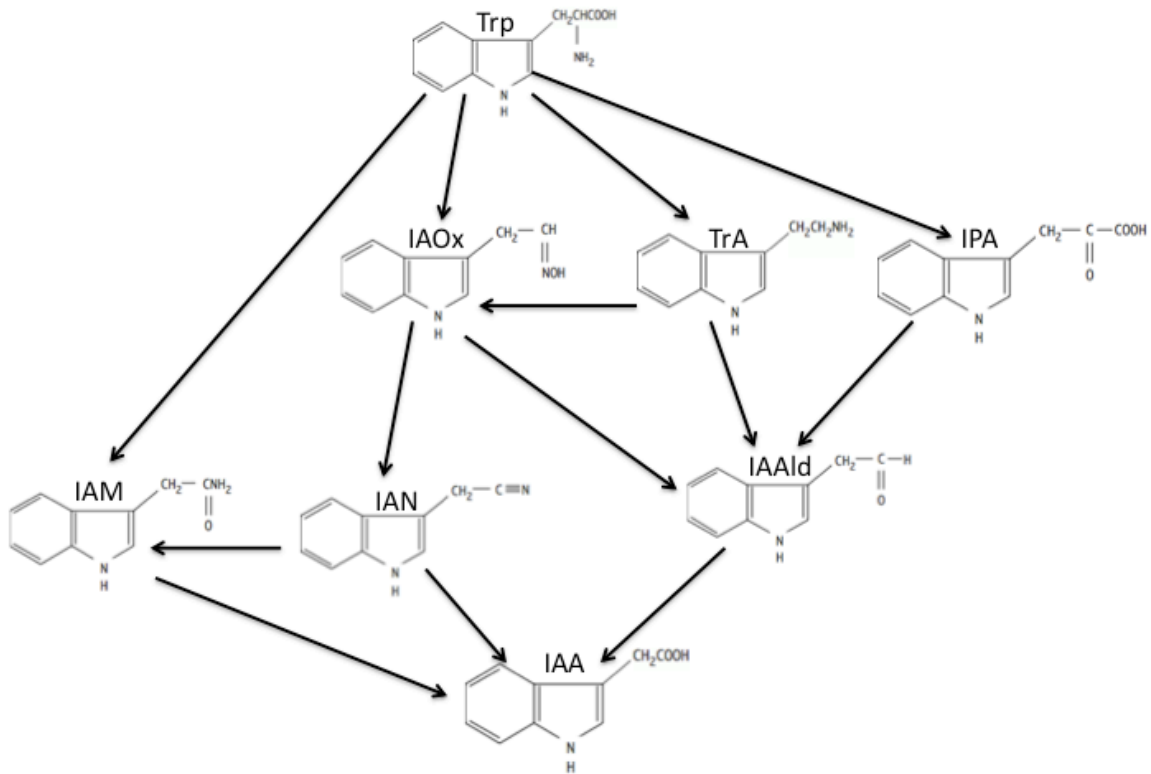


Figure 2. Tryptophan Dependent IAA Biosynthetic Pathways. Trp=tryptophan, IAOx=indole-3-acetaldoxime, TrA=tryptamine, IPA=indole-3-pyruvic acid, IAN=indole-3-acetonitrile, IAM= indole-3-acetamide, IAAld=indole-3-acetaldehyde, IAA=indole-3-acetic acid. Figure adapted from Prinsen et al., 1997.

THE INDOLE-3-PYRUVIC ACID PATHWAY

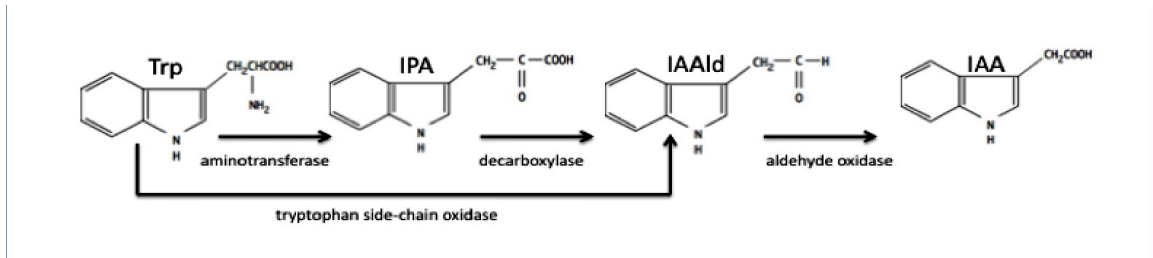


Figure 3. The Indole-3-Pyruvic Acid Pathway. Trp=Tryptophan, IPA=Indole-3-pyruvic acid, IAAlD=Indole-3-acetaldehyde, IAA=Indole-3-Acetic Acid. Figure adapted from Patten and Glick, 1996. .

Both plants and bacteria synthesize IAA via the indole-3-pyruvic acid (IPA) pathway. In fact, this is the most studied and well-characterized pathway in bacteria. First, the tryptophan precursor is transaminated to indole-3-pyruvic acid (IPA) by an aminotransferase enzyme. Subsequently, an indole-3-pyruvate decarboxylase decarboxylates indole-3-pyruvic acid (IPA) into indole-3-acetylaldehyde (IAAld), the rate limiting step (Costacura and Vanderleyden 1995; Spaepen, 2006). Finally, indole-3-acetylaldehyde (IAAld) is oxidized to the final indole-3-acetic acid product by an aldehyde oxidase (Fig. 2) (Costacura and Vanderleyden 1995; Spaepen, 2006; Pollmann et al., 2006). It is important to note that indolepyruvic acid can also be spontaneously converted to indoleacetaldehyde. However, it has been observed that *Enterobacter cloacae* strains produced more IAA from tryptophan when the indolepyruvate decarboxylase gene was present than strains without the gene (Koga et al.1994). This is evidence that this enzyme does contribute to IAA biosynthesis. Furthermore, the aminotransferase reversibly transaminates tryptophan to indolepyruvic acid, but has a dramatically lower Km for indolepyruvic acid than for tryptophan (Koga 1995). Therefore, indolepyruvic acid levels are kept low and are not likely to contribute significantly to spontaneous IAA biosynthesis. Since the indolepyruvate decarboxylase has a high affinity for indolepyruvic acid, even at low amounts of this substrate, it is efficiently converted to indoleacetaldehyde and further to IAA (Koga et al. 1994; Koga 1995). This pathway can be circumvented by a tryptophan side chain monooxygenase enzyme, which directly converts tryptophan into indole-3-acetylaldehyde (Figure 2). This is known as the tryptophan side chain oxidase (TSO) pathway (Oberhänsli et al., 1991).

Aromatic amino acid aminotransferases (AAT) have been reported in plant-associated bacteria such as *Azospirillum*, *Enterobacter*, *Gluconacetobacter*, *Pseudomonas* and *Rhizobium* (Kittell et al., 1989; Koga et al., 1994). Several different isoforms, able to utilize multiple substrate amino acids can exist within a bacterium (Kittell et al., 1989). This implies that these enzymes may catalyze biosynthetic and catabolic pathways in addition to IAA synthesis (Kittell et al., 1989; Pedraza et al., 2004). The indolepyruvate decarboxylase (IPDC), which is encoded by the *ipdC* gene has been cloned from several different bacteria including, *Enterobacter*, *Azospirillum* and *Erwinia* (Brandl et al., 2001; Koga et al., 1991; Malhotra & Srivastava, 2008; Patten & Glick, 2002; Zimmer et al., 1998b). Inactivation of IPDC can result in up to 90% reduction in IAA in *Azospirillum* and *Enterobacter* (Prinsen et al., 1993; Vande Broek et al., 1999; Patten and Glick, 2002). Diminished levels of IAA following disruption of the *ipdC* gene, confirms that IAA is predominantly produced via the IPA pathway in those bacteria.

THE INDOLE-3-ACETAMIDE PATHWAY

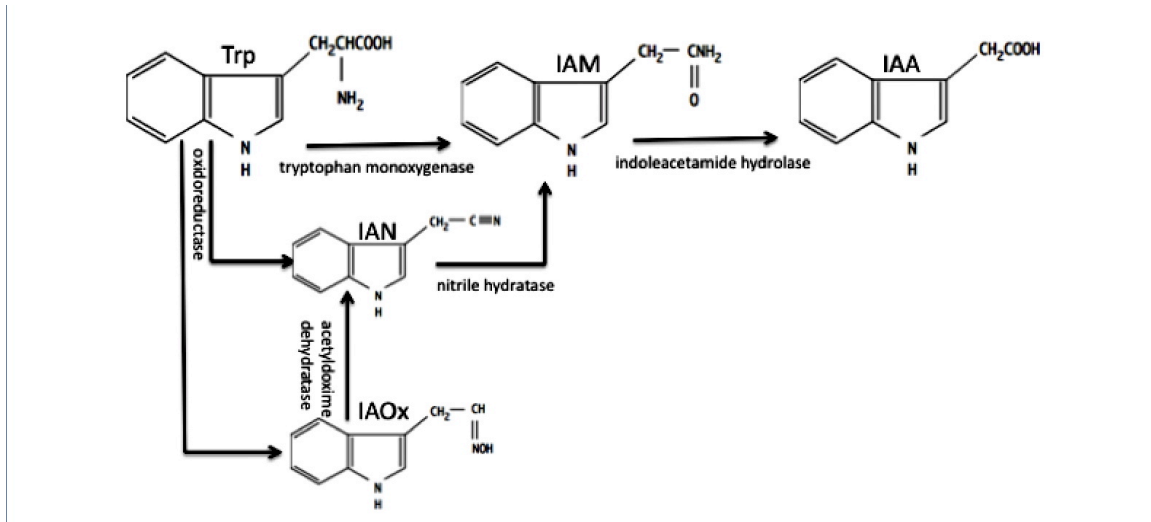


Figure 4. The Indole-3-Acetamide Pathway. Trp=tryptophan, IAM=indole-3-acetamide, IAN=indole-3-acetonitrile, IAA=indole-3-acetic acid, IAOx=indole-3-acetaldoxime. Figure adapted from Patten and Glick, 1996 and Prinsen et al., 1997.

The indole-3-acetamide (IAM) pathway has been described mainly in phytopathogenic bacteria, although it does occur in plants and plant growth promoting bacteria (Kochar et al., 2011). First, tryptophan is converted to the indole-3-acetamide (IAM) intermediate by a tryptophan monooxygenase enzyme (Figure 3). The second reaction is catalyzed by an IAM-specific hydrolase/amidase, which hydrolyzes indole-3-acetamide to the final IAA product (Figure 3) (Pollmann et al., 2006).

The genes mediating this pathway are *iaaM*/*tms-1* encoding tryptophan monooxygenase and *iaaH*/*tms-2* encoding indoleacetamide hydrolase/amidase enzymes (Comai & Kosuge, 1982; Schröder et al., 1984; Thomashow et al., 1984). These genes may be organized in an operon on a plasmid, as is the case for *Pseudomonas savastanoi*, or located on opposite DNA strands with a short intergenic promoter region like in *Agrobacterium tumefaciens* (Yamada et al., 1985a ; Gaffney et al., 1990; Mazzola & White, 1994; Costacura and Vanderleyden 1995). Phylogenetic analysis of the *iaaM* gene revealed that homologues exist in few bacteria. Moreover, the *iaaM* sequences fall into two groups (Patten et al., 2012). Group I genes include those that have been experimentally confirmed to encode tryptophan 2-monooxygenases in the plant pathogens *A. tumefaciens*, *P. syringae*, *P. agglomerans*, and *Dickeya dadantii* (Comai & Kosuge, 1982; Thomashow et al., 1984; Van Onckelen et al., 1986; Clark et al., 1993; Yang et al., 2007; Patten et al., 2012). Group II *iaaM* homologues occur in more diverse bacterial species. The function of the group II homologues in IAA biosynthesis remains to be determined experimentally. Tryptophan may not be a substrate of these group II enzymes, as a putative *iaaM* sequence from *P. putida* KT2440 (DavB) has been shown to

catalyze lysine degradation (Revelles et al., 2005). Perhaps group II *iaaM* homologues do not partake in IAA synthesis, although many are annotated as putative tryptophan monooxygenases based on sequence identity with group I homologues (Patten et al., 2012).

Nitrile hydratase enzymes link the IAN and IAM pathways by catalyzing the hydration of indole-3-acetonitrile (IAN) into indole-3-acetamide (IAM), which is then converted to the final product IAA by indole-3-acetamide hydrolase/amidase (Figure 3) (Vega-Hernández et al., 2002).

THE INDOLE-3-ACETONITRILE/ INDOLE-3-ACETYLDOXIME PATHWAY

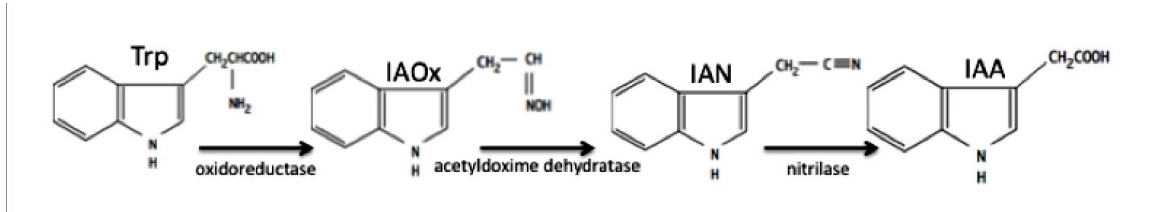


Figure 5. The Indole-3-Acetonitrile/Indole-3-Acetylaloxime Pathway. Trp=tryptophan, IAOx=indole-3-acetylaloxime, IAN= indole-3-acetonitrile, IAA=indole-3-acetic acid. Figure adapted from Patten and Glick, 1996 and Prinsen et al., 1997.

The indole-3-acetonitrile (IAN) pathway has been well studied in plants but neglected in bacterial studies (Kobayashi et al. 1993; Kobayashi and Shimizu 1994; Bartel and Fink 1994; Bartling et al. 1994). In this pathway, tryptophan is first converted into indole-3-acetaldoxime (IAOx) by an oxidoreductase enzyme. In plant studies of this pathway, cytochrome p450 oxidoreductase enzymes catalyze this step (Hull et al., 2000; Mikkelsen et al., 2000). Such an enzyme has not yet been characterized in bacteria. In plants such as *Arabidopsis thaliana*, indole-3-acetaldoxime (IAOx) is an intermediate that can be converted into different secondary metabolites besides indole-3-acetic acid (Hull et al., 2000; Mikkelsen et al., 2000). Inactivation of the cytochrome p450 oxidoreductases in plants eliminates the production of indole-3-acetaldoxime (IAOx) and results in only subtle growth defects. It appears that these genes and the indole-3-acetaldoxime intermediate are not major players in IAA biosynthesis in plants (Sugawara et al., 2009; Zhao, 2010). Moreover, the *cyp79b2/b3* genes encoding the cytochrome p450 oxidoreductases only occur in a small number of plant species, thus it is unlikely that they serve as universal IAA biosynthesis genes (Zhao, 2010).

In the second step, the indole-3-acetaldoxime intermediate is converted into indole-3-acetonitrile by an acetaldoxime dehydratase (Figure 4). The indole-3-acetonitrile intermediate is consequently converted directly to IAA by a nitrilase enzyme. Alternatively, nitrilase enzymes can convert the indole-3-acetonitrile to indole-3-acetamide, which is then converted to the final product IAA by IAM hydrolase/amidase (Layh et al., 1998; Piotrowski et al., 2001; O'Reilly C and Turner., 2003; Fernandes et al.,

2006; Martinkova and Kren, 2010; Zhao, 2012; Gong et al., 2012). This activity is similar to that of nitrile hydratase, which converts the nitrile into the amide product as mentioned earlier. Nitrilases and amidases make up part of a large superfamily composed of 13 branches, however only branch I nitrilases are implicated in IAA biosynthesis. Nitrile hydratases are not part of this superfamily (Pace and Brenner, 2001; O'Reilly and Turner, 2003; Gong et al., 2012). Nitrile compounds occur frequently in nature so nitrilase and nitrile hydratase enzymes are widespread among many different types of bacteria. While these enzymes can facilitate IAA biosynthesis, this is not necessarily their main role (Kim and Oriel, 2000). In plants, it has been suggested that nitrilases play a more important role in glucosinolate metabolism, camalexin homeostasis and cyanide detoxification than in IAA biosynthesis (Zhao et al., 2012). Usually, microbes contain either a nitrilase or a nitrile hydratase-amidase system, although some have both (Robinson and Hook, 1964; Harper, 1977; Harper, 1985; Kobayashi et al., 1990; Nagasawa et al., 1990; Layh et al., 1998; Prasad et al., 2007a; Martinkova and Kren, 2002; Prasad et al., 2005; Bandyopadhyay et al., 1986; Mathew et al., 1988; Mauger et al., 1988; Linton and Knowles, 1986; Bhalla et al., 1992, 1995; Prasad et al., 2009; Bhalla and Kumar, 2005).

INDOLE-3-ACETIC ACID AND PLANT GROWTH PROMOTING BACTERIA

Among the reported plant growth promoters that produce indole-3-acetic acid are those from genera such as *Pseudomonas*, *Rhizobium*, *Azospirillum*, *Enterobacter*, *Azotobacter*, *Klebsiella*, *Alcaligenes*, *Pantoea* and *Streptomyces* (Apine & Jadhav, 2011a). The secreted indole-3-acetic acid stimulates plant root hair formation and root growth, when it is within an ideal concentration range. However, bacterial IAA can also

inhibit primary root growth (Davies, 1995). For example, a wild-type IAA-producing *Pseudomonas putida* strain stimulates plant growth while its IAA overproducing mutant actually inhibits growth (Xie et al., 1996; Persello-Cartieaux et al., 2003). Dobbelaere et al., (1999), observed a decrease in wheat root length with increasing concentrations of IAA (10^{-9} to 10^{-4} M). This inhibitory effect was the same when the wheat seeds were inoculated with 10^9 bacteria per mL of the wild-type IAA-producing *Azospirillum brasilense* strain in the presence of exogenous Trp. In other cases, root growth inhibition can be observed at concentrations of 0.01 M IAA (Reid et al., 2011). Each plant has a unique capacity for IAA and the ideal concentration range can be extremely narrow (Spaepen et al., 2007). A well-developed root system is imperative for water and nutrient uptake and for anchoring plants in the soil. The plant reciprocates by providing the bacterial companion with nutritional exudates and an ideal shelter (Ahmed & Hasnain, 2010). Therefore, indole-3-acetic acid is a reciprocal signaling molecule in plant–microbe interactions, sustaining the symbiotic relationship that has evolved between host plants and their microbial allies (Malhotra & Srivastava, 2009).

In 1977, Thimann showed that the number of roots formed was greatly increased when oat seeds were germinated in an IAA solution. Then, in 1979, Tien et al., observed that roots of pearl millet seedlings showed a remarkable growth response when they were inoculated with IAA-producing *Azospirillum brasilense*. Moreover, the lateral roots were densely covered by root hairs, whereas very few hairs developed on uninoculated control plants (Tien et al., 1979). IAA at a concentration of 6×10^{-8} M also significantly increased shoot biomass (Tien et al., 1979). More recently, inoculation of wheat with

transconjugant *Azospirillum brasilense* (expressing the *ipdC* gene from a constitutive or a plant inducible promoter) causes an increase in root hair formation as compared to inoculation with the wild-type strain. Root hairs help take up nutrients, thus benefiting plant growth (Dobbelaere et al., 1999; Spaepen et al., 2008). Canola roots from seeds treated with IAA-producing *Pseudomonas putida* GR12-2 were 35% longer than the roots from uninoculated control seeds. The mutant, deficient in IAA biosynthesis, did not stimulate root growth (Patten and Glick, 2002). Isolates of *Pantoea agglomerans* were selected from legume roots and investigated for the ability to promote the growth of canola, lentil and pea (Sergeeva et al., 2007). There is a correlation between plant-growth promoting ability and the production of IAA by these strains (Sergeeva et al., 2007). The inoculation of *Arabidopsis* with an IAA-producing *Streptomyces* spp. resulted in a significantly increased plant biomass as compared to the untreated control. These *Streptomyces* are naturally endophytic to important medicinal plants. *Arabidopsis* plantlets inoculated with *Streptomyces* mutants that did not have a functional IAA biosynthetic pathway did not display significantly improved growth compared to the control. This particular spore-bearing endophytic streptomycete has the potential to serve as a promising inoculant for enhancing plant growth (Lin and Xu, 2013). Ahmed et al. (2012) observed that exogenous indole-3-acetic acid application, at a concentration of 8.5×10^{-4} M, markedly increased date palm fruit size with a reasonable reduction in the amount of fruit drop, which causes major economic losses every year. Therefore, foliar application of IAA at the unripe stage of fruit development or perhaps inoculation with an IAA-producing PGPB may be a means of increasing fruit yields (Ahmed et al., 2012).

INDOLE-3-ACETIC ACID AND PHYTOPATHOGENS

The beneficial aspects of bacterial IAA on plant growth have been well explored, but paradoxically, both plant-growth-promoting bacteria and phytopathogenic bacteria produce IAA. In fact, bacterial IAA plays a major role in plant disease and bacterial pathogenicity (Fu et al., 2011). High levels of IAA produced by phytopathogenic bacteria such as *A. tumefaciens*, *Erwinia herbicola* pv. *gypsophilae*, *Pseudomonas syringae* pv. *savastanoi* and *Pseudomonas syringae* pv. *syringae* causes necrotic lesions and gall tumour formation on host plants. The phytopathogens benefit by receiving nutrients such as gall-derived opines and plant metabolites. Losing the ability to produce IAA by mutagenesis reduces the virulence of these pathogens (Comai & Kosuge, 1982; Manulis et al., 1998; Surico et al., 1985).

IAA has been shown to increase the susceptibility of *Arabidopsis*, tobacco, sweet orange and rice to biotrophic and necrotrophic bacterial and fungal infection (Cernadas & Benedetti, 2009; Ding et al., 2008; Ferrari et al., 2008; Fu et al., 2011; Navarro et al., 2006). *Arabidopsis* and rice plants treated with the IAA analogs 2,4-dichloro phenoxy acetic acid (2,4-D) or 1-naphthal acetic acid (NAA) had more severe disease symptoms when infected with a phytopathogen than untreated plants (Fu et al., 2011).

Bacterial IAA compromises the integrity of the plant cell wall, the first barrier of defense against pathogens. It does this by inducing the expression of proteins responsible

for decreasing cell wall rigidity. For example, IAA is reported to induce the expression of expansins, which extend the cell wall while allowing phytopathogens to intrude (Fry et al., 1992; Brummel et al., 1994; Catala et al., 1997, 2000; Kochar, 2011). Overexpression of expansin in rice has been shown to increase its susceptibility to the bacterial pathogen *Xanthomonas oryzae* (Ding et al., 2008). IAA signaling has also been linked to the opening of stomata, which phytopathogens use as portals to colonize the plant (Melotto et al., 2006; Acharya & Assmann, 2009; Kazan & Manners, 2009).

Plant pathogenic bacteria use a type III secretion system to deliver effector proteins directly into the plant host cells. One such bacterial effector is AvrRpt2 produced by *Pseudomonas syringae*. When this effector protein is delivered into plant cells it induces native IAA biosynthesis. This overproduction of IAA may be one of the mechanisms used by the pathogen to colonize its host. Transgenic *Arabidopsis* plants that over express AvrRpt2 have elevated levels of free IAA and are more susceptible to *P. syringae* infection compared with wild-type plants (Chen et al., 2007). AvrRpt2 enhances IAA signaling by stimulating the degradation of the Aux/IAA negative regulators. When these repressor proteins are degraded, auxin response factors are no longer repressed, and auxin signaling cascades can proceed serving as a virulence mechanism to promote pathogenicity (Cui et al., 2013).

Salicylic acid is a plant defense signal that inhibits IAA signaling by stabilizing Aux/IAA repressor proteins (Wang et al., 2007; Cui et al, 2013). Studies revealed that an IAA-producing pathogenic *Pseudomonas syringae* strain promotes disease in *Arabidopsis*

by suppressing pathogenesis-related (PR) gene expression and salicylic acid-dependent defense responses. This suppression is paralleled by an increase in IAA levels (Fu et al., 2011). Plants deficient in salicylic acid also show increased IAA levels (Kazan & Manners, 2009).

Gonzalez-Lamothe et al. (2012) noted that the activation of auxin signaling in plants, induces the formation of conjugated forms of IAA via GH3 proteins. GH3 proteins conjugate IAA to amino acids and these conjugated forms of IAA promote plant disease. The study demonstrated that infection of *Arabidopsis* with *Botrytis cinerea* or *Pseudomonas syringae*, leads to transcriptional activation of auxin conjugating GH3 proteins and consequently to accumulation of IAA-Asp. IAA-Asp enhanced pathogen growth and activated virulence genes (Gonzalez-Lamothe et al., 2012).

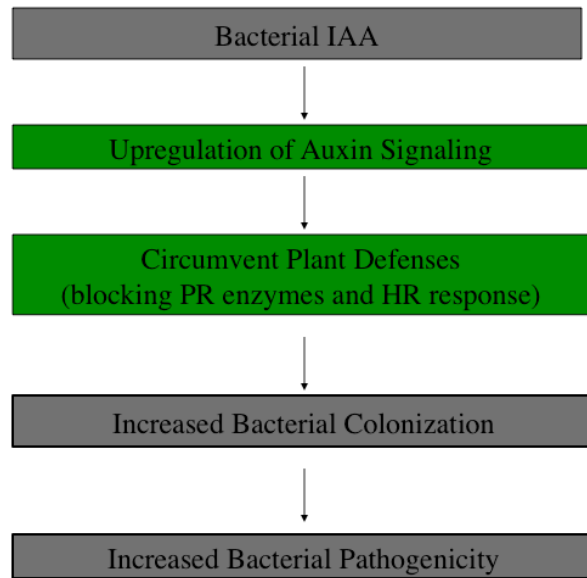


Figure 6. IAA in pathogenic plant/bacterial interactions. Signaling taking place in the plant is indicated by green boxes. Figure adapted from Spaepen et al., 2007.

FACTORS INVOLVED IN INDOLE-3-ACETIC ACID PRODUCTION IN BACTERIA

Determining the factors that control IAA biosynthesis in bacteria will allow us to maximize the beneficial effects of IAA and reduce the deleterious effects. The IAA secreted by rhizospheric bacteria acts in conjunction with the plant's endogenous IAA supply. Thus, the impact of bacterial IAA on plants can be either positive or negative, depending on the level of IAA produced and secreted and the sensitivity of the plant tissue to IAA (Ali et al., 2010; Glick, 1995). For instance, the plant root is most sensitive to fluctuations in IAA, and its response to different IAA concentrations ranges from elongation of the primary root, formation of lateral and adventitious roots, to inhibition of growth (Loper and Schroth, 1986; Davies, 1995; Xie et al., 1996; Beyerler et al., 1997). Plants have regulatory systems that maintain IAA homeostasis. However, phytopathogens that produce high levels of IAA may override the plant regulation system and impose detrimental effects on the plant (Sitbon et al., 1992; Patten & Glick, 1996; Pilet & Saugy, 1985; Pilet et al., 1979; Taiz & Zeiger, 1991).

The pathway(s) and the location of the IAA biosynthesis genes (on the chromosome or on a plasmid) influences the amount of IAA produced by that bacterium. IAA biosynthesis genes that reside on a high copy number plasmid have more gene copies to be transcribed as compared with those located on the chromosome (Brandl et al., 1996; Patten & Glick, 1996). In *Agrobacterium tumefaciens*, the Ti plasmid region containing the IAA biosynthesis genes is transferred and integrated into the host plant genome and transcribed from strong plant promoters. This direct transformation exposes plant cells to deleteriously high concentrations of IAA (Liu et al., 1982; Gaudin et al.,

1995; Sitbon et al. 1991). Endophytic bacteria such as *Pseudomonas syringae* pv. *savastanoi* also produce detrimental amounts of IAA. This bacterium colonizes the interior of the plant and secretes IAA directly into the plant cells (Smidt & Kosuge, 1978; Comai & Kosuge, 1980). Conversely, secretion of IAA by rhizobacteria exposes the plant to lower concentrations of IAA as the hormone may be degraded before it actually reaches the plant cell. The inoculum size of the bacteria also reflects the level of bacterially produced IAA imposed upon the plant, and therefore may determine whether that bacterium either promotes or inhibits plant growth. Another important factor is the level of expression of IAA biosynthesis genes in the rhizosphere, which is largely unknown (Harari et al., 1988; Loper & Schroth, 1986; Morgenstern & Okon, 1987).

Production of IAA by bacteria varies greatly among different species and is influenced by culture condition, growth stage, and availability of substrates (Shokri & Emtiazi, 2010a). In nature, it appears that IAA biosynthesis is finely-tuned according to the different environmental conditions that may be encountered by the bacteria in the soil and plant environment (Spaepen et al., 2007). The presence of tryptophan, vitamins, salt, oxygen, pH, temperature, carbon source, nitrogen source and growth phase are all potentially contributing factors in the regulation of IAA biosynthesis. Plant extracts or specific compounds present in the rhizosphere or on plant surfaces influence bacterial IAA biosynthesis. For example, flavonoids produced by plants stimulate IAA production in the symbiotic bacteria *Rhizobia* spp. (Prinsen et al., 1991; Theunis et al., 2004). Likewise, plant leaf extracts from oranges stimulate IAA production in *Xanthomonas* spp. (Costacurta et al., 1998). Evidently, different bacteria produce different amounts of IAA

under different conditions. The optimal conditions for IAA production may be a reflection of the ideal niche that the bacterium occupies, be it in the slightly acidic rhizosphere or at the physiological pH inside a plant. Controlling IAA production will require a better understanding of how all these factors can be optimized (Apine & Jadhav, 2011b).

Bacterial IAA production is linked to a reduction in growth rate or entry into the stationary growth phase. The sigma factor RpoS (σ^{38}) is effective at the onset of the stationary phase of growth (Latifi et al., 1996). This sigma factor is referred to as a general stress regulator in α -proteobacteria bacteria and was reported to promote IAA production by up-regulating the expression of IAA biosynthetic genes (Saleh & Glick, 2001; Patten & Glick, 2002a; Sun et al., 2009). Recombinant bacteria that constitutively produced RpoS also produced IAA earlier and continued to produce high levels compared with cells that produced natural levels of RpoS (Patten & Glick, 2002a).

THE ROLE OF INDOLE-3-ACETIC ACID IN BACTERIA

Bacterial IAA does not only have a physiological effect on plants and a role as a communication signal in plant-microbe interactions, it also serves a purpose in a bacterium itself. Perhaps most profoundly, IAA promotes better bacterial adaptation to stress conditions leading to improved survival and persistence in the plant environment (Bianco et al., 2006). The majority of bacteria cultured from plants are IAA-producers. Therefore, from an evolutionary perspective, having the ability to produce IAA must give the bacteria a selective advantage in that environment (Kim et al., 2011).

Escherichia coli was used as a model system for microarray analysis to show which genes displayed an altered expression level as a result of exogenous IAA treatment. The affected genes encode cell envelope proteins, or proteins involved in bacterial adaptation to harsh environmental conditions. Interestingly, the IAA-treated cells produced more trehalose, lipopolysaccharide (LPS), exopolysaccharide (EPS) and biofilm. IAA also conferred increased tolerance to heat and cold shock, UV-irradiation, osmotic and acid shock, oxidative stress, toxic antibiotics, detergents and dyes (Bianco et al., 2006a). *E. coli* does not typically encounter IAA in its natural environment, nor does it have the ability to produce IAA. However, upon exogenous exposure to IAA, the tricarboxylic acid (TCA) cycle and the glyoxylate shunt are activated. IAA treated cells produced more acetyl-CoA which goes into the phosphotransacetylase (Pta)-acetate kinase (Ack) pathway resulting in more acetate and less pyruvate production. The accumulation of acetate in IAA-treated cells confers an advantage in that during the transition to stationary phase, the cells can reabsorb acetate, activate it to acetyl-CoA and utilize it to generate energy. The NADH/NAD⁺ ratio is reduced in IAA-treated cells, avoiding repression of the TCA cycle's rate-controlling enzymes (Bianco et al., 2006b).

IAA can trigger the induction of genes related to bacterial stress resistance in bacteria associated with plants as well. *Sinorhizobium meliloti* cells treated with exogenous IAA, or modified to overproduce IAA, were exposed to various stress conditions such as acidity, osmotic shock, UV-irradiation and heat shock. Afterwards, viable bacterial cell counts were taken to see how IAA affected their survival. More

bacteria survived in both IAA-treated and IAA-overproducing strains compared with wild-type or non-treated strains (Bianco et al., 2009). Exogenous IAA treatment also promoted intracellular trehalose accumulation in *Sinorhizobium meliloti*. Moreover, an IAA over-producing strain had approximately 3 times more trehalose than the wild-type strain. Bacteria can use trehalose as a source of carbon and as an osmolyte that confers protection against freezing and desiccation (Bianco et al., 2009).

The production of lipopolysaccharide (LPS), exopolysaccharide (EPS) and biofilm was evaluated in both IAA-treated and IAA-overproducing *Sinorhizobium meliloti*. It was observed that the IAA-overproducer contained higher levels of LPS molecules and produced more biofilm as compared to wild-type *Sinorhizobium* (Bianco et al., 2009). It also produced more exopolysaccharide (EPS), a major component of biofilm. Increased LPS in the outer membrane protects the bacterial cells against the innate plant defense system. Likewise, the increased formation of biofilm likely serves as an important survival factor, enabling rhizobia to resist harsh environmental conditions and to improve their attachment to plant roots (Bianco et al., 2009).

PURPOSE OF THIS RESEARCH

The genome of one particularly effective strain of plant growth-promoting bacteria, *Pseudomonas putida* UW4, originally isolated from the University of Waterloo campus, has been completely sequenced. Seven separate genes that encode enzymes potentially involved in the biosynthesis of indole-3-acetic acid were identified (Duan, et al., 2012). These seven genes appear to be part of at least two different IAA biosynthesis

pathways. The proposed research is directed towards better understanding the IAA biosynthesis pathways operating in *Pseudomonas putida* UW4 by isolating, purifying and characterizing some of the implicated enzymes.

The seven genes that have been identified as putative IAA biosynthesis genes in *P. putida* UW4 are:

iaaM- a tryptophan monooxygenase

auxI- a tryptophan monooxygenase

ami- an indole-3-acetamide hydrolase/amidase

nthA and *nthB*- a putative nitrile hydratase composed of two separate subunits

nit- a nitrilase

pheD- a phenylacetylaldehyde dehydratase

Both the IAOx/IAN and IAM pathways are predicted to be operating in UW4 (Figure 7). We hypothesize that in the former pathway, the tryptophan precursor is first converted into the IAOx intermediate by an unknown enzyme. Subsequently, the phenylacetylaldehyde dehydratase (PheD) converts the IAOx intermediate into the IAN intermediate. This IAN substrate is either directly converted into IAA by nitrilase (Nit) or is converted into the IAM intermediate by nitrile hydratase (NthAB). In the IAM pathway, the two tryptophan monooxygenase enzymes (IaaM & Aux1) convert tryptophan to IAM. Once the IAM intermediate is produced, it is converted into IAA by amidase (Ami).

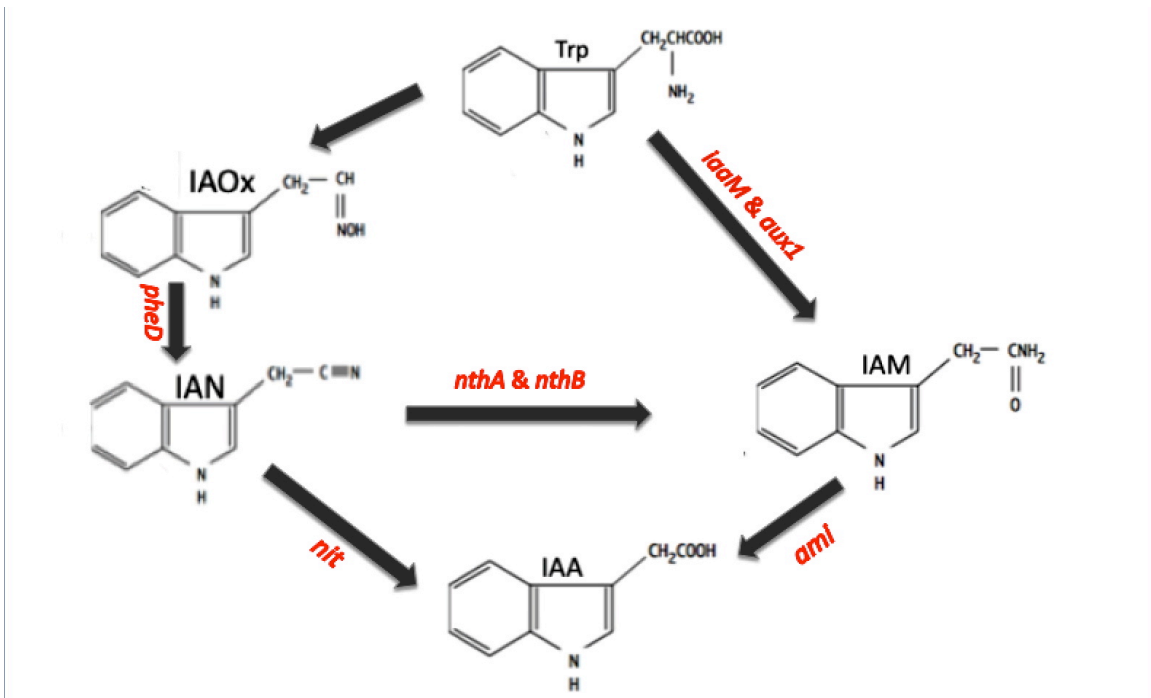


Figure 7. IAA biosynthetic pathways in *Pseudomonas putida* UW4

MATERIALS AND METHODS

BACTERIAL CULTURES

The bacterial strains and plasmids used in this study are described in Table 1. *Pseudomonas putida* UW4 (Duan et al., 2012) was grown and maintained aerobically at 30°C in tryptic soy broth (TSB) (Bacto™) supplemented with 100 µg/mL ampicillin. All *Escherichia coli* strains were maintained aerobically at 37°C in Luria –Bertani (LB) broth (Fischer Bioreagents®). When appropriate, 50 µg/mL kanamycin and isopropyl β-D-1-thiogalactopyranoside IPTG were added. Bacteriological grade agar (1.5 %) (Bioshop® Canada Inc.) was used as a solidifying agent for all media when needed. *E.coli* DH5a (Invitrogen, Life Technologies™) was used as an initial cloning host to maintain recombinant plasmids without any background basal protein expression. *E.coli* BL21 DE3 (Novagen, Merck KGaA©) was used as the host for recombinant protein expression. This expression host is designed for expression from pET vectors and contains an IPTG inducible T7 RNA polymerase (Novagen, Merck KGaA©).

Table 1. Bacterial strains, plasmids and constructs used in this study

Strain	Description	Reference
<i>Escherichia coli</i> DH5a	F ⁻ ϕ 80 <i>lacZ</i> ΔM15 Δ(<i>lacZYA-argF</i>) U169 <i>recA1 endA1 hsdR17</i> (<i>rk⁻, mk⁺</i>) <i>gal phoA supE44 λ thi⁻</i> 1 <i>gyrA96 relA1</i>	Invitrogen
<i>Escherichia coli</i> BL21 (DE3)	F ⁻ <i>ompT hsdS_B(r_B⁻m_B⁻) gal dcm</i> (DE3)	Novagen
Plasmid	Description	Reference
pET30b (+)	N-terminal His•Tag® /thrombin/ S•Tag™ /enterokinase configuration plus an optional C-terminal His•Tag	Novagen
Constructs	Description	Reference
pETnit	pET30b(+) vector with the <i>nit</i> gene from <i>P. putida</i> UW4 in the NdeI/XhoI site	This study
pETnthAB	pET30b(+) vector with the <i>nthAB</i> gene from <i>P. putida</i> UW4 in the NdeI/XhoI site	This study
pETP47K	pET30b(+) vector with the <i>p47K</i> gene from <i>P. putida</i> UW4 in the NdeI/XhoI site	This study
pETaux	pET30b(+) vector with the <i>aux</i> gene from <i>P. putida</i> UW4 in the NdeI/XhoI site	This study
pETiaaM	pET30b(+) vector with the <i>iaaM</i> gene from <i>P. putida</i> UW4 in the NdeI/XhoI site	This study
pETpheD	pET30b(+) vector with the <i>pheD</i> gene from <i>P. putida</i> UW4 in the NdeI/HindIII site	This study

IAA PRODUCTION BY *P. PUTIDA* UW4

Salkowski Assay

To test for IAA production by *P. putida* UW4 and to determine the amount of IAA produced, the Salkowski assay was first employed (Gordon and Weber, 1951; Glickmann and Desaux, 1995). This test is based on the reaction of Salkowski reagent (150mL H₂SO₄, 250 mL dH₂O, 7.5mL 0.5M FeCl₃) with IAA, which produces a characteristic pink colour change. The intensity of the colour is proportional to the amount of IAA produced and can be measured spectrophotometrically (Figure 8). Briefly, a starter culture of strain UW4 was grown in 5 mL TSB medium supplemented with 100 mg/mL ampicillin (final concentration) at 30°C overnight. The following day, 20 µl of the starter culture was used to inoculate 5 mL of Dworkin and Foster (DF) salts minimal medium supplemented with 0, 200 or 500 µg/mL tryptophan (Sigma). The cultures were incubated in a shaking water bath at 30°C for 24-72 hours or until they reached an OD₆₀₀ above 1 (i.e., in late log/stationary phase of growth). The bacterial cells were then collected by centrifugation in a Sigma 3-18K centrifuge at 2000 x g for 5 minutes. The supernatant was saved (IAA is secreted into the supernatant) and a 1 mL aliquot was mixed with 4 mL of Salkowski reagent. The mixture was allowed to stand at room temperature for 30 minutes, after which the absorbance at 535 nm was measured with a Varian CARY 50 BIO UV-Visible spectrophotometer. One mL of uninoculated DF salts minimal medium was used as a reference blank. The concentration of IAA was determined by comparison with a standard curve. IAA standards for the standard curve were prepared from a 100 µg/mL IAA stock solution (Sigma). The following final concentrations of IAA standards were used: 0, 1, 5, 10, 20, 40 µg/mL.

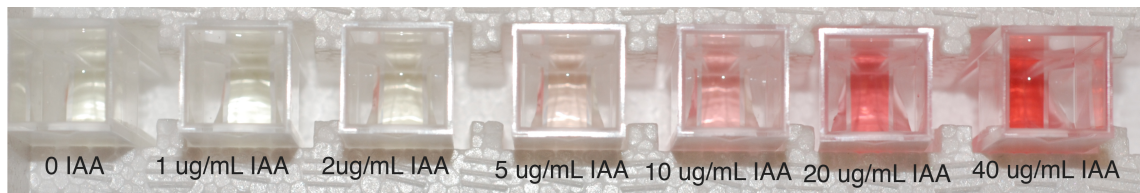


Figure 8. The Salkowski Assay of IAA Standards (0-40 $\mu\text{g/mL}$)

IAA HPLC Assay

To confirm the amount of IAA produced by *P. putida* UW4, HPLC analysis was employed as a more specific and analytical method. Fifty mL cultures of *P. putida* UW4 were grown in DF salts minimal media supplemented with 0, 250 or 500 µg/mL of tryptophan. The cultures were incubated in a shaking water bath at 30°C for 24-48 hours or until they reached an OD₆₀₀ above 1. The OD₆₀₀ was always consistent between all samples. After the incubation period, 20 µl of 1 mg/mL indole-3-propionic acid (IPA) was added to each culture. This is an internal standard that behaves similar to IAA during the extraction process and facilitates HPLC quantitation of IAA (Kim et al., 2006). The bacterial pellet was collected by centrifugation at 2000 x g for 15 minutes. The supernatant (containing the secreted IAA) was transferred to a clean 50 mL polypropylene tube (VWR® SuperClear™) and the pH was lowered to 2.5 with 1M HCl. An equal volume of HPLC-grade ethyl acetate was added to the supernatant and mixed rigorously via vortexing. The mixture was then centrifuged at 2000 x g for 5 minutes to separate the ethyl acetate fraction from the aqueous fraction. The upper ethyl acetate fraction was transferred to a clean 300 mL (Pyrex®, USA) round-bottom flask. The ethyl acetate extraction process was repeated twice more, each time collecting the upper phase and adding it to the round bottom flask. Rotary evaporation, under vacuum, of the ethyl acetate was then performed, maintaining the temperature below 50°C at all times. The remaining precipitate was then dissolved in 1 mL of 100% HPLC-grade methanol and syringe filtered through 0.45mm filter to remove any particulate matter. The samples were then analyzed by HPLC (Tien et al. 1979).

CLONING

Genomic DNA Isolation

Pseudomonas putida UW4 was grown in 5 mL TSB liquid culture supplemented with 100 mg/mL ampicillin (final concentration) at 30°C overnight in a shaking water bath. Genomic DNA was extracted according the manufacturers instructions. The Wizard® Genomic DNA purification kit (PROMEGA, REF A1120) was used for genomic DNA extraction.

Primers

All primers used for PCR were purchased from Sigma-Aldrich Canada. The primer sequences used in this study are listed in Table 2. Restriction sites in the primers are highlighted in grey. Start and stop codons were not included in any of the primer sequences because these codons are already present in the pET30b(+) expression vector. All primers have the NdeI restriction site in the forward primer and XhoI in the reverse primer preceded by a short 4 bp linker sequence to facilitate efficient digestion. The only exception is pheD-R, which has a HindIII site in the reverse primer due to an existing XhoI site within the gene.

To obtain the UW4 *nit*, *nthAB*, *P47K* (activator protein), *aux*, *iaaM* and *pheD* genes, the primers listed in Table 2 were used. Both the forward and reverse primer sequences were based on the fully sequenced *P. putida* UW4 genome from GenBank with the accession number CP003880.1. For the NthAB protein composed of the α and β subunits, the forward primer was designed starting from the second codon of the

α subunit, while the reverse primer was designed starting from the second last codon of the β subunit. The α -subunit, short intergenic region (42 bp) and β -subunit were amplified as a single fragment for cloning.

The primers were designed using the Sigma Genosys DNA calculator (Sigma-Aldrich), with melting temperatures (T_m) within 1- 2 °C of each other (forward and reverse), at least 50% GC content, no predicted primer dimer formations and weak/no secondary structure formation. The T_m of each primer was calculated without including the restriction enzyme site and the 4bp linker sequence because these sequences are overhangs and do not anneal to the template.

Table 2. Primers used to amplify the *nit*, *nthA*, *nthB*, *P47K*, *aux* and *iaaM* putative IAA biosynthesis genes. F represents the forward primer, while R represents the reverse primer.

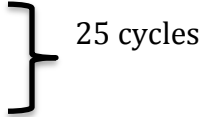
Name	Sequence	Description
nit-F	5'-TAATCATATGCCCAAATCAATCGTTGCGGC-3'	<i>nit</i> (NdeI)-fwd
nit-R	5'-ATTACTCGAGGGAAGTGAAGCGCACCCCC-3'	<i>nit</i> (XhoI)-rev
nthA-F	5'-TAATCATATGAGCGCCACTGTATCCCCAG-3'	<i>nthA</i> (NdeI)- fwd
nthB-R	5'-ATTACTCGAGTGCGGCCACCGTTTTTC-3'	<i>nthB</i> (XhoI)-rev
P47K-F	5'-TAATCATATGATTGACGGGGCCCTATC-3'	P47K (NdeI)- fwd
P47K-R	5'-ATTACTCGAGGGGTGACAATGCCTTGAG-3'	P47K (XhoI)- rev
aux-F	5'-TAATCATATGACTATCGGATCAAGCTACAAC-3'	<i>aux</i> (NdeI)-fwd
aux-R	5'-ATTACTCGAGGGTTTTGAGTTGGTAGTGC-3'	<i>aux</i> (XhoI)-rev
iaaM-F	5'- TAATCATATGAACAAGAACAATCGCCATCCTGCAG-3'	<i>iaaM</i> (NdeI)- fwd
iaaM-R	5'-ATTACTCGAGCTCGGGCAGGGCGATCG-3'	<i>iaaM</i> (XhoI)- rev
pheD-F	5'-TAATCATATGGAATCTGCGATCGATAAG-3'	<i>pheD</i> (NdeI)- fwd
pheD-R	5'-ATTAAAGCTTGGTTTCAGGGATCACC-3'	<i>pheD</i> (HindIII)- rev

PCR-Genomic DNA

Hot-start PCR was performed with KOD Hot Start DNA polymerase (Novagen, Mississauga, ON). The reaction mixture (50 µl total) was set up on ice and included: 5 µl KOD Hot Start Buffer (1X), 3 µl of 25 mM MgSO₄ (final 1.5 mM), 5 µl of 2M dNTPs (final 0.2 mM), 1.5 µl forward primer (final 0.3 mM), 1.5 µl reverse primer (final 0.3 mM), 100 ng of template genomic DNA, 1 µl of KOD Hot Start Polymerase and PCR grade water up to the final volume of 50 µl. The PCR reaction was performed in an Eppendorf MasterCycler Gradient Machine, using the following amplification conditions:

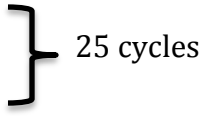
nit:

95°C- 2min
95°C-20 sec
71°C- 10sec
70°C-15 sec
70°C-5 min
end at 4°C



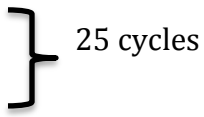
nthAB:

95°C- 2min
95°C-20 sec
67°C-10 sec
70°C-23 sec
70°C-5 min
end at 4°C



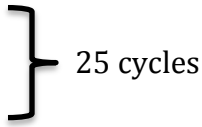
P47K:

95°C- 2min
95°C-20 sec
62°C-10 sec
70°C-22 sec
70°C-5 min
end at 4°C




aux:

95°C- 2min
95°C-20 sec
57°C-10 sec
70°C- 40 sec
70°C-5 min
end at 4°C




iaaM:

95°C- 2min
95°C-20 sec
72°C-10 sec
70°C- 34 sec
70°C-5 min
end at 4°C



pheD:

95°C- 2min
95°C-20 sec
55°C-10 sec
70°C- 21 sec
70°C-5 min
end at 4°C



pET30b(+) Plasmid Isolation and Digestion

pET30b(+) was isolated using the Bio Basic INC. BS414-100 Preps EZ-10 Spin Column Plasmid DNA Kit (VWR#CA99502-170) according to the manufacturer's instructions. Upon plasmid purification, the vector was subjected to a double digestion using NdeI and XhoI restriction enzymes (Fermentas FastDigest®). The following general digestion reaction mixture was prepared and incubated at 37°C for approximately one hour:

X amount of pET30b(+) plasmid isolated
1 μ l of each restriction enzyme per μ g of plasmid DNA
10X FastDigest® Green Buffer
Nuclease-free Water

The digestion mixture was cleaned-up to leave only the intended digestion products using the PROMEGA Wizard® SV Gel and PCR Clean-Up System (REF A9282) according to the manufacturer's instructions

Cloning into pET30b(+)

The PCR products from the above-described PCR reactions were separated by gel electrophoresis on a 0.8% (w/v) agarose gel. The band of interest, corresponding to each of the genes (*nit*, *nthAB*, *P47K*, *aux*, *iaaM*, *pheD*) was excised from the gel and purified using PROMEGA Wizard® SV Gel and PCR Clean-Up System (REF A9282) according to the manufacturer's instructions. Following gel purification, the fragment was double digested with NdeI and XhoI (Fermentas FastDigest®) to produce the sticky ends compatible with the digested pET30b(+) vector. The digestion mixture was cleaned-up using the PROMEGA Wizard® SV Gel and PCR Clean-Up System (REF A9282), to remove any unwanted digestion fragments and residual 10X FastDigest® Green Buffer. The desired digested fragments were then cloned into the pET30b(+) vector. A molar ratio of 3:1 vector:insert was used to clone the fragment into the plasmid vector. The amount of vector and insert DNA after digestion and purification was determined using a Nanodrop Spectrophotometer ND-1000 V3.8.1. The ligation reaction was set-up using T4 DNA Ligase system (Promega, Catalog #M1801) in the following manner:

100 ng of the digested pET30b(+)
Corresponding amount of the digested insert fragments (*nit*, *nthAB*, *p47K*, *aux*, *iaaM*,
pheD)
10X ligase buffer
1 μ l of T4 DNA Ligase
X ml of Nuclease-free water

Up to final volume of 10-20 μ l

The ligation mixture was incubated at 4°C overnight, then transformed into *E. coli* DH5a (Invitrogen) as described in the “General Protocols” section.

Post-transformation, several random colonies were picked and screened for the presence of the insert. Since this was a double-digest cloning, the orientation of the insert was already determined. Plasmid DNA was extracted from these colonies (refer to “General Protocols” section) double digested with NdeI and XhoI (Fermentas FastDigest®) and the products were run on a 0.8% (w/v) agarose gel. When the insert is present, two bands are visible, one corresponding to the size of the insert (*nit* = 924 bp, *nthAB*= 1305 bp, *P47K*= 1224 bp, *pheD*= 1059 bp, *aux*= 1947 bp, *iaaM*= 1683 bp) and a band corresponding to the size of the linearized vector (5237 bp). When no insert is present, there is only one band visible on the gel, corresponding to the empty linearized vector (5237 bp).

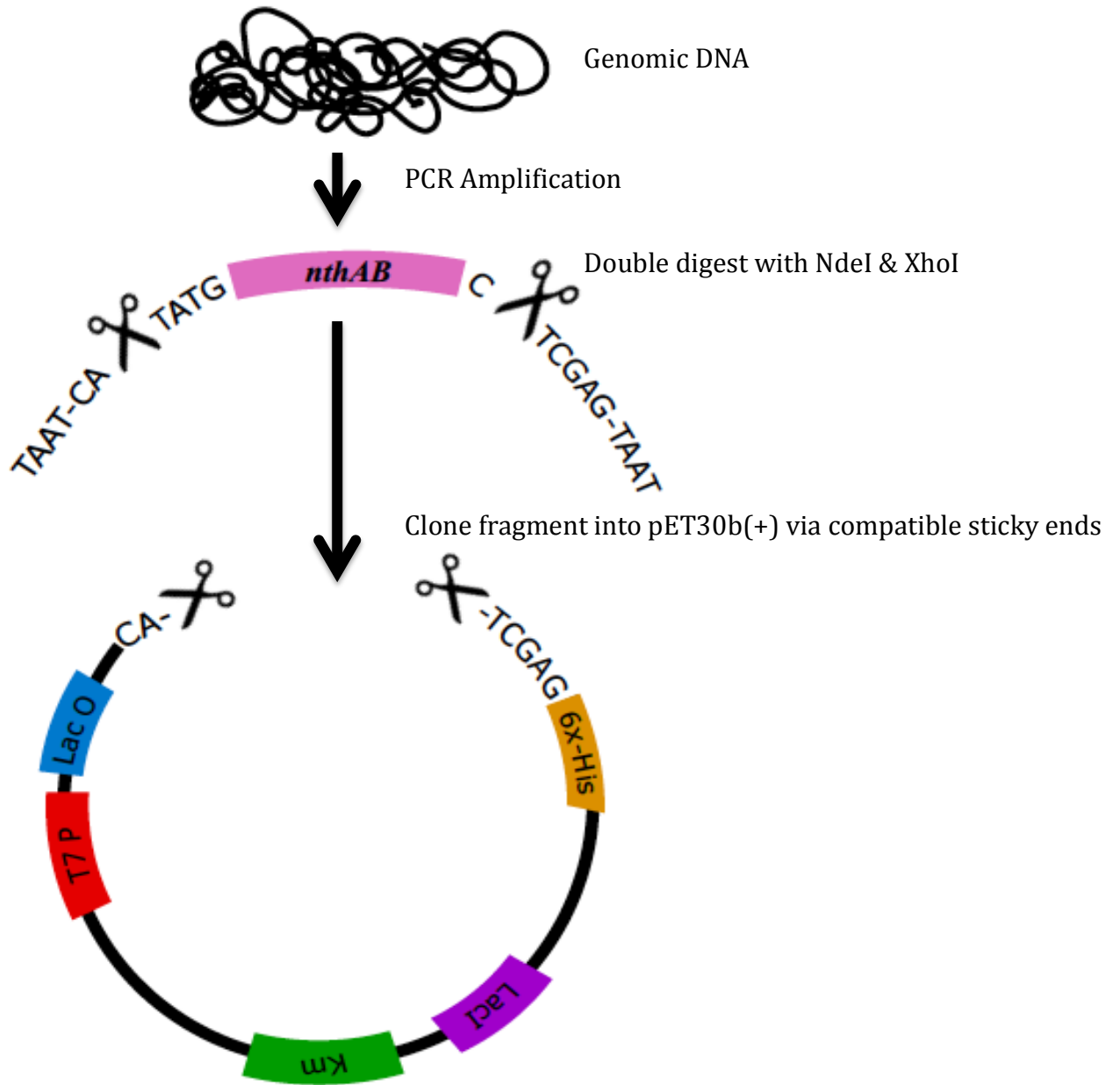


Figure 9. Cloning the *nthAB* gene into the pET30b(+) vector for expression.

PROTEIN EXPRESSION

Transformation into *E. coli* BL21 (DE3)

For the purpose of protein expression, the constructs pETnit, pETnthAB, pET47K, pETAux, pETiaaM and pETpheD were extracted from the *E. coli* DH5a cloning host and re-transformed into the *E. coli* BL21(DE3) expression host (refer to “General Protocols” section). To confirm that these constructs maintained the inserts, plasmid was extracted from the transformed *E. coli* BL21 (DE3) host, double digested with NdeI and XhoI or HindIII (Fermentas FastDigest®) and the products were run on a 0.8% (w/v) agarose gel. Note that in some cases, pETnthAB and pETP47K were co-transformed into the same *E. coli* BL21 (DE3) host cell, for co-expression of NthAB and the putative P47K activator protein together. To confirm that both plasmids (pETnthAB and pETP47K) were taken up together and maintained in the expression host, several random colonies were chosen from the transformation plate and plasmids were isolated from these colonies. Double digestion of the plasmid collection with NdeI and XhoI, resulted in two separate bands on an agarose gel, corresponding to the size of *nthAB* and *P47K*. Moreover, PCR amplification of these two genes from the isolated plasmids of the co-transformed host, reveals two separate PCR products, corresponding to *nthAB* and *P47K*.

Target Protein Expression

To determine whether the recombinant protein is expressed, a small-scale induction protocol was performed, followed by SDS-PAGE analysis. Three, 5 mL LB broth tubes supplemented with 50 µg/mL kanamycin were inoculated with pETnit,

pETnthAB and pET47K respectively and incubated in a 37°C shaking water bath overnight. These are the starter cultures. The following day, three 30 mL fresh LB tubes, supplemented with kanamycin were inoculated with 1 mL of each starter culture, and incubated at 37°C in a shaking water bath, until they reached mid-log phase (OD_{600} of 0.4- 0.8). At this time, 1 mL of culture was taken as an uninduced control. These cells were collected by centrifugation at 2000 x g for 5 minutes, the supernatant was discarded and the pellet was re-suspended in 100 ml of 1X SDS-PAGE loading dye (100 mM TRIS-HCl, pH 6.8, 4% (w/v) SDS, 0.2% (w/v) bromophenol blue, 20% (v/v) glycerol, 200 mM DTT). The uninduced sample was stored at -20°C until SDS-PAGE analysis. The remainder of the culture was induced with 0.1, 0.5 and 1 mM IPTG and grown at 30°C (pETnit) or room temperature (pETnthAB and pETP47K) with shaking for aeration. One mL samples were collected at various time points (1, 3, 6 hour and overnight induction) and processed as described above for the uninduced sample. All of the samples were run on a 10% (pETnit, pETpheD, pETAux, pETiaaM) or 12% (pETnthAB and pETP47K) SDS-PAGE gel as described in the “General Protocols” section.

Determining the Solubility of the Expressed Proteins

To determine whether the recombinant proteins were expressed in the soluble fraction, or aggregated as inclusion bodies in the insoluble fraction, the following protocol was followed: A 5 mL starter culture was prepared of which 1 mL was used to inoculate 30 mL of fresh LB supplemented with 50 µg/mL kanamycin. The culture was grown to mid-log phase ($OD_{600} = 0.4- 0.8$) in a shaking water bath at 37°C. A 1 mL

sample of this uninduced culture was taken, the pellet collected via centrifugation at 2000 x g for 5 minutes and re-suspended in 100 ml of 1X SDS-PAGE loading dye (100 mM TRIS-HCl, pH 6.8, 4% (w/v) SDS, 0.2% (w/v) bromophenol blue, 20% (v/v) glycerol, 200 mM DTT). The sample was stored at -20°C until SDS-PAGE analysis. The remaining culture was induced with 0.1 mM IPTG overnight in a shaking water bath at 30°C (pETnit) or at room temperature (pETnthAB and pETP47K). A 1 mL sample of each induced culture was taken and processed as described above for the uninduced sample. The remaining culture was collected by centrifugation at 2000 x g for 20 min at 4°C. The supernatant was discarded and the cell pellet was re-suspended in 5 mL lysis buffer (50 mM NaH₂PO₄, 300 mM NaCl, 10mM imidazole with 1 mg/mL lysozyme). Lysis buffer is added at a ratio of 5 ml per gram of cells (Kuhn, et al. 2012). This reaction was kept on ice for 30 min, after which it was sonicated 30X for 10 seconds each, with 10 second pauses, at 200W, using a sonic dismembrator (Fischer Scientific, Model 100). The lysate was kept on ice at all times during sonication to avoid overheating and possible protein denaturation. After sonication, the lysate was centrifuged at 8000 x g for 30 minutes at 4°C to separate the soluble and insoluble fractions. The supernatant (soluble fraction) was saved and kept at 4°C, while the pellet (insoluble fraction) was re-suspended in 5 mL of lysis buffer. A 20 µl sample of each fraction (soluble and insoluble) was taken and 4 µl of 5X SDS-PAGE loading dye was added. SDS-PAGE analysis was performed for the uninduced, induced, soluble and insoluble samples (Please refer to “General Protocols” section).

Culture Preparation for Large-Scale Expression and Purification

Two mL of a starter culture grown at 37°C overnight, was used to inoculate 500 mL of fresh LB broth supplemented with 50 mg/mL kanamycin (final concentration). The cultures were grown at 37°C with shaking for aeration, until the OD₆₀₀ reached 0.5. At this point the cultures were induced with 0.1 mM IPTG and incubated at 30°C (pETnit) or room temperature (pETnthAB and pETP47K) overnight. The following day, the cells were collected by centrifugation at 2000 x g for 20 minutes at 4°C. The cell pellet was washed with 20 mL of 50 mM KH₂PO₄ pH 7.5 (gentle vortexing) followed by centrifugation at 2000 x g for 10 minutes at 4°C. This wash step was repeated two more times to remove any IPTG, antibiotic or other media components that may interfere with enzyme assays. The washed pellet was re-suspended in 50 mL of binding buffer (20 mM sodium phosphate, 500 mM NaCl, 20 mM imidazole, pH 7.4) (for His GraviTrap™) and sonicated 30X for 30 seconds each with 10 seconds pauses in between each round. The lysate was kept on ice at all times during sonication. After sonication, the lysate was centrifuged at 10 000 rpm for 30 minutes at 4°C to separate the soluble and insoluble fractions. The soluble fraction was saved at 4°C for His GraviTrap™ purification.

Culture Preparation for Small-Scale Expression and Purification

One mL of a starter culture grown at 37°C overnight, was used to inoculate 100 mL of fresh LB broth supplemented with 50 mg/mL kanamycin. The cultures were grown at 37°C with shaking, until the OD₆₀₀ reached 0.5. At this point the culture was induced with 0.1 mM IPTG and incubated at 30°C (pETnit) or room temperature (pETnthAB and

pETP47K) overnight. The following day, the cells were collected by centrifugation at 2000 x g for 20 minutes at 4°C. The cell pellet was washed with 10 mL of 50 mM KH₂PO₄ pH 7.5 (with gentle vortexing) followed by centrifugation at 2000 x g for 10 minutes at 4°C. This wash step was repeated two more times to remove any remaining IPTG, antibiotic or other media components. The washed pellet was re-suspended in 10 mL of 50 mM KH₂PO₄ pH 7.5 and sonicated 10-15X for 10 seconds each with 10 seconds pauses in between each round. The lysate was kept on ice at all times during sonication. After sonication, the lysate was centrifuged at 10,000 rpm for 30 minutes at 4°C to remove cell debris and separate the soluble and insoluble fractions. The soluble fraction was saved at 4°C until His SpinTrap™ purification.

PROTEIN PURIFICATION

His GraviTrap™ Purification

The recombinant proteins, which have a C-terminal 6X His-tag, were purified under native conditions using His GraviTrap™ prepacked, single-use gravity-flow column containing precharged Ni Sepharose™ 6 Fast Flow. The protocol was followed according to the manufacturer's instructions (GE Healthcare, UK). This column has a protein binding capacity of 40 mg. The purified protein samples were analyzed by SDS-PAGE.

His SpinTrap™ Purification

The recombinant proteins, which have a C-terminal 6X His-tag were purified under native conditions using His SpinTrap™, which contains Ni Sepharose™ High Performance Medium according to the manufacturer's instructions (GE Healthcare, UK). These prepacked columns are used for rapid, small-scale protein purification, with a protein binding capacity of 750 µg. Note that for nitrilase (Nit) purification, 1mM

dithiothreitol (DTT) was added to the elution and binding buffers. The purified protein samples were analyzed by SDS-PAGE.

PROTEIN DESALTING /BUFFER EXCHANGE

Centrifugal Filter Tubes

Macrosep® Advance Centrifugal Devices (PALL Life Sciences, USA) and Amicon® Ultra Centrifugal Filters (Merck KGaA, Germany) were used for the purpose of buffer exchange and salt removal of the immobilized metal ion affinity chromatography (IMAC) samples from above. The protocol was followed according to the manufacturer's instructions. High salt and imidazole concentrations would interfere with FPLC purification and structural studies and thus had to be removed. Ultracel® 50K MWCO centrifugal devices (Amicon® Ultra-4) were used for Nit desalting, while 10K MWCO Omega Blue (Macrosep®) and 3K Amicon® (500mL) centrifugal devices were used for NthAB and P47K desalting.

Dialysis

Dialysis was also used for salt removal and buffer exchange of the immobilized metal ion affinity chromatography (IMAC) samples. Spectra/Por® molecularporous membrane tubing (Spectrum Medical Industries Inc. USA) was used for protein dialysis. MWCO 12-14,000 membrane was used for Nit dialysis, while MWCO 6- 8,000 membrane was used for NthAB and P47K dialysis (refer to "General Protocols" section).

DENSITOMETRY

Following SDS-PAGE analysis of GraviTrap and FPLC purified samples, densitometry was used to determine the relative purity of the protein. ImageJ 1.46R image analysis software was used to analyze the 1D SDS-PAGE gel images (National Institutes of Health, USA). The SDS-PAGE gels were scanned on a flat bed scanner in grey scale, resolution quality 600 dpi. The black ink intensity values were obtained for each protein band, and the background was subtracted. The values were normalized against control pure bovine serum albumin (BSA) protein band values.

FAST PERFORMANCE LIQUID CHROMATOGRAPHY (FPLC)

Purification by Anion Exchange FPLC

The protein samples that had been previously purified via immobilized metal ion affinity chromatography were further purified by FPLC. Fast Protein Liquid Chromatography (FPLC) purification separates proteins based on their different isoelectric points. A BIORAD Biologic Duo Flow FPLC system with an Econogradient pump and a Quad Tech UV-Vis detector was used. A 1 ml sample was injected onto a Q-column anion exchange column that was previously equilibrated with 20 mM TRIS-HCl pH 8. The column was run at a flow rate of 2 ml /min with monitoring of protein quantity at an absorbance of 280 nm. Proteins were eluted off the column by a 0-100% 1M NaCl linear gradient. One ml fractions were collected, pooled together and analyzed by SDS-PAGE. Prior to FPLC analysis, samples and buffers were filtered through 0.22 mm low protein binding Durapore membrane filters (Millex®-GV, Merck Millipore Ltd, IRL) to ensure they were free of particulate matter.

Native Size Determination by Size Exclusion Chromatography (SEC) FPLC

A HiPrep 26/60 Sephacryl S-300 High Resolution prepacked gel filtration column was used to estimate the native size of the NthAB and Nit proteins (GE Healthcare). The column was connected to a BIORAD Biologic Duo Flow FPLC system. The sample load volume was 1 mL, the flow rate was 0.8- 1.3 mL/min and 50 mM Tris, 150 mM NaCl pH 8 buffer was used for elution. Instructions were followed according to the column Manufacturer (GE Healthcare, 28-4026-53-AE). The following gel filtration standards were used to generate a standard curve: bovine thyroglobulin (670 kDa), ferritin (440kDa), aldolase (158 kDa), chicken ovalbumin (44 kDa) and horse myoglobin (17 kDa) (BIO RAD, Catalog #151-1901 and Pharmacia Catalog no. 17-0441- 01). The lyophilized standards were rehydrated and stored according to the BIO RAD instruction manual. Buffer exchange and desalting to remove imidazole was performed on His GraviTrap™ purified nit and nthAB samples prior to SEC FPLC.

ENZYME CHARACTERIZATION

Activity Assays

The recombinant proteins were tested for their ability to convert a nitrile substrate into its corresponding acid or amide product. Specifically, nitrilase (Nit) was tested for the ability to convert indole-3-acetonitrile (IAN) directly into indole-3-acetic acid (IAA), while nitrile hydratase (NthAB) was tested for the ability to convert indole-3-acetonitrile (IAN) into indole-3-acetamide (IAM).

Enzyme activity was generally assayed in a 1 mL reaction mixture containing the following:

50 µg of purified enzyme (Nit or NthAB)
1 mM IAN substrate
50 mM KH₂PO₄ pH 7.5 buffer
1 mL total volume

The reactions were set-up in 1.5 mL microcentrifuge tubes and incubated at appropriate temperatures and pHs for specific periods of time. The reactions were stopped by adding 100 µl of 1M HCl. The tubes were inverted several times to mix the contents and stored at 4°C until HPLC analysis.

Temperature Optima

To determine the ideal temperature conditions for both nitrilase (Nit) and nitrile hydratase (NthAB) activity, the above mentioned general reaction mixture was set up. The tubes were incubated at various temperatures (20-60°C for Nit) or (4-60°C for NthAB). Reactions were allowed to proceed for 3 hours.

pH Optima

To determine the ideal pH for both nitrilase (Nit) and nitrile hydratase activity (NthAB), the following buffers were used: sodium acetate at pH 5-5.5, sodium citrate at pH 6-6.5, potassium phosphate at pH 7-7.5, Tris-HCl at pH 8-8.5, glycine at pH 9. The above mentioned general reaction mixture was set up in the corresponding pH buffers.

The tubes were incubated at 30°C for nitrilase (Nit) and at room temperature for nitrile hydratase (NthAB) for 3 hours.

Time Curve

The utilization of the indole-3-acetonitrile (IAN) substrate and production of the IAA product by nitrilase (Nit) was monitored over time via HPLC. The general enzyme reaction mixture was prepared and immediately upon adding all the components, a 100 µl sample was removed. This sample represents time = 0 min. The remaining reaction mixture was incubated at 30°C and 100 µl samples were removed periodically at the following times: 15, 30, 60, 120, 180 and 360 minutes.

Optimizing NthAB Activity

To determine whether nitrile hydratase (NthAB) requires the putative P47K activator protein and an iron co-factor to be active, the following reactions were set-up:

50 µg or 100 µg of NthAB
NO iron
NO P47K
1 mM IAN substrate
50 mM KH₂PO₄ pH 7.5
1 mL total volume

50 µg or 100 µg of NthAB
0.001% iron
NO P47K
1 mM IAN substrate
50 mM KH₂PO₄ pH 7.5
1 mL total volume

50 µg or 100 µg of NthAB
NO iron
50 mg P47K
1 mM IAN substrate
50 mM KH₂PO₄ pH 7.5
1 mL total volume

50 µg or 100 µg of NthAB
0.001% iron
50 mg P47K
1 mM IAN substrate
50 mM KH₂PO₄ pH 7.5
1 mL total volume

The reaction mixtures were incubated at room temperature for 3 hours, after which the reaction was stopped as mentioned previously.

Note that 0.001% FeCl₃ was added to the growth culture at the same time as the ITPG was added for induction.

To determine the effect of different enzyme and substrate concentrations on the activity of NthAB, the following reactions were set-up:

100 or 150 µg/mL NthAB
0.5 or 1 mM IAN substrate
50 mM KH₂PO₄ buffer pH 7.5
1 mL total volume

The reaction mixtures were incubated at room temperature for 3 hours, after which the reaction was stopped as mentioned previously.

CONTROLS

To determine whether IAN and IAM are spontaneously converted to IAA, non-

enzymatic controls were set up as 1 mL reactions. For pH controls, 1 mM IAN or IAM was added to sodium acetate at pH 5, sodium citrate at pH 6, potassium phosphate at pH 7, Tris-HCl at pH 8, glycine pH 9 buffers. The tubes were incubated at 30°C for 3 hours. For temperature controls, 1 mM IAN or IAM was added to KH₂PO₄ pH 7.5 buffer. The tubes were incubated at temperatures between 22°C and 55°C for 3 hours. No enzyme was added.

To determine whether the *E.coli* expression host produces an IAN-converting enzyme without expressing the recombinant Nit/NthAB proteins, 100 mL cultures of either non-transformed *E.coli* BL21 (DE3) or *E.coli* BL21 (DE3) transformed with empty pET30b(+) were grown at 37°C until they reached mid-log phase (OD₆₀₀ of 0.4- 0.8). The cultures were induced with 0.1 mM IPTG for 3 hours. Cells were collected by centrifugation at 2000 x g for 20 minutes at 4°C. The cell pellet was washed with 10 mL of 50 mM KH₂PO₄ pH 7.5 followed by centrifugation at 2000 x g for 10 minutes at 4°C. This wash step was repeated twice more. The washed pellet was re-suspended in 10 mL of 50 mM KH₂PO₄ pH 7.5 and sonicated 10-15X for 10 seconds each with 10 second pauses in between each round. After sonication, the lysate was centrifuged at 8000 x g rpm for 30 minutes at 4°C . The soluble fraction was used for the enzyme assay. The reaction mixture (1 mL total volume) consisted of approximately 50 µg of crude protein extract and 1 mM IAN in 50 mM KH₂PO₄ pH 7.5 buffer. The reactions were incubated at 30°C for 3 hours. Samples were stored at 4°C until HPLC analysis.

HPLC ANALYSIS

HPLC analysis was performed at the University of Guelph in the HPLC facility of the Ontario Veterinary College, using a Waters Alliance® 2695 HPLC separations system (Mississauga, ON, Canada) which includes a Waters 2996 photodiode array detector. The system was connected to a PC with Empower 2 software (Waters®, Mississauga, ON, Canada) for data collection and processing. A Sunfire® C18 column (50 mm x 4.6 mm I.D., 2.5 µm, Waters®, Ireland) was connected with a Security Guard C18 guard column (4 mm x 3.0mm I.D., Phenomenex®, Torrance, CA, USA). Gradient HPLC was performed at room temperature using a mobile phase containing (A) water-acetic acid (1% v/v) and (B) acetonitrile-acetic acid (1% v/v). Starting with 80% A, the gradient began at 2 min and reached 60% A at 15 min. The flow rate was 1 mL/min. A 100 µL sample injection volume was used and the eluent was monitored at 280 nm. The retention times observed were 2.3 min for indole-3-acetamide (IAM), 5.2 min for indole-3-acetic acid (IAA), 7.5 min for indole-3-propionic acid (IPA) and 8.4min for indole-3-acetonitrile (IAN), respectively.

MULTIPLE SEQUENCE ALINGMENTS & PHYLOGENETIC ANALYSIS

Multiple sequence alignments were constructed for Nit, NthAB and P47K (activator) protein using MEGA 5.10 Software (Tamura et al., 2011). Nucleotide sequences were translated into amino acid sequences using the web-based software from the EMBL-EBI website <http://www.ebi.ac.uk/Tools/emboss/transeq/>. The amino acid sequence alignment was more conserved because the redundancy in the genetic code was accounted for. Protein Blast searches were performed on the Nit, NthAB and P47K proteins from *Pseudomonas putida UW4* to detect similar amino acid sequences in the

NCBI web site. Only non-redundant coding sequence hits that shared at least 50% identity with the UW4 proteins were included in the alignments. Each alignment was manually refined and the regions that could not be aligned reliably were removed. Maximum-likelihood trees were constructed using MEGA 5.10 Software. The nitrilase (Nit) alignment utilized a WAG substitution model with a gamma distribution and invariant sites (WAG+G+I) (Tamura et al., 2011). The WAG matrix (Whelan and Goldman, 2001) assumes that the process of amino acid replacement is very similar across all positions. To conserve protein function and structure, there are only certain positions that can change (Abascal et al., 2005). Non-uniformity of evolutionary rates among sites is modeled using a discrete gamma distribution (+G) (Nei and Kumar, 2000; Tamura et al., 2011). The WAG+G+I model chosen for this phylogenetic analysis considers a fraction of amino acids to be invariable ('+I') (Reeves, 1992; Yang, 1993). This model was chosen based on the goodness-of-fit to the dataset, which was indicated by the Bayesian information criterion (BIC) and Akaike information criterion (AICc) scores. Models with the lowest BIC scores describe the best substitution pattern (Hurvich and Tsai 1989; Posada and Buckley 2004; Schwarz 1978; Nei and Kumar, 2000; Tamura et al., 2011). The nitrile hydratase a and b subunits both utilized a WAG+G model for maximum likelihood analysis, while the P47K activator protein utilized a JTT + G model. Neighbour-joining and Maximum Parsimony trees were also constructed. One thousand bootstrap replicates were performed to assess the confidence for each clade of the tree based on the proportion of bootstrap trees showing that same clade (Efron et al., 1996).

GENERAL PROTOCOLS

The general protocols described in this section were routinely utilized for cloning and protein analysis.

PREPARATION AND TRANSFORMATION OF COMPETENT *E. COLI*

E. coli cells used in this study were made competent according to a standard protocol (Sambrook and Russel, 2001). Transformation of competent cells was performed using a standard heat-shock method as described by Sambrook and Russel (2001).

DETERMINATION OF PROTEIN CONCENTRATION

Protein concentrations were measured using the Bio-Rad Protein Assay, based on the Bradford (1976) method. The microtiter plate protocol (2.4) was followed according to the Manufacturers instructions (BIO RAD Laboratories).

SODIUM DODECYL SULFATE POLYACRYLAMIDE GEL ELECTROPHORESIS (SDS-PAGE)

Proteins were analyzed on 10 or 12% polyacrylamide gels. The gels were prepared according to protocol #6-7 (Scheppeler et al. 2000). Samples were prepared by adding the appropriate amount of protein and 1X SDS-PAGE loading buffer (10 mL of 5X SDS-PAGE loading buffer contains: 2.5 mL of 1.25M Tris (pH 6.8), 5 mL of 100% glycerol, 1g of SDS, 0.8g DTT, 1 mL of 1% bromophenol blue). The samples were boiled for 2-5 minutes, then cooled to room temperature. After loading the samples, the sample was run at 80 volts through the stacking gel and 150 volts through the separating

gel in 1X electrophoresis running buffer (10X running buffer contains 30g TRIS base, 144g glycine, 10g SDS, H₂O up to 1L). After electrophoresis, the gels were Coomassie-stained to visualize the protein bands (1L of stain contains: 1g Coomassie Blue R250, 100 mL glacial acetic acid, 400 mL methanol, 500 mL deionized H₂O) and destained (1L of destaining solution contains 200 mL methanol, 100 ml glacial acetic acid, 700 mL deionized H₂O) according to protocol #8 (Scheppeler et al. 2000).

DIALYSIS

Protein dialysis for the purpose of salt removal and buffer exchange were performed using Spectra/Por® 1 and 2 molecularporous membrane tubing (Spectrum Medical Industries Inc., USA). Approximately 5 cm of MWCO 12-14,000 membrane was used for Nit dialysis, and 5 cm of MWCO 6- 8,000 membrane was used for NthAB and P47K dialysis. Dialysis was performed according to the manufacturer's instructions found in the Spectrum Product Instruction Manual (SpectrumLabs.com)

RESULTS

CLONING IAA GENES

The putative IAA biosynthesis genes (*pheD*, *iaaM*, *nit*, *nthA*, *nthB*, *aux*) and the activator protein gene *P47K*, were KOD-PCR amplified from *P. putida* UW4 genomic DNA. The forward PCR primers contained an NdeI restriction site, while the reverse primers contained an XhoI site (with the exception of the *pheD* reverse primer which contains a HindIII site). The amplification products were analyzed on agarose gels as seen in Fig. 10. The bands representing amplified IAA biosynthesis genes were extracted from the gel and purified with the PROMEGA Wizard® SV Gel and PCR Clean-Up System (REF A9282). The purified fragments were double digested with NdeI and XhoI/HindIII and then cloned into pET30b(+) via compatible sticky ends. These constructs were transformed into *E. coli* DH5a cloning host and then into the *E. coli* BL21(DE3) expression host. To confirm that the host contains the desired vector+insert, plasmid was isolated and double digested with NdeI and XhoI. The digestion products were analyzed on an agarose gels. Two bands, one corresponding to the size of insert and the other to the size of linearized vector (5237 bp) were observed on the gel (Fig. 11). A third band between 6000-7000bp was also present; this band represents incomplete plasmid digestion products.

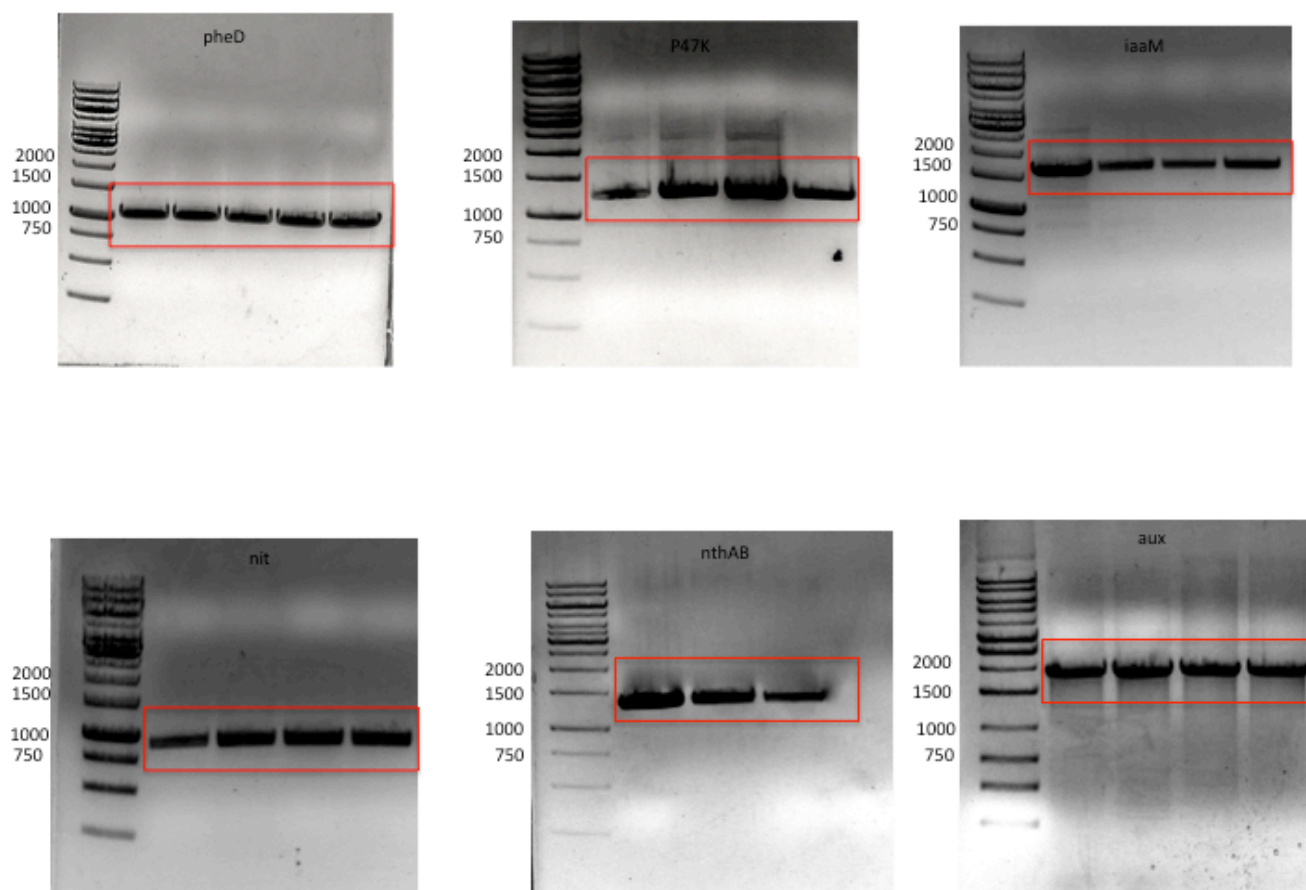


Figure 10. KOD-PCR of putative IAA genes from *P. putida* UW4 genomic DNA. PCR primers contain NdeI (Forward) and XhoI (Reverse) restrictions sites. *pheD*= 1059 bp, *P47K*=1224 bp, *iaaM*= 1683bp, *nit*=924bp, *nthAB*=1305bp, *aux*=1947bp. Thermo Scientific GeneRuler 1 kb DNA ladder was used.

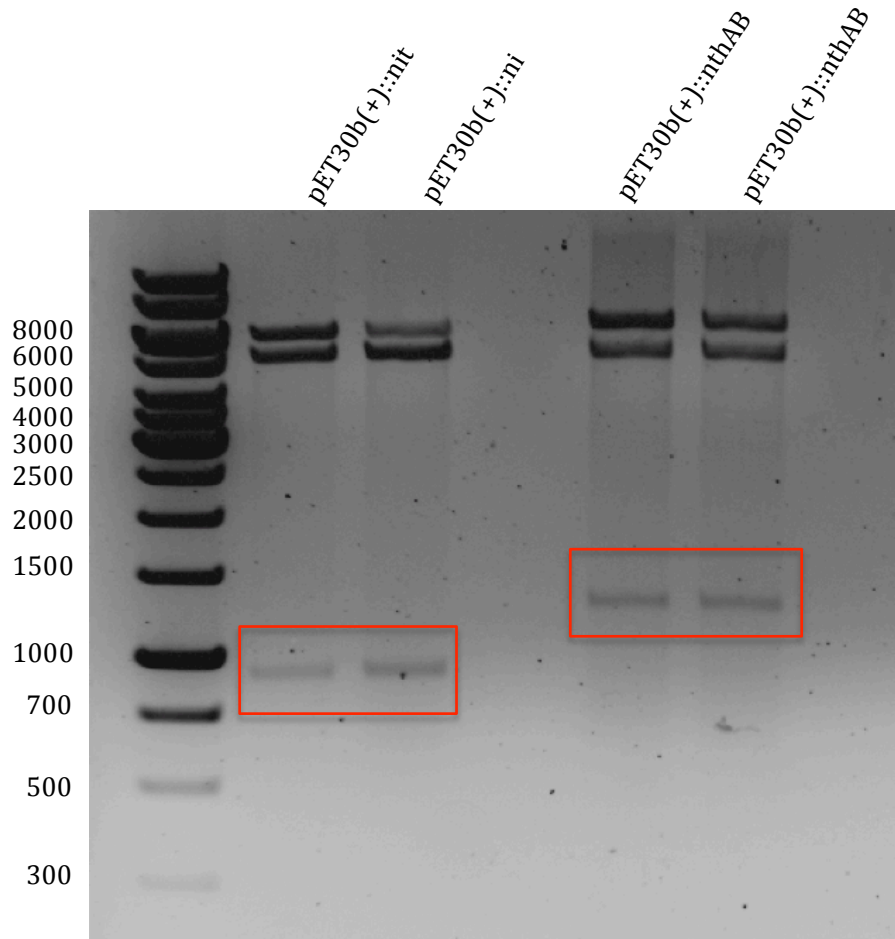


Figure 11. Confirming the cloning of *nit* and *nthAB* into pET30b(+) by double digestion of plasmid DNA with NdeI + XhoI. The bands within the red rectangles correspond to the amplified and cloned inserts (*nit*=924 bp and *nthAB* =1305 bp). The upper bands represent incomplete digestion products. VWR 1 kb DNA ladder was used.

DETERMINING IF THE PUTATIVE IAA PROTEINS ARE EXPRESSED AND SOLUBLE

For protein expression, the amplified IAA genes were cloned into the pET30b(+) vector and this construct was then transformed into the expression host *E. coli* BL21 (DE3). Expression cultures were induced with IPTG concentrations of 0.1, 0.5 and 1 mM to determine the ideal induction concentration. To determine the time required for induction, cultures were induced for various times up to 16 hours at both 30°C and room temperature (~22°C). Samples were collected at different times and analyzed by SDS-PAGE. The recombinant proteins are expressed at all of the different IPTG concentrations tested and the amount of protein gradually increases over time (Refer to Fig. 12-15). Uninduced cells and host cells that did not carry the recombinant genes did not show expression of the target proteins.

After determining that the recombinant proteins were well expressed, protein solubility was assessed. For substrate-feeding enzyme assays and structural studies, the recombinant protein must be expressed in the soluble active form. After separating the soluble and insoluble fractions and examining them by SDS-PAGE, it was evident that the majority of the expressed proteins were in the insoluble form. However, in some instances a small amount of protein was soluble and was able to be purified. Nitrilase (Nit) had a larger fraction of soluble protein compared to nitrile hydratase (NthAB). In an attempt to maximize soluble expression, other culture conditions were tested. These conditions included decreasing the induction temperature to 15°C, inducing expression later in the growth phase, decreasing the induction time and changing the expression host

to *E. coli* Lemo21(DE3), which offers the possibility of tunable expression by adding the sugar L-rhamnose. L-rhamnose controls the level of lysozyme (*lysY*), the natural inhibitor of T7 RNA polymerase (New England BioLabs Inc). Notwithstanding these modifications, the recombinant proteins were still found mostly in the insoluble fraction.

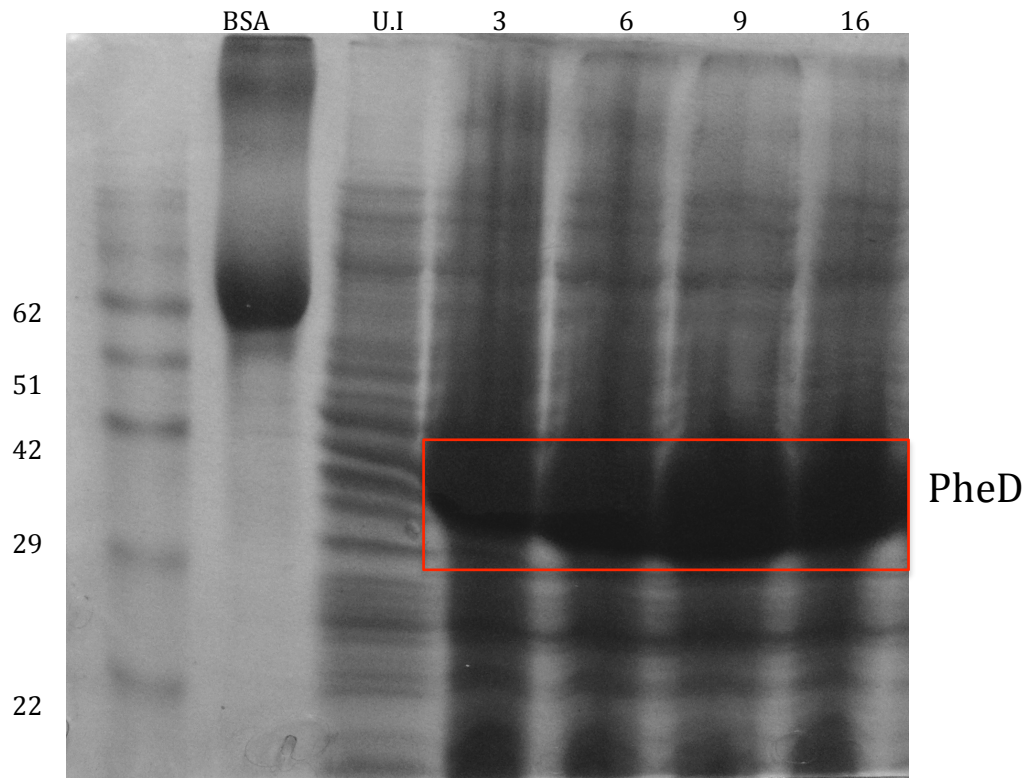


Figure 12. Examining PheD protein expression with SDS-PAGE. The culture was induced with 0.1 mM IPTG and 1 mL samples were taken at various time points between 3-16 hours. The protein ladder on the left side is marked in kDa. Protein is efficiently expressed at this IPTG concentration. U.I. = uninduced sample, BSA=loading control

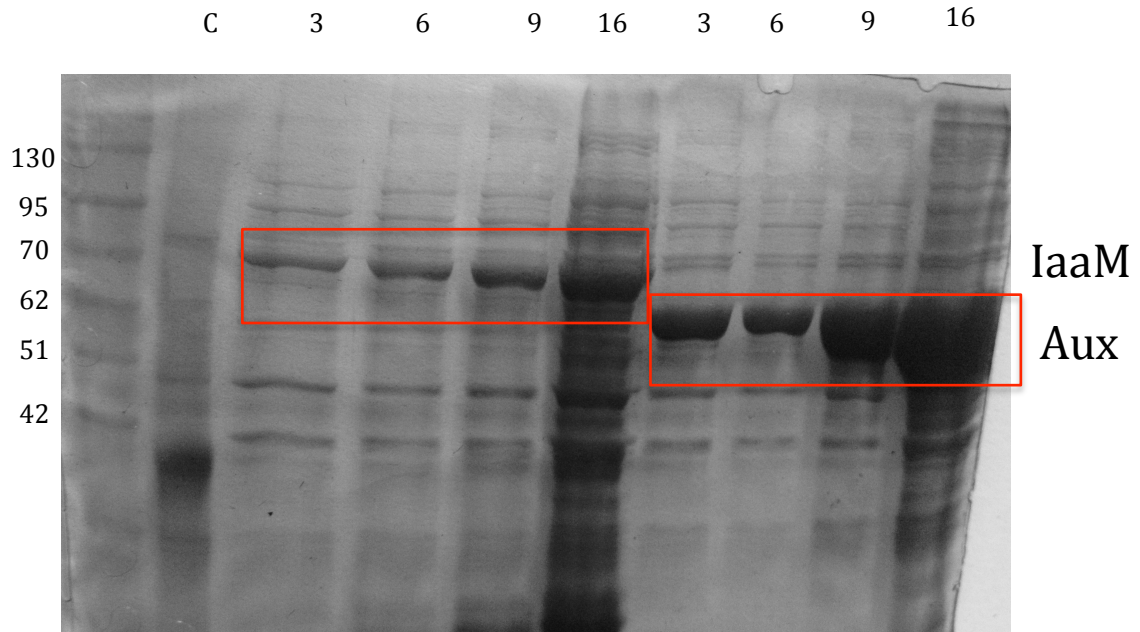


Figure 13. Examining IaaM and Aux protein expression with SDS-PAGE. The culture was induced with 0.1 mM IPTG and 1 mL samples were taken at various time points between 3- 16 hours. The protein ladder on the left side is marked in kDa. Protein is efficiently expressed at this IPTG concentration and increases proportionally over time. C= loading control

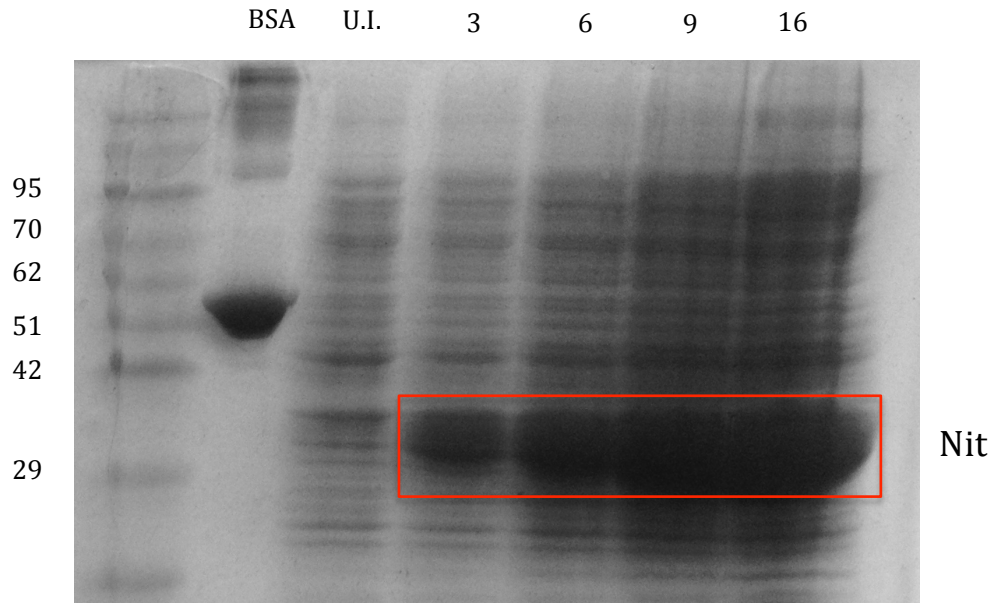


Figure 14. Examining Nit protein expression with SDS-PAGE. The culture was induced with 0.1 mM IPTG and 1 mL samples were taken at various time points between 3- 16 hours. The protein ladder on the left side is marked in kDa. Protein is efficiently expressed at this IPTG concentration and increases proportionally over time. U.I. = uninduced sample, BSA=loading control

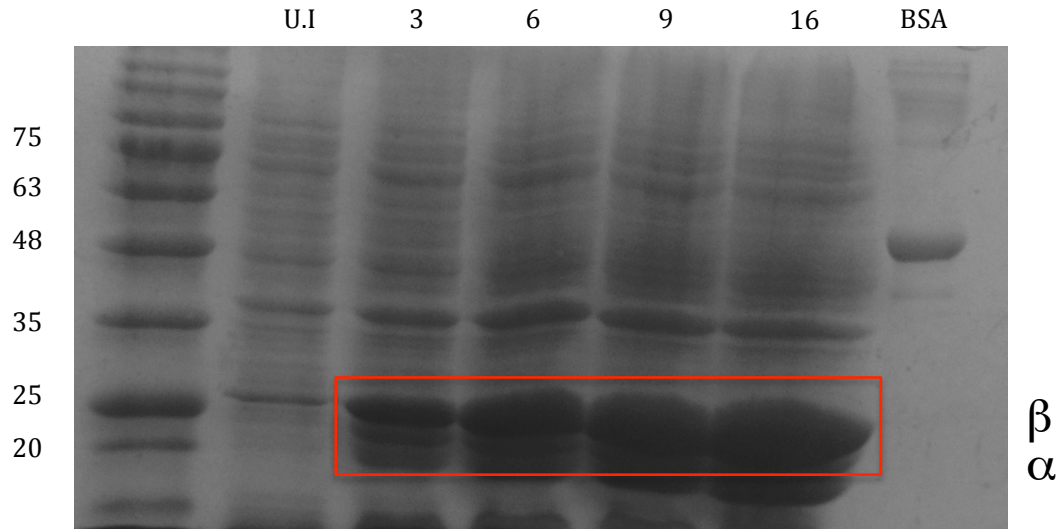


Figure 15. Examining NthAB protein expression with SDS-PAGE. The culture was induced with 0.1 mM IPTG and 1 mL samples were taken at various time points. The protein ladder on the left side is marked in kDa. Protein is efficiently expressed at this IPTG concentration and expression increases proportionally over time. U.I. = uninduced sample, BSA=loading control

PROTEIN PURIFICATION

Although all the putative recombinant IAA-biosynthesis proteins were over expressed in *E. coli* BL21, only Nit and NthAB were purified for enzyme assays. Both Nit and NthAB recombinant proteins were expressed in the soluble form and both were predicted to utilize the same IAN substrate, thus they were chosen for purification and enzyme assays. Although the majority of recombinant protein appeared as insoluble aggregated forms, traces of soluble proteins were detected. A scaled up expression protocol, utilizing a larger culture, allowed for enough soluble protein to be purified and used in enzyme assays. Denaturing conditions could have been used to process the insoluble inclusion bodies, however, in order to maintain active proteins, non-denaturing conditions were preferred.

The recombinant proteins were expressed with a 6X His-tag on the C-terminal end. This allowed for purification by His SpinTrap™ and His GraviTrap™ Ni Sepharose columns. The 32.9 kDa Nit, 22.3 kDa NthAB a-subunit, 24.7 NthAB b-subunit and 45.5 kDa P47K activator proteins are shown on an SDS-PAGE gel after His-tag purification in Figure 16. The nitrilase protein was further purified by anion exchange FPLC to obtain a higher purity (Figure 17).

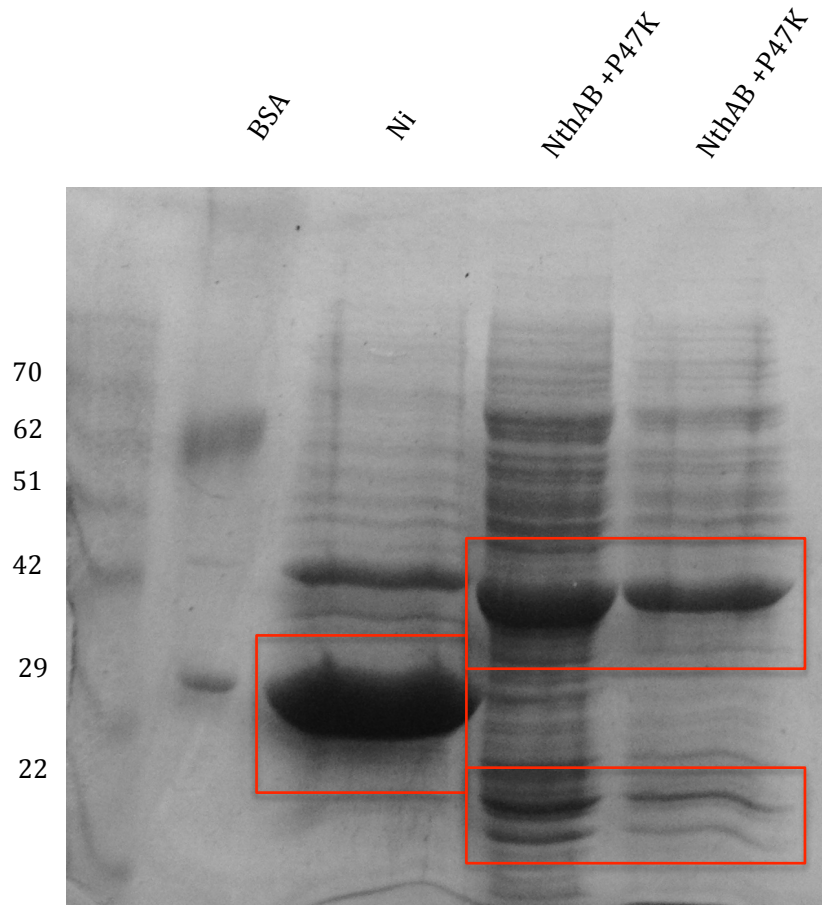


Figure 16. SDS-Page of Nit, NthAB and P47K (putative activator) proteins after His SpinTrap purification. BSA= loading control.

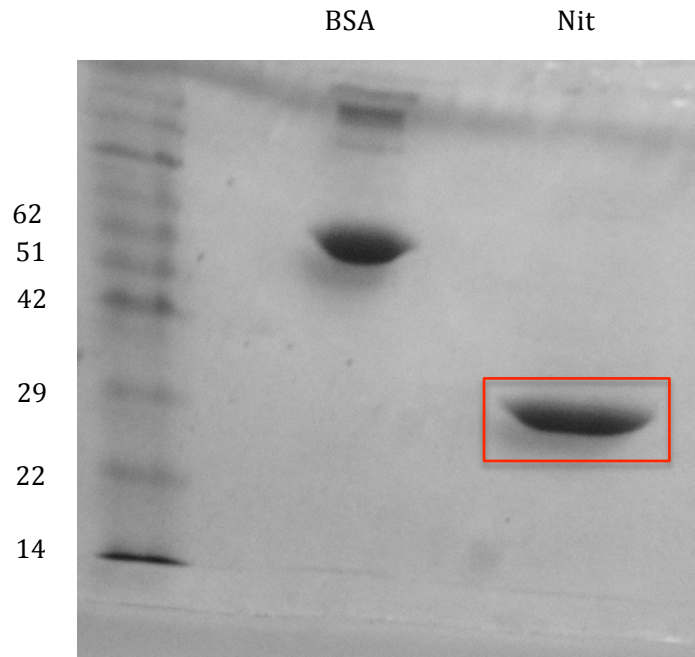


Figure 17. SDS-PAGE of Nit protein after anion exchange FPLC purification. BSA= loading control.

DETERMINING THE NATIVE SIZE OF PROTEINS

FPLC with a gel filtration size exclusion chromatography column was performed in order to determine the native size of nitrilase (Nit) and nitrile hydratase (NthAB) proteins. Five gel filtration standard proteins were used to produce a standard curve (Figure 20). Blue dextran (MW= 2000 kDa) was used to determine the void volume of the column. Nitrilase (Nit) was recovered in eight elution fractions which were pooled together, concentrated in an Ultracel® 50K MWCO centrifugal device and analyzed by SDS-PAGE (Figure 18). From the standard curve (Figure 20) the estimated size of native nitrilase is approximately 470 kDa, i.e. it is an oligomer of at least 15 subunits. The molecular mass of the individual subunit is ~ 32.9 kDa as calculated by ExPASy software and as estimated from the calibration curve (Figure 19). The predicted size of native nitrile hydratase is between 450-550 kDa, suggesting that it is also an oligomer. The molecular mass of the individual a and b subunit is 22.3 kDa and 24.7 kDa respectively.

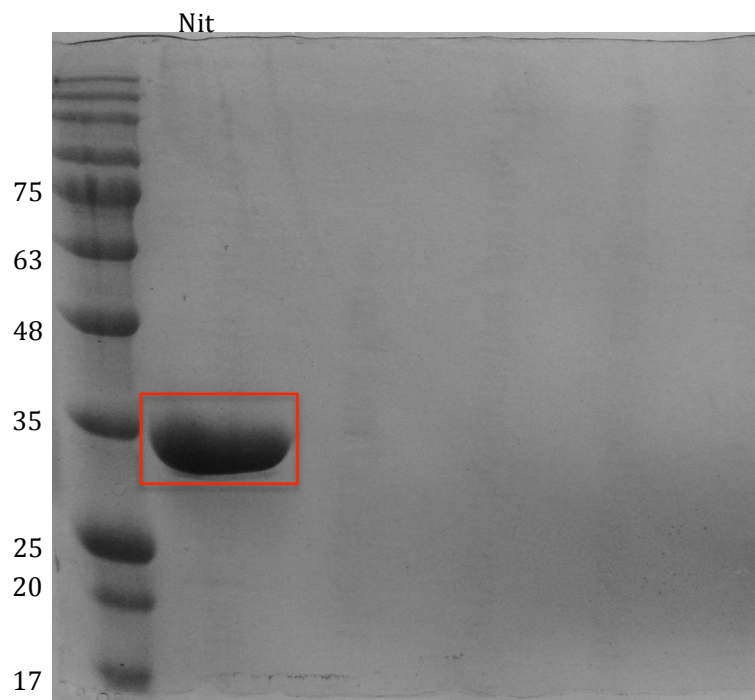


Figure 18. SDS-PAGE of Nit protein after SEC FPLC. Fractions #50-57 were collected and pooled together. The band highlighted in red corresponds to a 32.9 kDa Nit subunit.

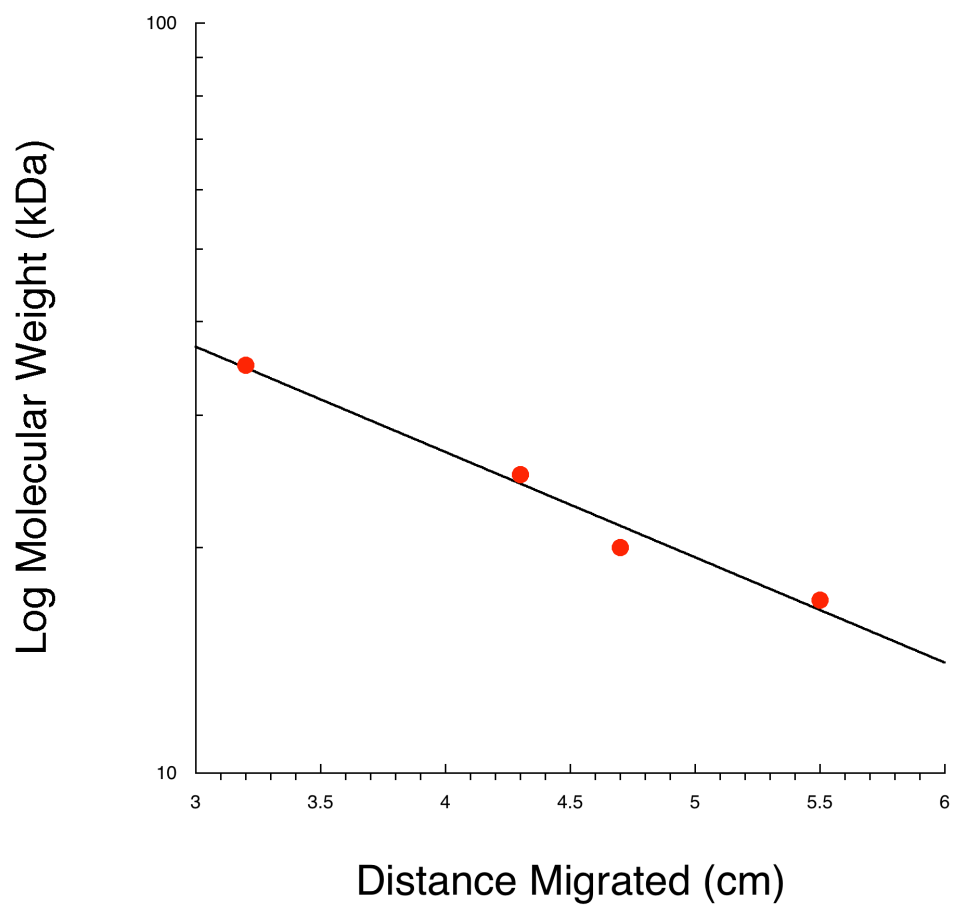


Figure 19. SDS-PAGE Protein Molecular Weight Calibration Curve. The Y-axis represents the log molecular weight of the protein ladder standards. The x-axis represents the distance that the proteins migrated in the SDS-PAGE.

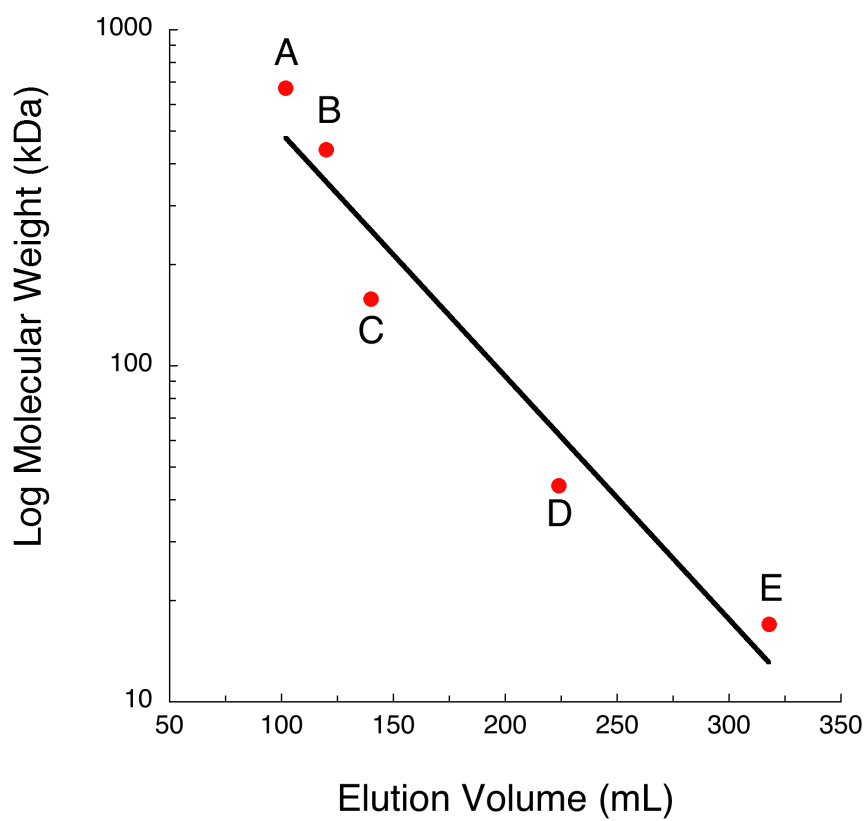


Figure 20. Size Exclusion Gel Chromatography Protein Standard Curve. A= bovine thyroglobulin (670kDa), B= Ferritin (440kDa), C= Aldolase (158kDa), D= chicken ovalbumin (44 kDa), horse myoglobin (17 kDa).

CONTROLS

Negative controls were performed to confirm that IAN is not spontaneously converted to IAM or IAA. Likewise spontaneous conversion of IAM to IAA was investigated. Different temperatures and pHs, similar to those used in enzyme activity studies were tested. The IAN substrate shows no spontaneous conversion at any of the temperatures or pHs tested, while IAM shows a small amount (<2%) of spontaneous conversion into IAA at the temperatures and pHs tested with the exception of pH 6 (Table 3 and 4). This spontaneous conversion only occurs at high concentrations of IAM (1 mM).

Negative controls were also performed to test whether the *E. coli* expression host produces an enzyme capable of converting the IAN substrate into IAM or IAA. These controls confirm that the activity observed in the enzyme assays is all attributable to the expression of the recombinant Nit or NthAB enzymes from *P. putida* UW4. Crude protein extracts from nontransformed *E. coli* BL21 (DE3) or *E. coli* BL21 (DE3) transformed with empty pET30b(+) vector did not show any activity with the IAN substrate (Table 5).

Table 3. Spontaneous, non-enzymatic conversion of IAN into either IAM or IAA, as well as conversion of IAM into IAA, at different temperatures. Initial IAN concentration = 1 mM.

Temperature (°C)	[IAN] mM	[IAM] mM	[IAA] µg/mL
30	1	0	0
40	1	0	0
45	1	0	0
50	1	0	0
55	1	0	0
22	0	1	1.37
30	0	1	3.42
40	0	1	1.51
45	0	1	2.07
50	0	1	1.51
55	0	1	1.3

Table 4. Spontaneous, non-enzymatic conversion of IAN into either IAM or IAA, as well as conversion of IAM into IAA, at different pH values. Initial IAN concentration = 1 mM.

pH	[IAN] mM	[IAM] mM	[IAA] µg/mL
5	1	0	0
6	1	0	0
7	1	0	0
8	1	0	0
9	1	0	0
5	0	1	0.65
6	0	1	0
7	0	1	1.70
8	0	1	0.30
9	0	1	0.67

Table 5. Testing crude extracts from non-transformed *E. coli* BL21(DE3) and *E. coli* BL21(DE3) transformed with the empty pET3-b(+) vector for the ability to convert the IAN substrate into IAM or IAA. Triplicates were performed.

Sample	IAM ($\mu\text{g/mL}$)	IAA ($\mu\text{g/mL}$)	IAN ($\mu\text{g/mL}$)
<i>E. coli</i> BL21 (DE3)	-	-	251.0
<i>E. coli</i> BL21 (DE3)	-	-	181.0
<i>E. coli</i> BL21 (DE3)	-	-	166.0
<i>E. coli</i> BL21 (DE3):: pET30b(+)	-	-	173.0
<i>E. coli</i> BL21 (DE3)::pET30b(+)	-	-	187.0
<i>E. coli</i> BL21 (DE3)::pET30b(+)	-	-	195.0

ENZYME CHARACTERIZATION

The conversion of the IAN substrate into the IAM and IAA products by Nit over time was monitored by HPLC (Figure 21). The amount of both products increased with time. There is approximately three times more IAM formed than IAA at all the time points tested. The reaction was allowed to progress for up to 48 hours and both IAM and IAA continued to accumulate to 18.9 $\mu\text{g/mL}$ and 6.1 $\mu\text{g/mL}$ respectively (data not shown). These results indicate that the nitrilase enzyme is slow acting and stable at 30°C.

The effects of temperature and pH on the activity of Nit and NthAB were also investigated. Enzyme assays included 50 $\mu\text{g/mL}$ of each respective enzyme and 1 mM of the IAN substrate. The formation of products was analyzed by HPLC. Figure 26. shows an HPLC chromatogram of the NthAB assay products at 22°C. Nit was observed to be most active at 50°C (Figure 22) and pH 6 (Figure 23). Three to five times more IAM is produced than IAA. NthAB is most active at 4°C (Figure 24) and pH 7.5 (Figure 25).

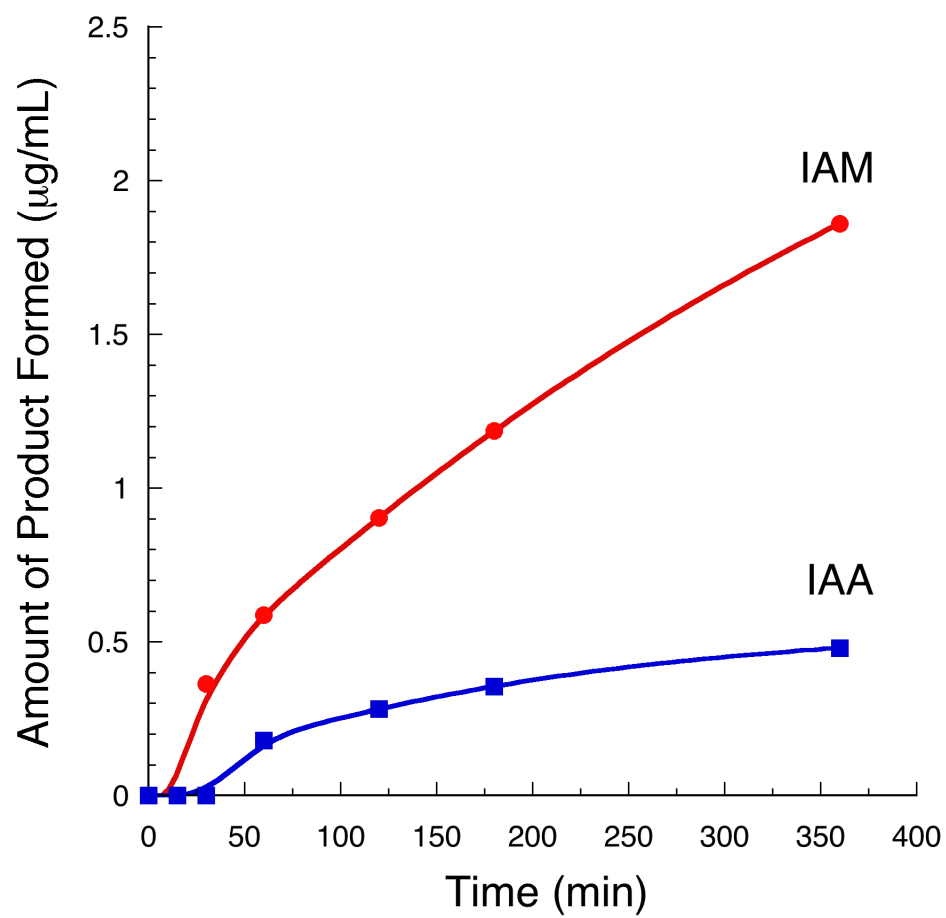


Figure 21. Nit activity over time. The amounts of both IAM and IAA increase over time.

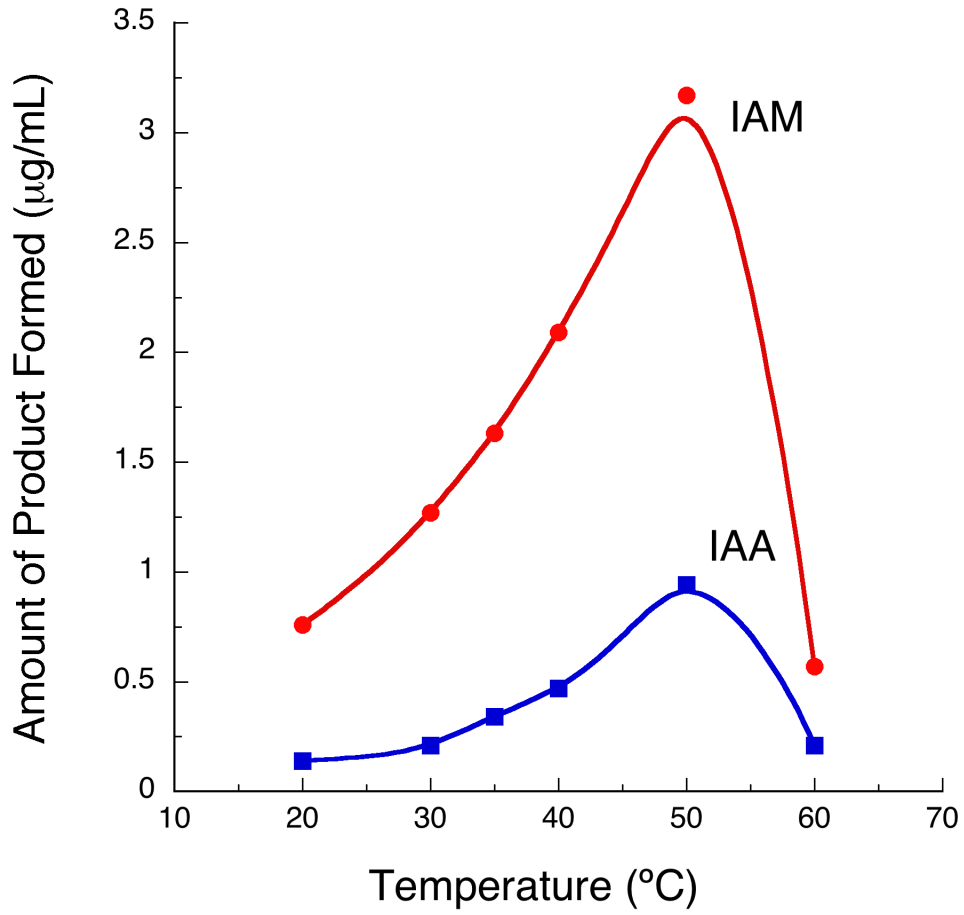


Figure 22. Temperature rate profile of Nit from *P. putida* UW4.

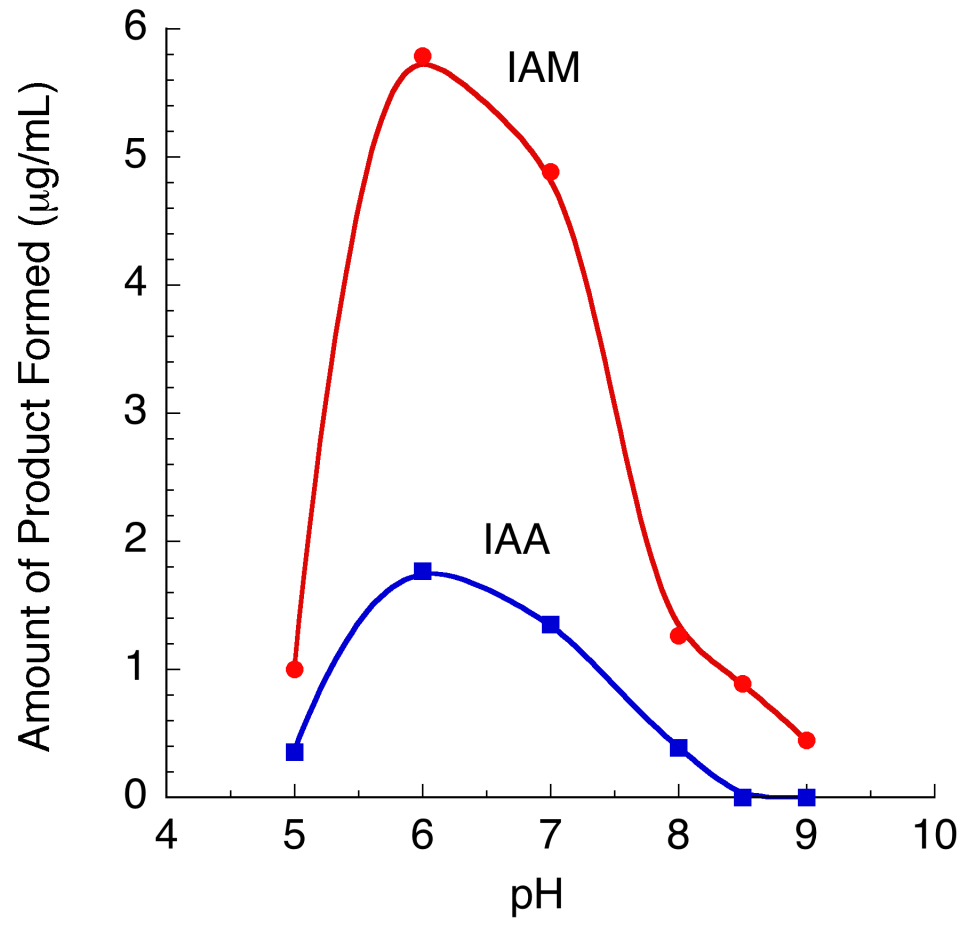


Figure 23. pH – rate profile of Nit from *P. putida* UW4.

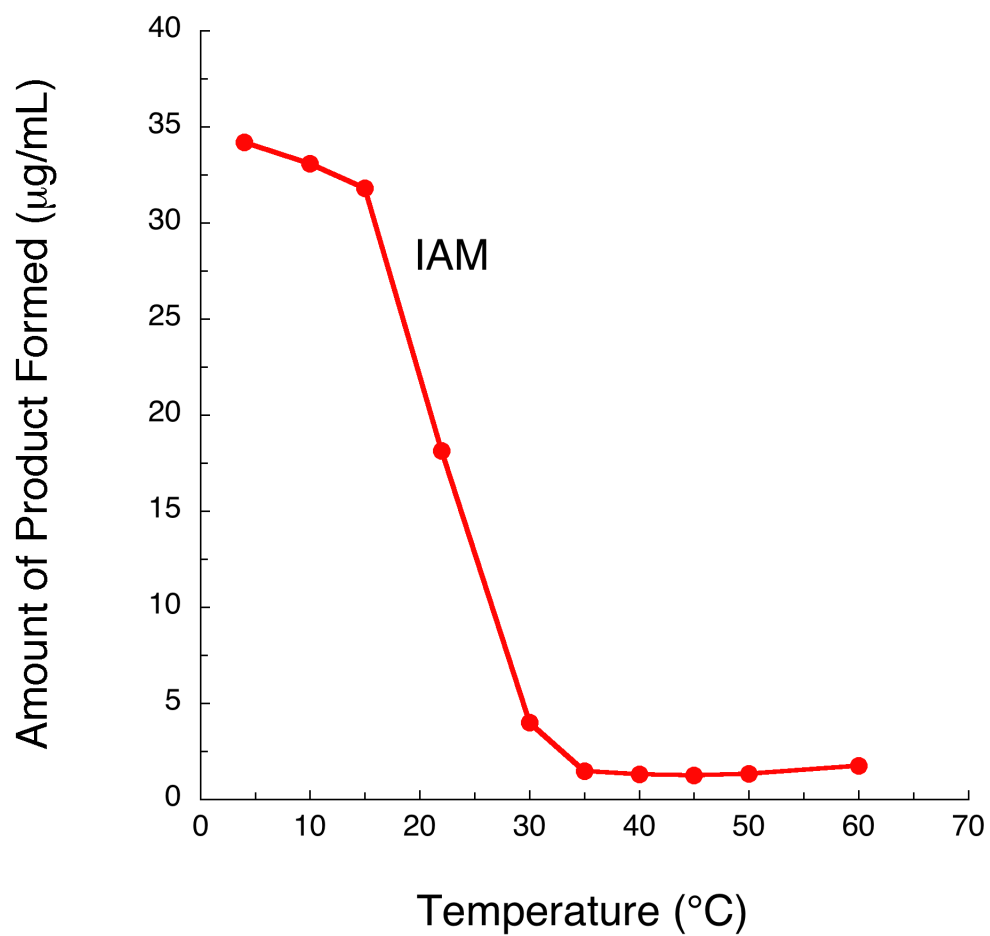


Figure 24. Temperature rate profile of NthAB from *P. putida* UW4.

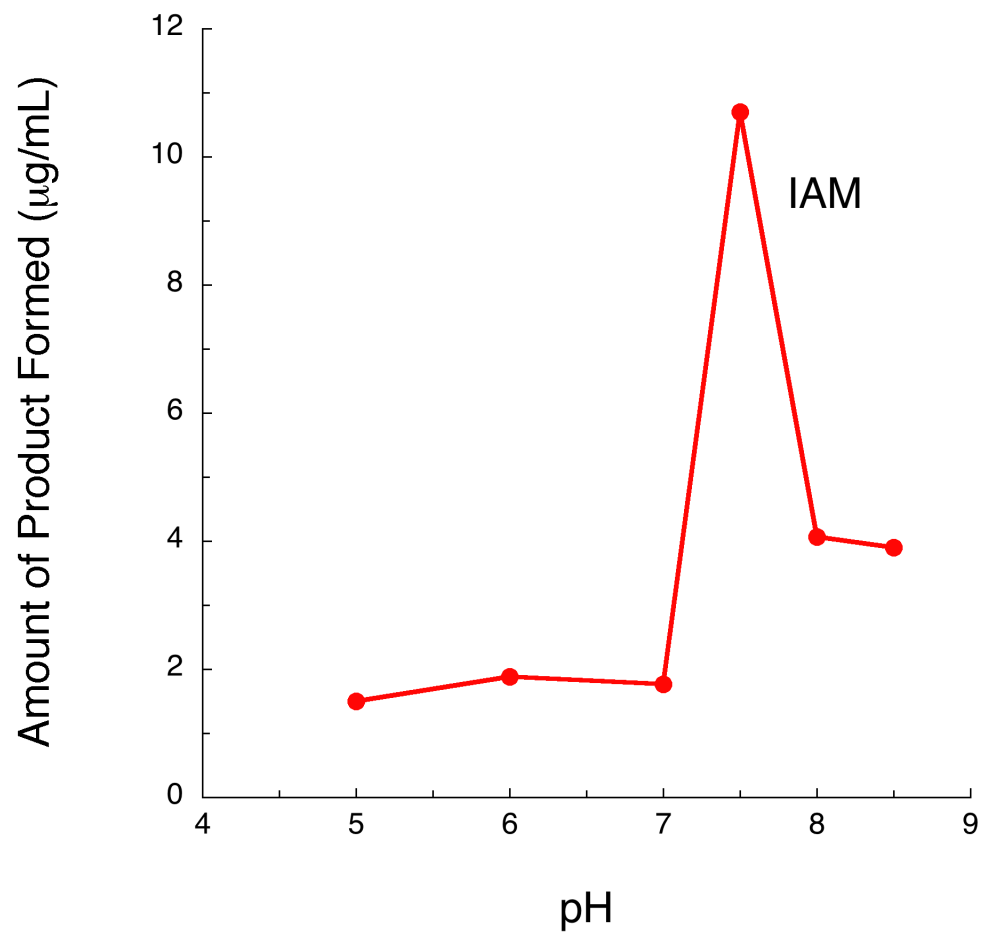


Figure 25. pH – rate profile of NthAB from *P.putida* UW4.

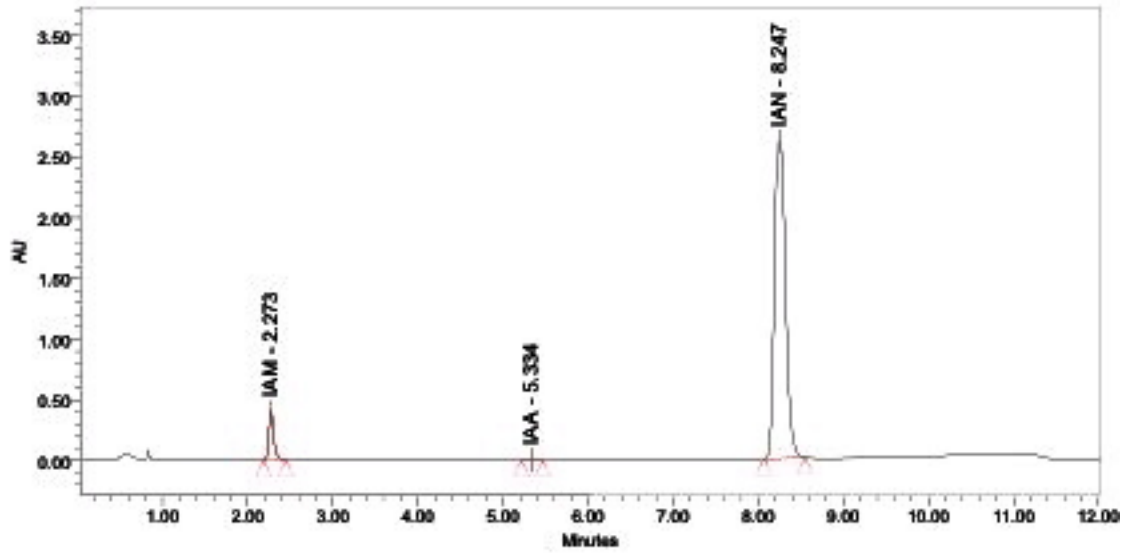


Figure 26. HPLC separation of NthAB assay products at room temperature. The peaks correspond to 18.15 $\mu\text{g/mL}$ IAM, 0.148 $\mu\text{g/mL}$ IAA and 246 $\mu\text{g/mL}$ of IAN.

OPTIMIZING NthAB ACTIVITY

P. putida UW4 NthAB is a metalloenzyme with a nonheme iron atom in its catalytic center. This enzyme may be linked to a putative P47K activator protein, which is found directly downstream of the *nthAB* β -subunit gene. Therefore, the dependence of the enzyme on the iron co-factor and the activator protein was investigated. Cultures expressing both NthAB and P47K (co-transformed) or just NthAB, either in the presence or absence of iron was tested for activity. These enzyme assays were performed at room temperature ($\sim 22^{\circ}\text{C}$) and a pH of 7.5. Iron (0.001% FeCl_3) was added to the expression culture as the bacterium was being induced. The results show that NthAB is active in the absence of iron and activator protein. However, when iron is added, the activator protein was required for NthAB to be active (Table 6).

In addition, the effect of different concentrations of NthAB enzyme and IAN substrate on activity was investigated. At a constant NthAB concentration, a higher IAN substrate concentration resulted in more IAM product being formed. At a constant level of IAN substrate, a higher NthAB enzyme concentration resulted in more product being formed (Table 7).

Table 6. Determining whether the Fe co-factor and P47K activator protein are needed for NthAB activity. Two different concentrations of NthAB protein were tested (50 and 100 $\mu\text{g}/\text{mL}$) for the ability to convert IAN substrate into IAM product.

Sample	[Enzyme] $\mu\text{g}/\text{mL}$	0.001% Fe (+/-)	P47K Activator (+/-)	[IAN] mM	[IAM] ($\mu\text{g}/\text{mL}$)	[IAA] $\mu\text{g}/\text{mL}$
NthAB	50	-	-	1	76.25	0
NthAB	100	-	-	1	150.23	0
NthAB	50	+	-	1	0	0
NthAB	100	+	-	1	0	0
NthAB	50	-	+	1	1.83	0
NthAB	100	-	+	1	12.6	0
NthAB	50	+	+	1	2.31	0
NthAB	100	+	+	1	41.02	0

Table 7. NthAB activity assay at different concentrations of enzyme (100 or 150 $\mu\text{g}/\text{mL}$) and substrate (0.5 or 1 mM). The production of both IAM and IAA products was monitored by HPLC.

[NthAB] $\mu\text{g}/\text{mL}$	[IAN] mM	[IAM] $\mu\text{g}/\text{mL}$	[IAA] $\mu\text{g}/\text{mL}$
100	0.5	102.9	0.583
100	1	114.4	0.647
150	0.5	124.2	0.518
150	1	158.7	1.148

IAA QUANTIFICATION

The amount of IAA produced by *P. putida* UW4 when supplemented with 0, 250 or 500 $\mu\text{g/mL}$ of tryptophan was analyzed by HPLC. IAA is secreted out of the bacterial cells into the culture media and can then be extracted using ethyl acetate. Table 8. shows triplicate measurements of IAA produced and secreted by UW4 . When tryptophan is not added, IAA is not detectable. Tryptophan is a precursor of IAA biosynthesis, and thus is required for production. On average, *P. putida* UW4 produces 3.05 $\mu\text{g/mL}$ and 3.17 $\mu\text{g/mL}$ of IAA when supplemented with 250 and 500 $\mu\text{g/mL}$ tryptophan respectively (Table 8). A known amount of IPA is added to the culture media prior to ethyl acetate extraction as an internal standard. This allows for quantification of IAA and determining the efficiency of the extraction process. Figure 28. shows a chromatogram of an IAA fraction from one of the cultures supplemented with 500 $\mu\text{g/mL}$ tryptophan. IAM, IAA, IPA and IAN standards (Sigma) were used to generate a standard curve. Figure 27. shows HPLC separation of these standards. IAM elutes first, while IAN has the highest retention on the column.

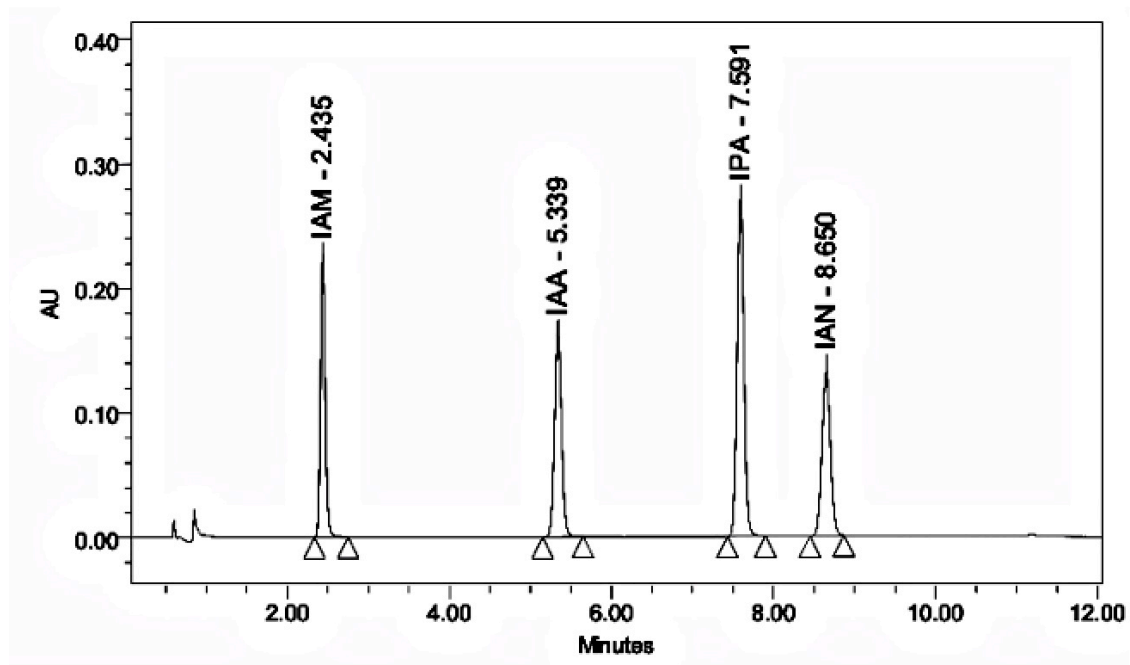


Figure 27. HPLC separation of a mixture of four standards (IAM, IAA, IAN 10 $\mu\text{g/mL}$, IPA 20 $\mu\text{g/mL}$). The injection volume is 100 μl . These standards were used to generate standards curves for IAA quantification.

Table 8. The amount of IAA present in the ethyl acetate extract of *P. putida* UW4 culture solution supplemented with 0, 250 or 500 $\mu\text{g/mL}$.

Replicate #	[Tryptophan] $\mu\text{g/mL}$	[IAA] $\mu\text{g/mL}$
1	0	0
2	0	0
3	0	0
1	250	3.54
2	250	2.31
3	250	3.31
1	500	3.70
2	500	2.84
3	500	2.96

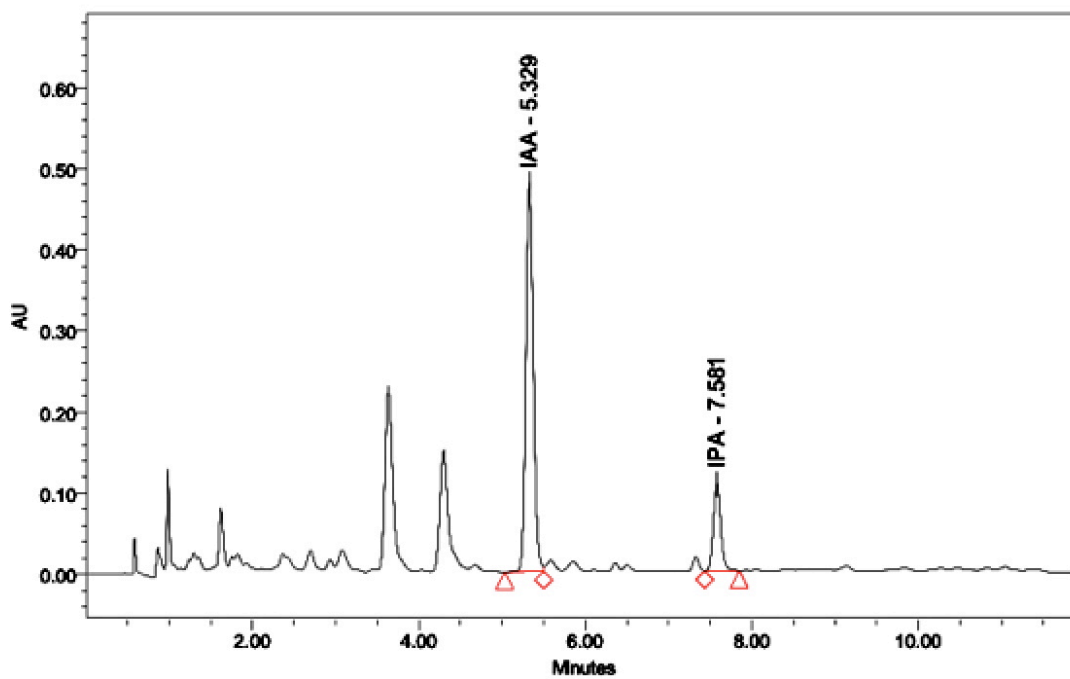


Figure 28. HPLC separation of an IAA fraction from an ethyl acetate extract of *P. putida* UW4 culture solution. The culture was supplemented with 500 $\mu\text{g}/\text{mL}$ tryptophan (replicate #1). IPA was added as an internal standard.

NITRILASE MOTIFS

Sharma and Bhalla (2012), manually determined four groups of conserved motifs that can be used to distinguish between aromatic and aliphatic nitrilases. These motifs were determined based on conserved regions in a multiple sequence alignment of aliphatic and aromatic nitrilases, using the Multiple EM for Motif Elicitation (MEME) software tool. ScanProsite, PRATT and Gblocks sequence pattern analysis tools further validated the identified motifs (Sharma and Bhalla, 2012). In this study, a multiple sequence alignment of bacterial, fungal and plant nitrilase amino acid sequences retrieved from the NCBI protein database was constructed. The aligned sequences share at least 50% identity with *P. putida* UW4 nitrilase. A motif search revealed that the UW4 nitrilase contains all four of the manually designed motifs reported for aromatic nitrilases. The Glu-Lys-Cys catalytic triad was identified in all of the sequences examined and each of the first three motifs have one amino acid of this active site (E-K-C). The four motif patterns in UW4 nitrilase were found to be between positions 40-50, 127-139, 165-178, 204-212 respectively. This is in agreement with the expected positions for aromatic nitrilase motifs as described by Sharma and Bhalla, 2012. Table 9. lists the motifs identified in the UW4 nitrilase.

Table 9. Nitrilase Motif Patterns. Letters (designating specific amino acid residues) in [] represent variable sites. Bold letters represent the catalytic triad (**E-K-C**). *P. putida* UW4 motifs are close to those manually determined for aromatic nitrilases by Sharma and Bhalla 2012.

Type of Nitrilase	Manually Designed Motif	<i>P. putida</i> UW4 Nitrilase Motif
Aliphatic	[FL]-[ILV]-[AV]-F-P- E -[VT]-[FW]-[IL]-P-[GY]-Y-P-[WY]	
Aliphatic	R-R- K -[LI]-[KRI]-[PA]-T-[HY]-[VAH]-E-R	
Aliphatic	C -W-E-H-[FLX]-[NQ]-[PT]-L	
Aliphatic	[VA]-A-X-[AV]-Q-[AI]-X-P-[VA]-X-[LF]-[SD]	
Aromatic	[ALV]-[LV]-[FLM]-P- E -[AS]-[FLV]-[LV]-[AGP]-[AG]-Y-P	V-V-M-P- E -A-L-L-G-G-Y
Aromatic	[AGN]-[KR]-H-R- K -L-[MK]-P-T-[AGN]-X-E-R	A-K-H-R- K -L-M-P-T-G-T-E-R
Aromatic	C -W-E-N-[HY]-M-P-[LM]-[AL]-R-X-X-[ML]-Y	C -W-E-N-M-M-P-L-L-R-T-A-M-Y
Aromatic	A-X-E-G-R-C-[FW]-V-[LIV]	A-H-E-G-R-C-F-V-V

PHYSICOCHEMICAL PROPERTIES OF NITRILASE

Sharma et al. 2009, report that aliphatic and aromatic nitrilases can be differentiated based on their amino acid sequence and physicochemical properties. The physicochemical properties of the *P. putida* UW4 nitrilase were deduced from *in silico* analysis of the amino acid sequence using the ProtParam of Expert Protein Analysis System (ExPASy) from the proteomic server of Swiss Institute of Bioinformatics, in order to predict aromaticity or aliphaticity. The parameters listed in Table 10. for the UW4 nitrilase are closer to those reported for aromatic nitrilases, supporting the prediction that *P. putida* UW4 nitrilase has aromatic substrate specificity. The average parameter values for aliphatic and aromatic nitrilase as seen in Table 10, were those reported by Sharma et al. 2009. The protein instability index estimates the stability of the protein *in vivo*. This parameter is based on the frequency of occurrence of certain dipeptides in the protein sequence, which exists predominantly in either stable or unstable proteins. An instability index smaller than 40 is predicted as stable, while a value above 40 predicts instability (Guruprasad et al., 1990). The nitrilase of UW4 has an instability index of 32.37 and is considered stable. The aliphatic index of a protein calculates the relative volume occupied by aliphatic side chains. This parameter was based on the observation that the amino acid composition of thermostable proteins invariably shows a high content of Ala, Val, Ileu, and/or Leu. Mesophilic proteins with high aliphatic index values (>90) are generally thermostable (Atsushi, 1980). The nitrilase of UW4 has a high aliphatic index of 94.43 and is considered thermostable. The grand average of hydropathicity parameter is based on assigning each amino acid a value reflecting its relative hydrophilicity and hydrophobicity. The sum of hydropathy values of all the

amino acids, divided by the number of residues in the sequence is then calculated to give the grand average of hydropathicity for that protein. Increasing positive values indicate greater hydrophobicity (Kyte and Doolittle, 1982). The nitrilase of UW4 has a relatively low grand average hydropathicity value of 0.099 and is considered hydrophilic.

Table 10. Physicochemical properties of aliphatic, aromatic and *P. putida* UW4 nitrilases. Average values are those reported by Sharma and Bhalla, 2009.

Parameters	Average Value for Aliphatic Nitrilases	Average Value for Aromatic Nitrilases	<i>P. putida</i> UW4 Nitrilase (Nit)
Number of amino acids	352	310	307
Molecular Weight (kDa)	38 274.1	33 693.5	32 847.7
Theoretical pI	5.50	5.51	5.69
No. of Negatively Charged Residues	41.7	35.8	34
No. of Positively Charged Residues	30.3	29.2	28
Extinction Coefficients (M ⁻¹ cm ⁻¹) at 280nm	50 213	43 975	40 210
Instability Index	41.2	38.5	32.37
Aliphatic Index	89.4	89.8	94.43
Grand Average of Hydropathicity	0.10	0.01	0.099

MULTIPLE SEQUENCE ALIGNMENTS

A total of 115 nitrilase amino acid sequences from bacteria, fungi and plants were aligned using MEGA 5.0 software (Figure 29). The alignments were manually refined and regions that could not be reliably aligned were removed. The four protein sequence motifs that were manually designed by Sharma and Bhalla (2012) to identify aromatic nitrilases were highlighted (Figure 29). These four motifs were present in all of the sequences analyzed.

Nitrile hydratases are metalloenzymes that have either cobalt or iron metal ions in the catalytic center (Kobayashi and Shimizu, 1998; Endo et al. 2001). These enzymes contain two subunits (a and b). A total of 73 microbial nitrile hydratase a- subunit amino acid sequences were aligned (Figure 30) in the same manner as the nitrilase genes. The primary sequences of each subunit are well conserved among different bacteria, however there is no strong homology between the two different subunits (Endo et al. 2001). The cobalt nitrile hydratases have the conserved V-C-T-L-C-S-C active site, while the iron-type have V-C-S-L-C-S-C. Both types of metal enzymes were included in the alignment. The active site was highlighted along with the sites that were 100% conserved among all the sequences analyzed (Figure 30). *P. putida* UW4 nitrile hydratase contains an iron-type active site.

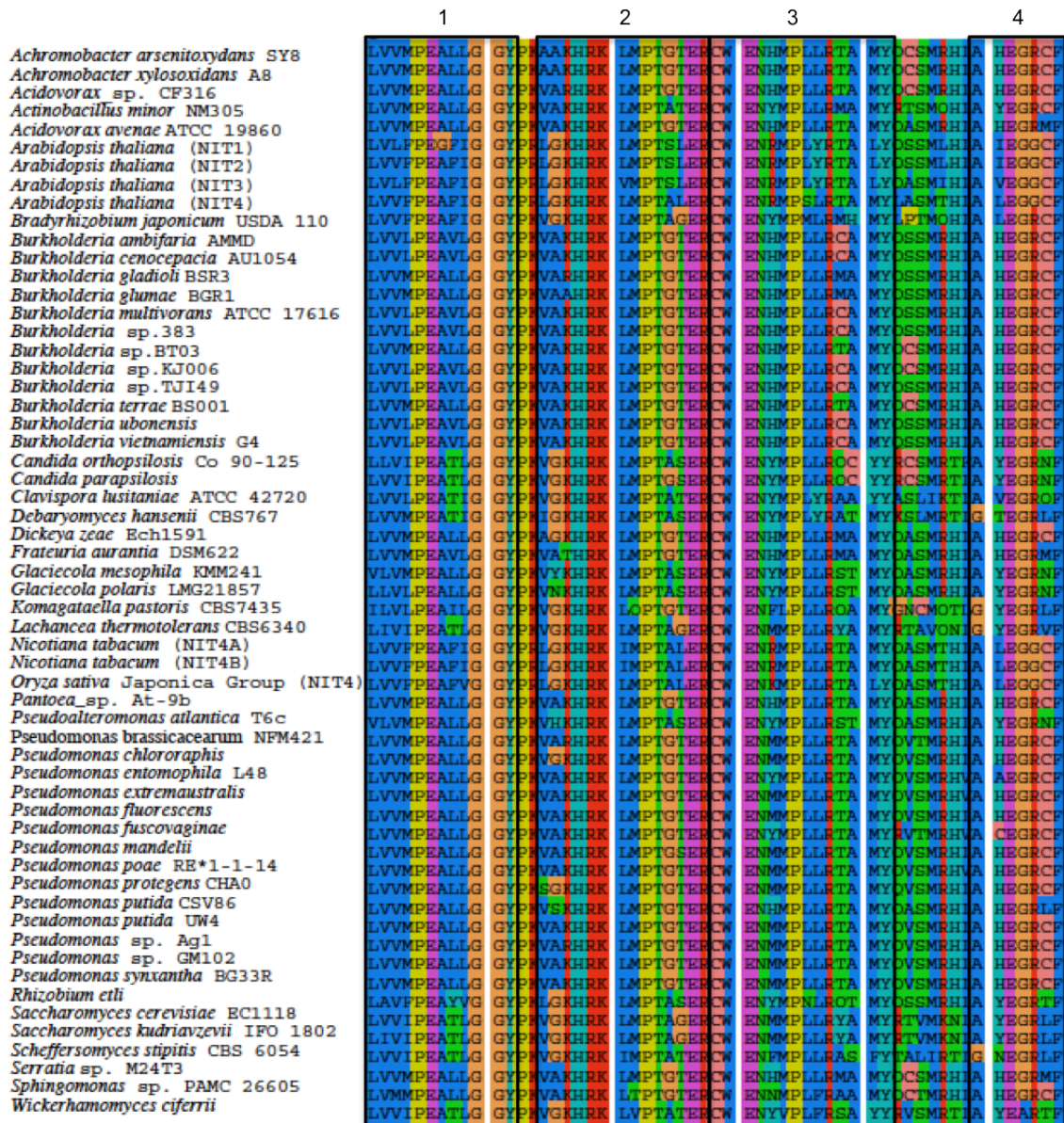


Figure 29. Multiple sequence alignment of nitrilase proteins. The black rectangles highlight the four different motifs (1-4) determined by Sharma and Bhalla (2012). Motif 1 includes residues #40-50, Motif 2 includes residues #126-139, Motif 3 includes residues #165-178, Motif 4 includes residues #204-210. Only 58 representatives out of 115 total aligned protein sequences are shown in this diagram.

Active Site

<i>Pseudomonas putida</i> UW4	VIVCSLCSCT	NWPVLGLPPE	WYK
<i>Pseudomonas chlororaphis</i>	VIVCSLCSCT	NWPVLGLPPE	WYK
<i>Pseudomonas putida</i> F1	VIVCSLCSCT	NWPVLGLPPE	WYK
<i>Pseudomonas synxantha</i>	VIVCSLCSCT	NWPVLGLPPE	WYK
<i>Pseudomonas fluorescens</i>	VIVCSLCSCT	NWPVLGLPPE	WYK
<i>Burkholderia ambifaria</i> AMMD	VIVCSLCSCT	NWPVLGLPPE	WYK
<i>Burkholderia cenocepacia</i> AU 1054	VIVCSLCSCT	NWPVLGLPPE	WYK
<i>Burkholderia gladioli</i> BSR3	VIVCSLCSCT	NWPVLGLPPE	WYK
<i>Burkholderia graminis</i>	VIVCSLCSCT	NWPVLGLPPE	WYK
<i>Burkholderia phytofirmans</i> PsJN	MVVCTLCSCY	PWPVLGLPPV	WYK
<i>Burkholderia</i> sp. BT03	MVVCTLCSCY	PWPVLGLPPI	WYK
<i>Burkholderia terrae</i> BS001	MVVCTLCSCY	PWPVLGLPPI	WYK
<i>Herbaspirillum seropedicae</i> SmR1	VIVCSLCSCT	NWPVLGLPPE	WYK
<i>Herbaspirillum</i> sp. GW103	VIVCSLCSCT	NWPVLGLPPE	WYK
<i>Acinetobacter calcoaceticus</i>	VIVCSLCSCT	NWPVLGLPPE	WYK
<i>Acinetobacter</i> sp. ADP1	VIVCSLCSCT	NWPVLGLPPE	WYK
<i>Acinetobacter</i> sp. NIPH 542	VIVCSLCSCT	NWPVLGLPPE	WYK
<i>Variovorax paradoxus</i> S110	VIVCSMCSCT	NWPVLGLPPE	WYK
<i>Acidovorax avenae</i> ATCC 19860	VIVCSLCSCT	NWPVLGLPPE	WYK
<i>Rhodococcus</i> sp. R312	VIVCSLCSCT	AWPILGLPPT	WYK
<i>Rhodococcus</i> sp. LCF30	VIVCSLCSCT	AWPILGLPPT	WYK
<i>Bacillus</i> sp. SW2-21	VIVCSLCSCT	AWPILGLPPT	WYK
<i>Microbacterium</i> sp. SS1-15	VIVCSLCSCT	AWPILGLPPT	WYK
<i>Microbacterium</i> sp. AJ115	VIVCSLCSCT	AWPILGLPPT	WYK
<i>Gordonia polyisoprenivorans</i> VH2	VIVCSLCSCT	AWPILGLPPT	WYK
<i>Sphingobium japonicum</i>	VIVCTLCSCY	AWPILGLPPT	WYK
<i>Streptomyces violaceusniger</i> Tu4113	VVVCTLCSCY	PWPVLGLPPS	WYK
<i>Rhodopseudomonas palustris</i> DX-1	MVVCTLCSCY	PWPVLGLPPV	WYK
<i>Pseudonocardia</i> sp. P1	VVVCTLCSCY	PWPVLGLPPS	WYK
<i>Mycobacterium smegmatis</i> JS623	LVVCTLCSCY	PWPILGLPPK	WYK
<i>Mycobacterium tusciae</i> JS617	LVVCTLCSCY	PWPTLGLPPK	WYK
<i>Ruegeria lacuscaerulensis</i>	MVVCTLCSCY	PWPLLGIPPG	WYK
<i>Ruegeria</i> sp. R11	MVVCTLCSCY	PWPLLGIPPG	WYK
<i>Silicibacter lacuscaerulensis</i> ITI-1157	MVVCTLCSCY	PWPLLGIPPG	WYK
<i>Silicibacter</i> sp. TrichCH4B	MVVCTLCSCY	PWPLLGIPPG	WYK
<i>Rhodobacteraceae bacterium</i> KLH11	MVVCTLCSCY	PWPLLGIPPG	WYK
<i>Rhodobacterales bacterium</i> Y4I	MVVCTLCSCY	PWPLLGIPPG	WYK
<i>Bradyrhizobium</i> sp. ORS285	MVVCTLCSCY	PWPVLGLPPV	WYK
<i>Roseobacter</i> sp. SK209-2-6	MVVCTLCSCY	PWPLLGIPPG	WYK
<i>Ruegeria mobilis</i> F1926	IVVCTLCSCY	PWPLLGIPPG	WYK
<i>Ruegeria pomeroyi</i> DSS-3	MVVCTLCSCY	PWPLLGIPPG	WYK
<i>Agrobacterium tumefaciens</i>	MVVCTLCSCY	PWSVLGLPPA	WYK
<i>Ricinus communis</i>	LVVCTLCSCY	PWPVLGLPPT	WFK
<i>Microvirga</i> sp. WSM-3557	MVVCTLCSCY	PWPVLGLPPV	WYK

Figure 30. Multiple sequence alignment of nitrile hydratase α - subunit protein. The black rectangle highlights the metal binding active site. Only 44 representatives out of 73 total aligned protein sequences are shown in this diagram.

PHYLOGENETIC TREES

Nitrilase (Nit), nitrile hydratase α (NthA) and β (NthB) subunits and P47K activator amino acid sequences were used for phylogenetic analysis. Amino acid sequences were chosen as opposed to nucleotide sequences to avoid misleading phylogenetic signals as a result of codon bias in the third position. All protein phylogenies were constructed under maximum likelihood (ML) using the MEGA 5.1 program (Tamura et al., 2011). The trees were inferred with different evolutionary models, best fitted to each type of data set being analyzed. The nitrilase tree utilized a WAG+G+I model, nitrile hydratase α and β subunits both utilized a WAG+G model and P47K activator utilized a JTT+G model. Neighbour-joining (NJ) and Maximum Parsimony trees were also constructed. For each approach taken, 1000 bootstrap replicates were performed. Only the phylogeny inferred using the maximum-likelihood (ML) method is shown in Figures (31-34), however bootstrap values from neighbor joining (NJ) and maximum parsimony (MP) analyses are also included in the trees shown.

Figure 31. Nitrilase phylogeny inferred using Maximum-likelihood method. The results of a ML-bootstrap analysis are shown in black, whereas the values in blue and purple are from neighbour-joining and maximum parsimony bootstrap analysis respectively. Plants are shown in green, yeasts in brown and bacteria in grey boxes.

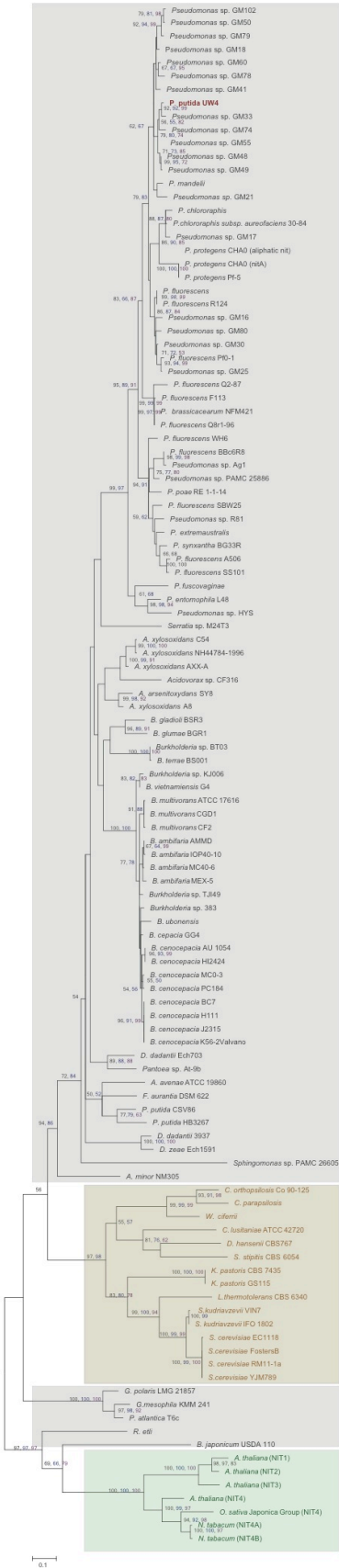


Figure 32. Nitrile hydratase α -subunit phylogeny inferred using ML method. The results of a ML-bootstrap analysis are shown in black, whereas the values in blue and purple are from neighbour-joining and maximum parsimony bootstrap analysis respectively. Iron-type nitrile hydratases are shown in red and cobalt-type in blue boxes.

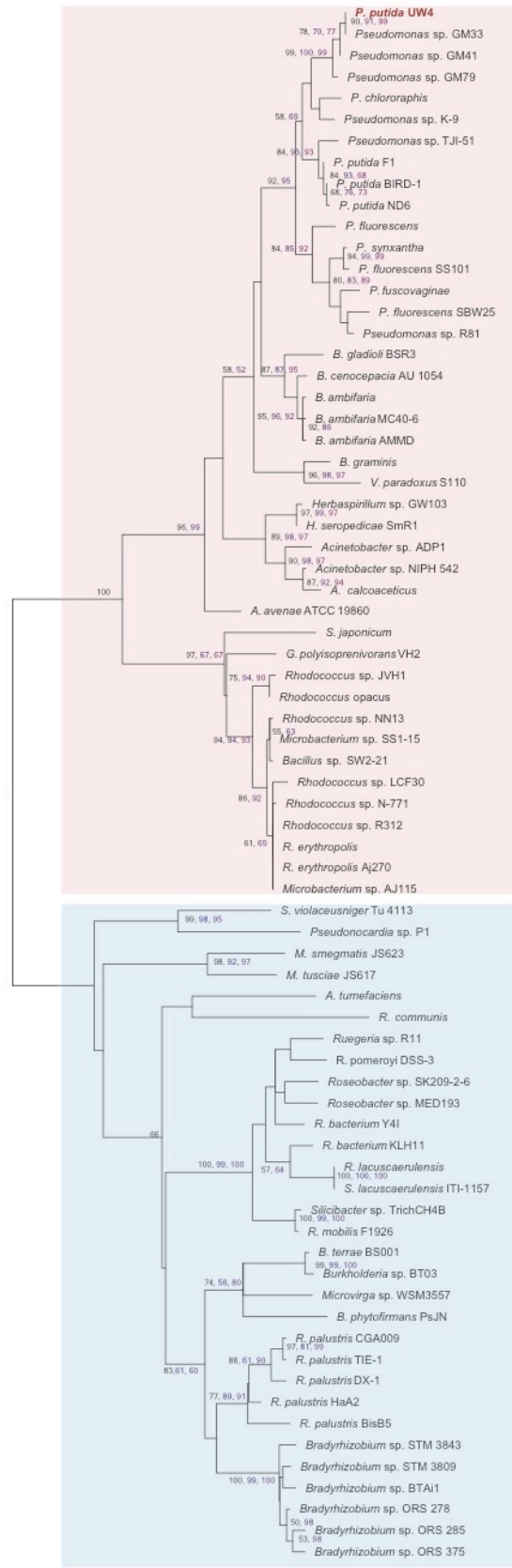


Figure 33. Nitrile hydratase β -subunit phylogeny inferred using ML method. The results of a ML-bootstrap analysis are shown in black, whereas the values in blue and purple are from neighbour-joining and maximum parsimony bootstrap analysis respectively.

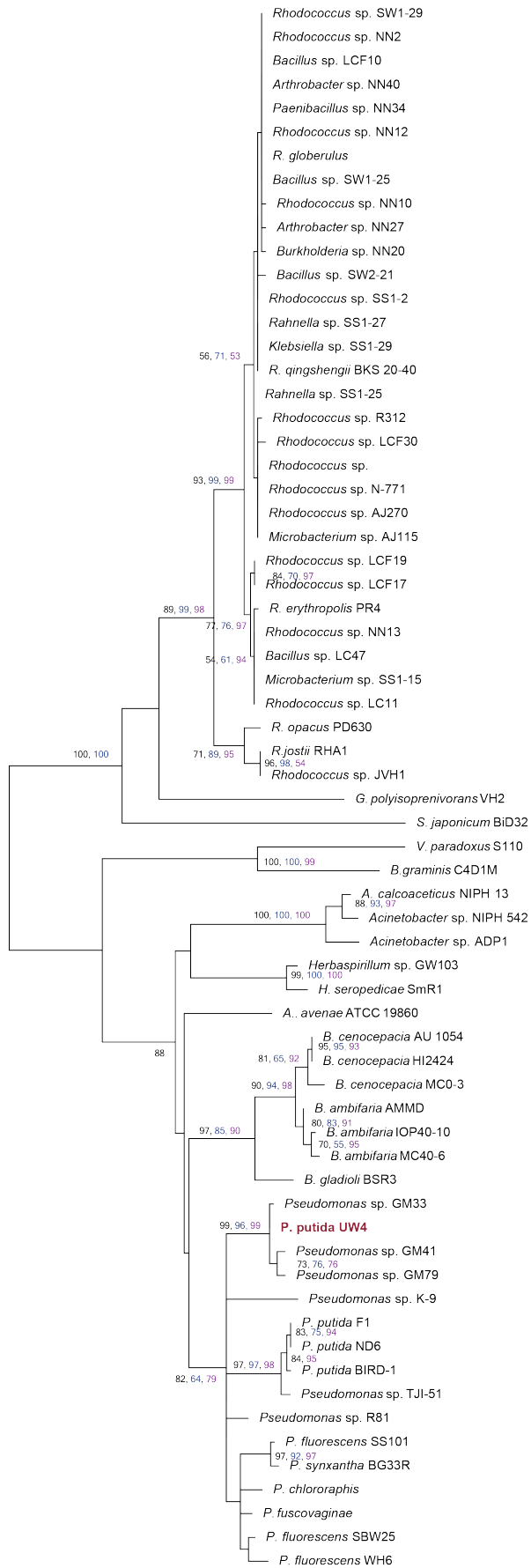
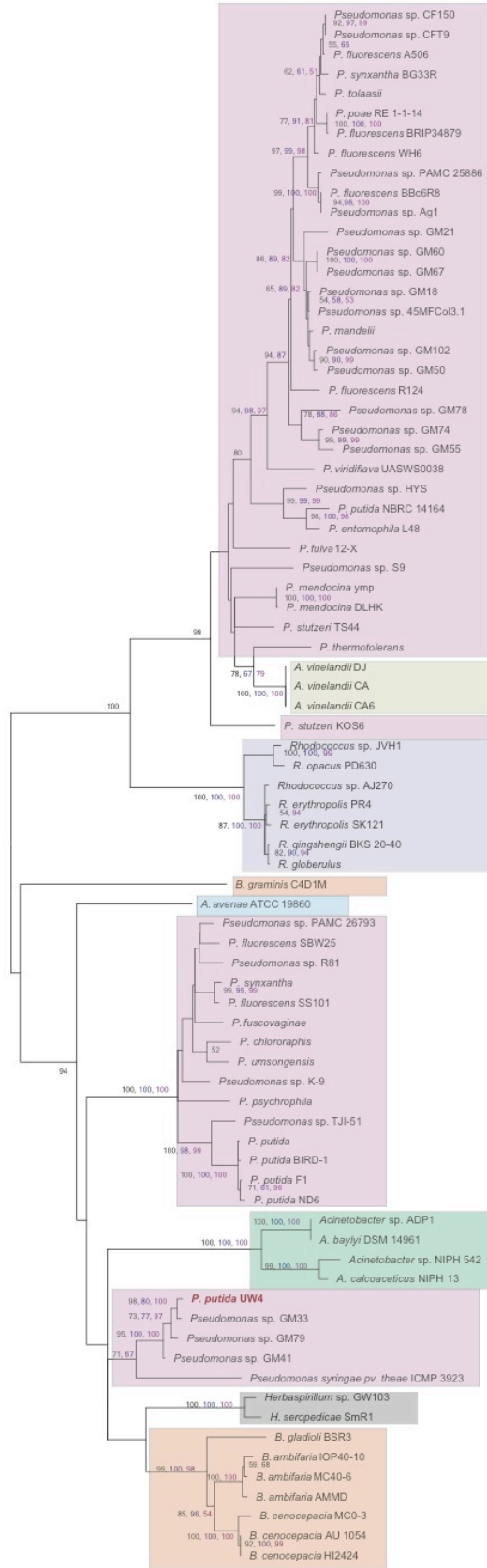


Figure 34. P47K activator protein phylogeny inferred using the ML method. The results of a ML-bootstrap analysis are shown in black, whereas the values in blue and purple are from neighbour-joining and maximum parsimony bootstrap analysis respectively. Each bacterial species is represented by a different coloured box.



DISCUSSION

Pseudomonas putida UW4 is a plant-growth promoting bacterium, isolated from the rhizosphere of common reeds on the campus of the University of Waterloo (Glick et al. 1995). One of the mechanisms that this bacterium employs to facilitate plant growth is the production of indole-3-acetic acid (IAA) phytohormone. Quantification of the amount of IAA secreted into the culture media of UW4 revealed that it can produce up to 3.7 µg/mL IAA, upon exogenous supplementation with 500 µg/mL tryptophan (Table 8). IAA has hormonal action at concentrations as low as 10^{-7} M (0.02 µg/mL) in plants (Kobayashi et al., 1993).

Recently, the complete genome of UW4 has been sequenced and several genes have been annotated as putative IAA biosynthetic genes (Duan et al., 2012). These genes include *nit*, *nthA*, *nthB*, *ami*, *pheD*, *aux*, *iaaM*, and are predicted to mediate the IAM and IAN pathways of IAA biosynthesis (Figure 7).

The aim of this research was to determine the IAA biosynthesis pathways operating in *Pseudomonas putida* UW4. Biochemical approaches were taken to isolate and purify some the enzymes encoded by putative IAA biosynthesis genes. The focus here was on two particular enzymes, nitrilase and nitrile hydratase. Characterizing these enzymes allows for a better understanding of how IAA is produced by UW4. Subsequent substrate feeding assays can then facilitate a better understanding of the role of each enzyme.

NITRILASE

Nitrilase enzymes are part of a large superfamily with over 180 known members. This superfamily is classified into 13 branches, of which only branch I is known to have true nitrilase activity (Pace and Brenner, 2001). Eight of the remaining branches have amidase or amide-condensation activities and consist of aliphatic amidases, β -ureidopropionases, β -alanine synthases and N-carbamyl-D-amino acid amidohydrolases (Pace and Brenner, 2001). Members of branch I (EC 3.5.5.1) exist in plants, animals, fungi and bacteria. Nitrilase enzymes are common in bacteria that associate with plants, perhaps playing a role in this ecological relationship (Pace and Brenner, 2001).

Members of the nitrilase superfamily catalyze the hydrolysis of non-peptide carbon-nitrogen bonds. Specifically, branch I nitrilases convert nitriles to their corresponding carboxylic acids, releasing ammonia in the process (Podar et al., 2005). This branch of nitrilase enzymes is implicated in IAA biosynthesis. The substrate specificity and enantioselectivity of nitrilases is specific to different sub-branches. For example, some Branch I nitrilases prefer aliphatic nitriles, while others act on aromatic/heterocyclic or arylacetonitriles (Podar et al., 2005; Banerjee et al., 2002). The *P. putida* UW4 nitrilase characterized in this study was found to act on the aromatic heterocyclic indole-3-acetonitrile substrate.

Nitrilase Enzyme Activity

Nitrile compounds exist all throughout the environment, some being natural plant products such as cyanoglycosides, cyanolipids, ricinine and phenylacetonitrile. Other nitriles have mutagenic, and carcinogenic properties. Industries release artificial nitriles via industrial wastewater, while agriculture uses nitrile herbicides, which pollute the environment. Enzymatic hydrolysis of toxic nitriles is an attractive means of bioremediation, but perhaps more profoundly, nitrile-degrading enzymes are used to produce useful amides and carboxylic acids. In fact, nitrilase has proven to be a key enzyme in the commercial production of nicotinic and mandelic acids (Komeda et al., 1996; Gong et al., 2012).

With most of the attention being on exploiting bacterial nitrilases for industrial processes, their role in the biosynthesis of IAA has been neglected. Genes encoding nitrilase enzymes capable of converting indole-3-acetonitrile (IAN) into IAA, have been identified in *Arabidopsis*, tobacco, Chinese cabbage and rice (Bartling et al., 1992, 1994; Bartel and Fink, 1994; Hillebrand et al., 1996; Zhou et al., 1996a, 1996b; Tsunoda and Yamaguchi, 1995; Bischoff et al., 1995). *Arabidopsis* contains four nitrilase genes (NIT7, NIT2, NIT3, and NIT4) that display different expression patterns. The NIT1 gene is strongly expressed in the portion of the plant most sensitive to the effects of exogenous indole-3-acetonitrile (IAN) (Bartel and Fink, 1994). This suggests that the sensitivity to IAN is due to its conversion into IAA by the NIT1 enzyme (Normanly et al., 1997). Although these nitrilase genes participate in IAA production, it has been suggested that

their primary roles in plants are glucosinolate metabolism, camalexin homeostasis, and cyanide detoxification. Glucosinolates and camalexin are plant secondary metabolites that serve a role in plant defense against insects, herbivores and microbial pathogens (Redovnikovi et al., 2008; Zhao et al., 2012). Moreover, secondary metabolites that contain nitrile groups are a rich source of macronutrients and may be processed by nitrilases to utilize the nitrogen in the form of ammonia (Janowitz et al., 2009).

Few plant-associated microbes that produce IAA via nitrilase enzyme have been studied for this characteristic. Kobayashi et al., 1993, characterized an indole-3-acetonitrile-specific nitrilase from *Alcaligenes faecalis* JM3. This enzyme does not act on substrates with a cyano group directly bound to an aromatic or heterocyclic ring, such as benzonitrile and cyanopyridine. Instead it is highly specific for arylacetonitriles such as indole-3-acetonitrile, benzyl cyanide and thiopheneacetonitrile. Howden et al. (2009) also identified an arylacetonitrilase in the plant pathogen *P. syringae* B728a that was capable of hydrolyzing indole-3-acetonitrile (IAN) to IAA.

In this study, a nitrilase enzyme capable of producing both IAA and indole-3-acetamide (IAM) has been identified in the plant growth-promoting bacterium *P. putida* UW4. Enzyme assays using purified UW4 nitrilase and indole-3-acetonitrile (IAN) as substrate, confirmed that this enzyme has the ability to act upon this arylacetonitrile. Other substrates were not tested, thus the substrate specificity of this enzyme cannot be inferred. Previous characterization of nitrilases from various bacteria (Table 12) reveals diverse substrate specificities and the ability of a single nitrilase to act upon multiple nitriles (i.e. aromatic, aliphatic, arylactenonitriles). The K_m values for some of these

nitrilases range from 1.2×10^{-2} to 9×10^{-6} M, depending on the type of substrate (Table 11).

Therefore, it is possible that indole-3-acetonitrile (IAN) is neither the only nor the preferred substrate that UW4 nitrilase can act upon.

Bacteria	Formation	Molecular Weight (kDa)	Optimum Temperature (°C)	Optimum pH	Substrate	Km (M)	Reference
<i>Pseudomonas</i> sp.	inducible				N-Methyl(ethyl)-3-cyano-4-methoxy-2-pyridone (nicine)	1.9x10 ⁻⁵	Robinson and Hook, 1964
<i>Pseudomonas</i> sp. 13	inducible	1000	55	9	β-Cyano-L-alanine	8.3x10 ⁻²	Yanase et al., 1982
<i>P. fluorescens</i> DSM 7155	inducible	130	55	9	Arylacetone nitriles (racemic 2-methoxy-mandelonitrile phenylacetone nitrile, 2-Phenylpropionitrile, 2-Phenylbutyronitrile)	8.7x10 ⁻⁵	Layh et al., 1998
<i>P. putida</i>	inducible	412	40	7	Arylacetone nitriles	1.3x10 ⁻²	Banerjee et al., 2006
<i>P. aeruginosa</i> 10145	inducible		40	8	Aromatic nitriles (racemic 2-phenyl-2-amino-acetonitrile, benzonitrile)		Alonso et al., 2008
<i>P. putida</i> MTCC 5110	inducible		40	8	mandelonitrile		Pawar et al., 2012
<i>P. fluorescens</i> EBC191	inducible		45	7	Phenylacetone nitriles, heterocyclic arylacetone nitriles (indole-3-acetonitrile, Mandelonitrile, benzonitrile) aliphatic nitriles		Kizlak et al., 2005
<i>P. fluorescens</i> Pf-5	inducible	138	45	7	Aliphatic mononitriles, aliphatic dinitriles, aromatic nitriles	1.8x10 ⁻²	Kim et al., 2009
<i>A. faecalis</i> JM3	inducible	275	45	7.5	Arylacetone nitriles		
<i>A. faecalis</i> ATCC 8750	inducible	460	40-45	7.5	Arylacetone nitriles (mandelonitrile)	3.3x10 ⁻⁴	Nagasawa et al., 1990
<i>A. faecalis</i> ZJUTB10	inducible		35	7.7-8.5	Mandelonitrile	9 x10 ⁻⁶	Kobayashi et al., 1993
<i>Alcaligenes</i> sp. ECU0401	constitutive	376	40	8	Aliphatic nitriles, aromatic nitriles (Mandelonitrile)	5.8x10 ⁻³	Yamamoto et al., 1992
<i>A. faecalis</i> MTCC 10757	inducible		35	8	Aliphatic nitriles, aromatic nitriles	2.2x10 ⁻²	Xue et al., 2011
<i>R. rhodochrous</i> J1	Inducible	78	45	7.6	Aliphatic, aromatic nitriles		Nageshwar et al., 2011
<i>R. rhodochrous</i> PA-34	inducible	45	35	7.5	Aromatic, aliphatic nitriles		Kobayashi et al., 1989
<i>R. rhodochrous</i> K22	inducible	650	50	5.5	Aromatic nitriles	4.5x10 ⁻²	Mathew et al., 1988
<i>R. rhodochrous</i> NCIMB 11216	inducible	45.8	30	8	Aromatic nitriles	1.9x10 ⁻²	Bhalla et al., 1992
<i>Rhodococcus</i> sp. NDB1165	inducible		45	8	Aromatic and unsaturated aliphatic nitriles	2.1x10 ⁻²	Kobayashi et al., 1990
<i>R. erythropolis</i> ZJB-0910	inducible		30	7.5	β-Hydroxy aliphatic nitrile	0.1	Hoyle et al., 1998
<i>Novcardia</i> sp. NCIB 11216	inducible	560		8	Aromatic nitrile	1.0x10 ⁻²	Prasad et al., 2007
<i>N. globerula</i> NHB-2	inducible				4-cyanopyridine		Dong et al., 2010
<i>Acinetobacter</i> sp. AK226	inducible	580	50	8	Aliphatic, heterocyclic nitriles		Harper, 1977
<i>Klebsiella ozaenae</i>	constitutive	37	35	9.2	Bromoxynil		Sharma et al., 2012
<i>Klebsiella pneumoniae</i>	constitutive		35	8	toxylin, bromoxynil, chloroxynil	3.1x10 ⁻⁴	Yamamoto and Komatsu, 1991
<i>Comamonas testostearni</i> sp.	inducible				Aliphatic nitriles		Stalker et al., 1988
<i>Bacillus pallidus</i> Dae521	inducible	600	65	7.6	Aromatic nitriles		Detzel et al., 2012
<i>Bacillus subtilis</i> ZJB-063	constitutive	60	80	7.4	Arylacetone nitriles	9.2x10 ⁻⁴	Lévy-Schi et al., 1995
<i>Pyrococcus abyssi</i> GE5	inducible	570	65	7.4	Aliphatic dinitriles		Almatawah et al., 1999
<i>Acidovorax facilis</i> 72W	inducible	455	65	7.4	Aliphatic dinitriles	9.5x10 ⁻³	Zheng et al., 2008
<i>Bradyrhizobium japonicum</i> USDA110	inducible				Mandelonitrile, phenylacetone nitrile	5.6x10 ⁻²	Mueller et al., 2006
<i>Halomonas nitrilica</i> sp. nov	inducible				Aryl aliphatic nitriles	2.6x10 ⁻⁴	Chauhan et al., 2003
<i>Streptomyces</i> sp. MTCC 7546	inducible				Aliphatic nitriles (acrylonitrile)		Zhu et al., 2007
<i>Arthrobacter nitroguaiacolicus</i> ZJUTB06-99	inducible		40	6.5	Aliphatic (acrylonitrile) and aromatic nitriles	1.2x10 ⁻²	Chmura et al., 2008
<i>Grobacillus pallidus</i> RAP-8	inducible	600			Aromatic nitriles		Nigam et al., 2009
<i>Burkholderia</i> sp.	inducible	484.5			Mandelonitrile, Acetonitrile, Adiponitrile, Glutaronitrile, Benzonitrile	8.4x10 ⁻⁵	Shen et al., 2009
<i>Burkholderia cenocepacia</i> 12315	inducible	450	45	8	Arylacetone nitriles, aliphatic nitriles, heterocyclic nitriles	1.4x10 ⁻⁴	Williamson et al., 2010
<i>Rhodobacter sphaeroideus</i> 1HS-305	inducible	560	40	7	Aliphatic and aromatic nitriles, aliphatic dinitriles, (3-cyanopyridine)	7.3x10 ⁻²	Seffernick et al., 2009
							Wang et al., 2013

Table 11. Characterization of various nitrilase enzymes from different bacteria

Nitrilase Temperature and pH Optima

Optimal activity for the *P. putida* UW4 nitrilase was observed at 50°C and a pH of 6. This data agrees well with other reported pseudomonad nitrilases, which have temperature optimums between 40-55°C as well as with several rhodococci nitrilases (Table 12). The UW4 enzyme retained greater than 50% activity at 55°C, however activity decreased significantly (~84%) at 60°C. An 89% decrease in activity was also reported for another *P. putida* nitrilase at 70°C (Banerjee et al., 2006). On the other hand, *P. fluorescens* DSM7155 nitrilase retained 80% activity at 60°C (Layh et al., 1998). The UW4 nitrilase appears to be a relatively thermostable enzyme. This is supported by the activity observed at 50°C and by the physicochemical properties reported in Table 10. This enzyme has an instability index of < 40 and a high aliphatic index of 94.43. Both of these values are indicative of high protein stability (Guruprasad et al., 1990; Atsushi et al., 1980).

The pH optima (pH 6) of the UW4 nitrilase is slightly lower than other reported pseudomonads, which display maximum activity at pHs between 7-9. Instead, it is more similar to that of *R. rhodochrous* K22 (pH 5.5) and *Arthrobacter nitroguajacolicus* ZJUTB06-99 (pH 6.5) (Table 11). However, the enzyme retained greater than 83% activity at pH 7 and thus is comparable to other pseudomonad nitrilases. Plant roots generally make the surrounding soil slightly acidic by expelling protons (H⁺) in the process of ammonium uptake. On the other hand, when plant roots take up nitrate (NO₃⁻), the roots release bicarbonate (HCO₃⁻), which increases the rhizosphere pH (McNear, 2013). Perhaps these fluctuations in rhizospheric pH can influence the activity of the

enzymes produced by rhizospheric bacteria. In general, neutrophiles have internal pH values of 7.5 to 8.0 (Booth, 1985). The enzyme systems in these bacteria evolve to operate within these pH ranges (Booth, 1985). *P. putida* UW4 is a rhizosphere inhabitant that produces a nitrilase most active in slightly acidic to neutral conditions (pH 6-7). This enzyme is predicted to be cytoplasmic and is not secreted into the rhizosphere. However, if the cytoplasmic pH is affected by the rhizospheric pH outside of the cell, this in turn may affect the activity of the nitrilase enzyme.

Native Size of Nitrilase

Microbial nitrilases are generally known to be multimeric enzymes, typically composed of 4–22 identical subunits (Thuku et al. 2009). Table 12 shows the native molecular sizes of several characterized nitrilases from different bacteria. These sizes range from 37 kDa (*Klebsiella ozaenae* nitrilase) to 1000 kDa (*Pseudomonas* sp. 13 nitrilase). The native molecular weight of *P. putida* UW4 nitrilase was predicted to be at least 470 kDa using size exclusion gel filtration FPLC. The individual subunit is ~ 32.8 kDa, which means the native conformation consists of at least 15 subunits. Similarly large native sizes have been reported for the nitrilases of *R. rhodochrous* K22 (650 kDa), *Bacillus pallidus* Dac521 (600 kDa), *Geobacillus pallidus* RAPc8 (600 kDa), *Acinetobacter* sp. AK226 (580 kDa), *Acidovorax facilis* 72W (570 kDa) and *Rhodobacter sphaeroides* LHS-305 (560 kDa) (Table 12).

Amide Production by Nitrilase

The conversion of indole-3-acetonitrile (IAN) by the UW4 nitrilase resulted in the formation of indole-3-acetamide (IAM) as well as IAA. Moreover, there was significantly more amide product (3-5X) produced than carboxylic acid. This side-activity does not conform to the commonly accepted acid-producing nitrilase mechanism. Even so, reports can be found on nitrilases producing modest amounts of amides. Kiziak et al., 2005 report that 43% of *O*-acetylmandelonitrile and 28% of (R)-*O*-acetylmandelonitrile were converted to the respective amides by the *Pseudomonas fluorescens* EBC191 nitrilase. Moreover, 80% of the mandelonitrile substrate was converted to mandelic acid and 20% to the mandelic acid amide (Kiziak et al., 2005). Approximately 5 % of the products from *Fusarium oxysporum* nitrilase were amides (Goldlust & Bohak, 1989). *Rhodococcus sp.* strain ATCC 39484 nitrilase produced 2% amide from phenylacetonitrile (Stevenson et al., 1992), while the ricinine-specific nitrilase from *Pseudomonas sp.* produced 7–10% amide. The *Arabidopsis* Nit1 converted 2-fluoroarylacetonitriles mostly to the amides, with only trace amounts of the corresponding carboxylic acids being formed. On the other hand, this enzyme converted aliphatic nitriles mostly to the corresponding acids. Perhaps the high electron-withdrawing substituents (fluorine or nitro-groups) are responsible for the increased amount of amide formation (Effenberger & Osswald, 2001; Osswald et al., 2002). Fernandes et al. (2006) suggest that elevated temperature and low pH promote the formation of acid, whereas a low temperature and increased pH promote the formation of the amide. This inference was based on nitrile hydrolysis by a recombinant nitrilase from *Pseudomonas fluorescens* EBC that had an acid:amide ratio of ~20 at pH 9 and ~25 at pH

5. Increasing the reaction temperature from 5°C to 40°C changed the acid:amide ratio from 11 to 38 (Fernandes et al., 2006). In this study, UW4 nitrilase produced 3.2X more amide than acid at pH 8 and 2.8X more amide at pH 5. Moreover, at a temperature of 30°C there was ~6X more amide than acid produced, while at 60°C only ~3X more amide was produced. From these results, it appears that the reaction temperature has a greater impact on the amount of amide vs acid produced than the pH. In any case, it is apparent that some microbial nitrilases have dual abilities and can be exploited for both classic acid production and “nitrile hydratase-like” amide production, UW4 nitrilase being one of these types of enzymes (Kiziak et al., 2005). While the amide-producing ability of UW4 nitrilase is not unique to this enzyme, the large amount of amide produced compared to the amount of acid is atypical for bacteria.

NITRILE HYDRATASE

Nitrile hydratases (E C 4.2.1.84) catalyze the hydration of nitriles to the corresponding amides. These enzymes are heterodimers composed of α and β subunits and can be classified as ferric or cobalt nitrile hydratases, depending on the type of metal co-factor in their active site (Lu et al., 2003). The metal ion is contained within the α subunit. These metalloproteins require metal ion trafficking, correct protein folding and assembly of the two subunits, as well as cysteine residue oxidization to be active (Lu et al., 2003). In our study, the heterodimer formation of the two-subunit NthAB was confirmed by expressing only the β -subunit with a C-terminal His-tag to facilitate purification. After purification both subunits are present, which implies that the α -subunit associated with the tagged β -subunit in solution and was then purified as a heterodimer.

Had the two subunits existed as individual monomers in solution, the purification step would have only yielded the tagged β -subunit. Throughout their biogenesis, nitrile hydratases may exist in three different forms; the precursor, cysteine oxidized, and cysteine oxidized and nitrosylated. The iron co-factor binds most tightly in cysteine oxidized and nitrosylated proteins and least tightly in precursor without any post-translational modification (Lu et al., 2003).

Some Fe-type nitrile hydratases lose all their catalytic activity upon aerobic incubation of the bacteria in the dark (inactive state) and are immediately re-activated upon light irradiation (active state) (Nagamune et al., 1990). When the protein is in the inactive state, the iron center associates with an endogenous nitric oxide (NO) molecule produced by the bacteria. Light causes the photo-dissociation of the NO molecule, converting the protein into the active form (Noguchi et al., 1995; Noguchi et al., 1996; Odaka et al., 1997; Nojiri et al., 1998). The *P. putida* UW4 iron-type nitrile hydratase does not seem to have this feature, as one of the enzyme assays was conducted in the dark cold room at 4°C and the enzyme remained active.

Nitrile Hydratase Enzyme Activity

Nitrile hydratases have been exploited as industrial biocatalysts in the commercial synthesis of acrylamide, nicotinamide and 5-cyanovaleramide (Hann et al. 1999 ; Kobayashi and Shimizu 2000). Like nitrilases, these enzymes can act on different types of nitrile substrates. For example the *Rhodococcus erythropolis* AJ270 enzyme can convert aliphatic, aromatic and heterocyclic nitriles into the corresponding amides

(Blakey et al. 1995 ; O'Mahony et al. 2005). Nitrile hydratases have been reported in different bacteria, however, their ability to synthesize IAA from indole-3-acetonitrile via the indole-3-acetamide intermediate remains to be confirmed experimentally (Patek et al., 2009; Coffey et al., 2010; Patten et al., 2012). Few studies have explored this enzyme's involvement in IAA biosynthesis. Nitrile hydratases from *Agrobacterium*, *Rhizobium* and *Bradyrhizobium* have been shown to convert indole-3-acetonitrile (IAN) into indole-3-acetamide (IAM), which is then converted into IAA by the sequential action of an amidase (Kobayashi et al., 1995; Vega-Hernandez et al., 2002).

Several cobalt and ferric nitrile hydratase enzymes from different bacteria have been characterized with respect to their substrate preferences, optimum temperature and pH (Table 12). The substrate specificity can be for aliphatic, aromatic and arylacetonitriles. For example the iron-type nitrile hydratase of *P. chlororaphis* B23 acts upon propionitrile, n-butyronitrile and acrylonitrile with high activity and is labeled as an aliphatic nitrile hydratase (Nagasawa et al., 1987). The cobalt-type nitrile hydratase of *Rhodococcus sp.* strain YH3-3 acts on various alkyl and aryl nitriles with high activity and is labeled as both an aliphatic and aromatic nitrile hydratase. Iron-type nitrile hydratases have narrower substrate specificity, preferring alkylnitriles, whereas the cobalt-type enzyme can act on a broad range of alkyl, aryl and arylalkyl-nitriles (Nagasawa et al., 1986; Nagasawa et al., 1987; Endo and Watanabe, 1989; Nagamune et al., 1990; Nagasawa et al., 1991; Payne et al., 1997; Banerjee et al., 2002). Maximum activity of some of these enzymes has been reported at temperatures ranging from 20-60°C and pHs of 6-8.8 (Table 12).

Bacteria	Formation	Metal Type	Molecular Weight (kDa)	Optimum Temperature (°C)	Optimum pH	Substrate	Activator Requirement	Reference
<i>Rhodococcus rhodochromus</i> J1 (Low MW)	inducible	Co	101	40	8.8	aromatic nitriles		(Okada et al., 1997)
<i>Rhodococcus rhodochromus</i> J1 (High MW)	inducible	Co	505	35-40	6.5	aliphatic nitriles		(Okada et al., 1997)
<i>Rhodococcus</i> sp. YH3-3	inducible	Co	130			aliphatic nitriles		(Kato et al., 1999)
						aromatic nitriles		(Yamaki et al., 1997)
<i>Pseudomonas putida</i> NRRL-18668	constitutive	Co	54	60		acrylonitrile		
<i>Rhodococcus erythropolis</i>	constitutive	Co	65	20	7	aliphatic nitriles	yes	(Alfani et al., 2001)
<i>Agrobacterium tumefaciens</i> IAMB-261	inducible	Co and Fe	102	35	7.5	aromatic nitriles		Kamble et al., 2013
<i>Rhodococcus</i> sp. N774	constitutive	Fe	70	35	7.7	indole-3-acetonitrile		(Kobayashi et al., 1995)
<i>Rhodococcus</i> sp. N771	constitutive	Fe	70	30	7.8	aliphatic nitriles	yes	(Endo and Watanabe, 1989)
<i>Agrobacterium tumefaciens</i> d3	inducible	Fe	69	40	7	aliphatic nitriles	yes	(Yamada and Kobayashi, 1996)
<i>Brevibacterium</i> sp. R 312	constitutive	Fe	85	25	7.8	2-arypropionitrile		(Bauer et al., 1994)
<i>Pseudomonas cholovoraphis</i> B23	constitutive	Fe	100	20	7.5	aliphatic nitrile	yes	(Nagasawa et al., 1986)
<i>Corynebacterium</i> sp. C5	constitutive	Fe	61.5	60	8-8.5	aliphatic nitriles		(Nagasawa et al., 1987)
<i>Bacillus</i> sp. RAFP8	constitutive	Fe	-	-	7	aliphatic dinitrile		(Yamamoto et al., 1992b)
<i>Brevibacterium imperialis</i>	constitutive	-	-	-	6	Alkyl nitrile		(Pereira et al., 1998)
<i>Arthrobacter</i> sp. J1	inducible	-	420	35	7	acrylonitrile	yes	(Alfani et al., 2001)
<i>Rhodococcus equi</i> A4	inducible	-	74	40	8	aliphatic nitriles		(Asano et al., 1982a)
<i>Rhodococcus rhodochromus</i> PA-34	inducible	Fe	86	30	7	3-cyanopyridine		(Prepechalova et al., 2001)
<i>Rhodococcus</i> AJ270	inducible	Fe	-	-	-	Aromatic nitriles	yes	(Prasad et al., 2009)
						aliphatic nitriles		Blakey et al., 1995
						hetero-aromatic nitriles		
<i>Bacillus pallidus</i> Dae521	constitutive	-	111	50	7-7.5	aliphatic nitriles		(Cramp and Cowan, 1999)

Table 12. Characterization of various nitrile hydratase enzymes from different bacteria

Nitrile Hydratase Temperature & pH Optima

In this study, maximum activity of the *P. putida* UW4 iron-type nitrile hydratase was observed at 4°C and a pH of 7.5. The pH optimum is narrow, as activity decreased by 82% at pH 7 and by 64% at pH 8, however it agrees well with most other reported nitrile hydratases, which have maximum activity at a pH between 7-8 (Table 13). The enzyme retained greater than 50% of its activity at 10-20°C, however, the activity decreased significantly (>3X) as the temperature increased above 20°C. Since this is a heterodimeric enzyme, the elevated temperature may adversely affect enzyme stability, causing the two subunits (α and β) to dissociate. On the other hand, the interaction with an activator protein such as P47K might be required for the nitrile hydratase to be active at temperatures above those reported to be optimal in this study (i.e >20°C). However, it has been reported that the nitrile hydratase activator protein is inactive at temperatures above 30°C (Rzeznicka et al., 2010). Perhaps the high nitrile hydratase activity that was observed at low temperatures (4°C) is due to the activator being active and interacting with the nitrile hydratase only at such low temperatures. When the activator is inactivated at higher temperatures, the activity of nitrile hydratase consequently decreases.

Generally, the nitrile hydratases of mesophilic bacteria exhibit maximum activity at ambient temperatures between 20-40°C (Prasad and Bhalla, 2009). However, there are reports of thermophilic nitrile hydratases from *Bacillus* RAPc8 and *Pseudonocardia thermophila* JCM3095, which prefer 60°C (Pereira et al., 1998; Yamaki et al., 1997). *P. putida* UW4, inhabits Canadian soils, in which it would often be exposed to cold temperatures. While the optimum growth temperature of this bacterium is 25-30°C, it

grows at temperatures as low as 4°C (Cheng et al., 2007). The activity of most enzymes decrease at low temperatures, however, remarkably UW4 nitrile hydratase activity does not. This enzyme's ability to produce indole-3-acetamide (IAM) at 4°C gives UW4 the potential to produce and secrete IAA into the plant rhizosphere in spring, when the soil temperature is low and new plantlets require IAA for growth.

Native Size of Nitrile Hydratase

The molecular masses of native nitrile hydratases range from 54-505 kDa (Table 13). Most are composed of 2-4 subunits, with reported subunit molecular weights of ~25-30 kDa (α -subunit) and 25-35kDa (β -subunit) (Banerjee et al., 2002). The *P. putida* UW nitrile hydratase α -subunit has a predicted molecular weight of 22.3 kDa and the β -subunit 24.7 kDa. Preliminary results from size exclusion gel filtration FPLC suggest that the *P. putida* UW4 nitrile hydratase is a multimeric enzyme with a native molecular size between 450-550 kDa. Similarly large native sizes have been reported for the nitrile hydratase of *R. rhodochrous* J1 (505 kDa) (Okada et al., 1997) and *Arthrobacter sp.* J1 (420 kDa) (Asano et al., 1982a). Further investigations must be made in order to determine the exact native size of this enzyme.

Nitrile Hydratase Activator Proteins

Some nitrile hydratase genes are flanked by sequences encoding activator proteins, which in some cases are essential for functional expression of both Fe and Co type enzymes. This is the case for bacteria such as *Rhodococcus sp.* N771, N774 and

Pseudomonas chlororaphis B23. The activator from *Rhodococcus sp.* N-771 shares amino acid sequence similarity with the ATP-dependent iron transporter from *Magnetospirillum sp.* AMB and with the cobalt transporter (*nhlF*) from *R. rhodochrous* J1 (Nakamura et al., 1995; Komeda et al., 1997; Nojiri et al., 1999). It also has a cysteine-rich motif similar to copper chaperones and resembles their activity by helping the target protein obtain a functional conformation. When the *Rhodococcus sp.* N-771 nitrile hydratase is expressed without the activator protein, a large proportion of the α and β subunits misfold and are subsequently cleaved by proteases, while others were expressed as inclusion bodies (Ikehata et al. 1989; Lu et al., 2003). The recombinant nitrile hydratase from *Rhodococcus erythropolis* AJ270 expressed in *E. coli*, showed highest activity in constructs co-expressing the P44k activator protein from the same plasmid. Co-expressing the P44K protein on a separate plasmid than the nitrile hydratase, decreased active expression (Song et al., 2008). *Pseudomonas putida* 5B cobalt-type nitrile hydratase also requires co-expression of a P14K activator and the presence of cobalt for functional expression in *E. coli*. The P14k activator aids in the incorporation of the cobalt ion into the active site of nitrile hydratase (Wu et al., 1997). The cobalt nitrile hydratases of *Pseudomonas putida* NRRL-18668 and *Rhodococcus jostii* RHA1 also require P14K and AnhE activators, respectively (Okamoto et al., 2010; Wu et al., 1997; Liu et al., 2013).

The *P. putida* UW4 iron-type nitrile hydratase does not require an activator protein for activity although there is a putative P47K activator encoded downstream of the β -subunit. The nitrile hydratase enzyme displayed highest activity in the absence of

both iron and P47K (Table 6). When exogenous iron was added to the growth medium, the enzyme did not display any activity. Perhaps this enzyme requires trace amounts of iron, which are already present in the nutrient growth medium and additional iron supplementation has inhibitory effects. When nitrile hydratase was co-expressed with the P47K activator and iron, it displayed ~27% of the activity of nitrile hydratase alone. In the absence of iron but in the presence of activator, the activity was ~8% of nitrile hydratase alone. The nitrile hydratase and P47K activator were co-expressed thus the exact proportion of each enzyme in the assay could not be determined, only the total enzyme concentration. Therefore, perhaps the difference in activity between the nitrile hydratase alone vs. with activator, was a result of less nitrile hydratase being present in the latter sample. When the total enzyme concentration was increased from 50 mg/mL to 100 mg/mL, the activity of nitrile hydratase alone increased by ~50%, while that of nitrile hydratase, P47K activator and iron increased by ~95%. These preliminary results suggest that the P47K protein is not essential for UW4 nitrile hydratase activity, however the possibility that P47K is involved in iron trafficking cannot be ruled out.

Nitrilase vs. Nitrile Hydratase

Both nitrilase and nitrile hydratase act on nitrile substrates, however enzyme assays show that generally, the specific activity of nitrile hydratase is much higher than that of nitrilase (Kobayashi and Shimizu, 2000). The two enzymes have completely different reaction mechanisms; nitrilase has an active cysteine residue involved in the hydrolysis of the nitrile, whereas nitrile hydratase has the metal ion in the catalytic site (Kobayashi and Shimizu, 2000). To highlight the remarkable difference in activity

between these two enzymes, the specific activities of nitrilase vs nitrile hydratase from different bacteria are listed in Table 13. The difference between the *P. putida* UW4 nitrilase vs nitrile hydratase activity was also evident in this study. In some instances, the UW4 nitrile hydratase activity was ~25X higher than that of UW4 nitrilase. The time course assay of nitrilase activity shows the accumulation of products over time for up to 6 hours (Figure 21). However, the reaction was allowed to progress for 48 hours at 30°C and ~10X more product accumulated by this point (data not shown in Figure 21). These results indicate that the nitrilase enzyme is slow acting and stable. Although the specific activity of nitrilase is low, it is enough to produce IAA concentrations capable of exerting hormonal action in plant cells.

Bacteria	Substrate	Enzyme	Specific Activity (units/mg)	Reference
<i>Nocardia</i> sp. NCIB 11215	benzonitrile	nitrilase	1.74	Harper, 1985
<i>Nocardia</i> sp. NCIB 11216	benzonitrile	nitrilase	15.7	Harper, 1977
<i>Arthrobacter</i> sp. J-1	benzonitrile	nitrilase	1.31	Bandyopadhyay et al., 1986
<i>R. rhodochrous</i> J1	benzonitrile	nitrilase	15.9	Kobayashi et al., 1989
<i>Klebsiella ozaenae</i>	bromoxynil	nitrilase	25.7	Stalker et al., 1988
<i>R. rhodochrous</i> K22	crotononitrile	nitrilase	0.737	Kobayashi et al., 1990
<i>A. faecalis</i> JM3	indole-3-acetonitrile	nitrilase	14.8	Kobayashi et al., 1993
<i>Pseudomonas chlororaphis</i> B23	propionitrile	nitrile hydratase	1840	Nagasawa et al., 1987
<i>Brevibacterium</i> R312	propionitrile	nitrile hydratase	1890	Nagasawa et al., 1986
<i>Rhodococcus</i> sp. N-774	propionitrile	nitrile hydratase	1260	Endo and Watanabe, 1989

Table 13. The specific activity of nitrilase and nitrile hydratase enzymes from various bacteria

THE GENES

Searching the sequenced *P. putida* UW4 genome for IAA-associated genes revealed the presence of orthologous genes in other IAA-producing bacteria such as *P. fluorescens* SBW25 and *P. putida* F1 (Duan et al. 2012). The putative IAA-biosynthesis genes in UW4 were identified based on sequence similarity to IAA biosynthesis genes from different bacteria. However, the enzymes encoded by these genes must be experimentally confirmed to synthesize IAA.

Each of the seven putative IAA biosynthesis genes was PCR amplified from genomic DNA of wild-type *P. putida* UW4. The primers used for this amplification were designed to contain restriction enzyme sites (NdeI, XhoI/HindIII) that would facilitate directional cloning in the pET30b(+) expression vector. The initiation codons of all of the subcloned genes is at the NdeI site of pET30b(+). Thus, in these constructs, each gene is preceded by a ribosome binding sequence with an appropriate interval sequence, which is optimal for expression in *E. coli*. For the two-subunit nitrile hydratase protein (NthAB), the b subunit is expressed using the original ribosomal binding sequence of *P. putida* UW4 that is contained within the short intergenic region between the a and b subunit. The isolated ORFs of each of the amplified and cloned genes are as follows: *nit*-924bp, *nthAB*-1305bp, *ami*-1515, *pheD*-1059bp, *aux*-1947bp, *iaaM*-1683bp, *P47K*-1224bp. However, since the project focused on the Nit and NthAB enzymes specifically, only their respective gene organizations were analyzed.

Genetic Organization on the UW4 Chromosome

Nitrile Hydratase

The genetic organization of IAA genes on the bacterial chromosome may reveal how the IAA biosynthetic pathways are regulated. For example, the literature suggests that there is a difference in the gene cluster arrangement and expression pattern between cobalt and iron-type nitrile hydratases (Lu et al., 2003). Generally iron-type nitrile hydratases exist in an operon consisting of *nhr2*, *nhr1*, *ami*, *nha1* (a), *nha2* (b), and *nha3*. These six genes encode nitrile hydratase regulator 2, regulator1, amidase, nitrile hydratase α subunit, nitrile hydratase β subunit and nitrile hydratase activator, respectively (Lu et al., 2003). The *nhr1* gene encodes a protein similar to the positive regulators NhlC and NhhC of the *R. rhodochrous* J1 nitrile hydratases (Kobayashi and Shimizu 1998; Komeda et al., 1996) and to the AmiC negative regulator of the amidase operon from *P. aeruginosa* (Wilson and Drew, 1991, 1995). The *nhr2* gene shares homology with the metalloregulatory transcriptional repressors SmtB/ArsR and with MerR transcriptional activators (Brown et al. 2003; Busenlehner et al.2003; Cervantes and Murillo 2002). This organization of genes is typically found in iron-type nitrile hydratase gene clusters including those of *P. chlororaphilis* B23 (Nishiyama et al. 1991) *R. erythropolis* JCM6823 (Duran et al. 1993) and *Rhodococcus* sp. N-774, N-771, R312 (Ikehata et al. 1989; Mayaux et al. 1990; Nojiri et al. 1999). Amidase (*ami*) genes are often found adjacent to nitrile hydratase (*nthAB*) genes as they convert the amide product of the nitrile hydratase to the corresponding carboxylic acid (Song et al., 2008). Genes encoding predicted amidases are found to be encoded upstream of a predicted nitrile hydratase in *R. jostii* RHA1, *A. radiobacter* K84, *B. japonicum* USDA 110 and *Ruegeria*

pomeroya DSS-3 (Patten et al., 2012). Xie et al., 2003, were the first to demonstrate a genetic relationship between aldoxime dehydratase, nitrile hydratase and amidase in *R. globerulus*. In this bacterium, the iron-type nitrile hydratase operon contains an AraC-like transcriptional activator and an aldoxime dehydratase gene upstream of the *nhr2* gene.

The *P. putida* UW4 nitrile hydratase gene cluster is organized as follows: AraC transcriptional activator (*AraC*), phenylacetyldoxime dehydratase (*pheD*), hypothetical protein (putative COG4313 protein involved in meta-pathway of phenol degradation), amidase (*ami*), nitrile hydratase a subunit (*nthA*), nitrile hydratase b subunit (*nthB*) and cobalamin synthesis protein/putative GTPase (*P47K* activator) (Figure 35). The nitrile hydratase gene cluster of UW4 includes neighboring amidase and phenylacetyldoxime dehydratase enzymes as were described for *R. globerulus* (Xie et al., 2003). We hypothesize that the phenylacetyldoxime dehydratase (*pheD*) converts the intermediates IAOx into IAN, which is then converted into IAM by nitrile hydratase (*nthAB*). The IAM intermediate is subsequently converted into the final product IAA by the amidase (*ami*) (Figure 7). The organization of these four IAA- genes (*pheD*, *nthA*, *nthB* and *ami*) in a putative operon reflects their concerted action in IAA biosynthesis.

Nitrilase

Since genes that are involved in a common metabolic process are often clustered in operons, analyzing the genetic neighbourhood of nitrilase genes might provide some insight into the function of this broad enzyme (Podar et al., 2005; Howden et al., 2009). Kiziak et al., (2005), report that the nitrilase from *Pseudomonas fluorescens* EBC191 is

able to hydrolyze mandelonitrile. The nitrilase gene is located close to a group of genes that encode enzymes in the mandelate pathway (Kiziak et al., 2005). The nitrilase gene from *Bacillus* sp. OxB-1 is upstream of the phenylacetaldoxime dehydratase gene, whose product converts phenylacetyldoxime and indoleacetaldoxime into phenylacetoneitrile and indole-3-acetonitrile, respectively (Kato et al., 2000). Once the indole-3-acetonitrile intermediate is formed, nitrilase can convert it directly into IAA (Howden et al., 2009). The nitrilase regions of *Pseudomonas syringae* B728a and DC3000 are highly conserved. The gene upstream of nitrilase encodes a putative phenylacetaldoxime dehydratase (Feil et al., 2005) and the gene downstream a putative positive transcriptional regulator belonging to the AraC family. *Rhodococcus rhodochrous* J1 and *Bacillus* sp. OxB-1 nitrilase regions also contain an AraC-type transcriptional regulator. This regulator has been shown to be essential for nitrilase activity in *R. rhodochrous* (Kato et al., 2000; Komeda et al., 1996; Howden et al., 2009).

There are eight genes belonging to the nitrilase superfamily in the genome of *P. putida* UW4 (Duan et al., 2012). However, only one of these enzymes (Nit-protein I.D AFY19658.1) has been experimentally confirmed to have true nitrile hydrolyzing activity; i.e. in this study. The remaining seven genes encode putative cyanide hydratases and aliphatic nitrilases with unknown substrate specificities and activities. The genetic organization of all eight putative nitrilase genes has been examined and is shown in Figures 36 and 37.

The *P. putida* UW4 nitrilase (*nit*) gene characterized in this study is organized as

follows: hypothetical protein, *LysR* transcriptional activator, nitrilase (*nit*), COG0365 Acyl-coenzyme A synthetases/AMP-fatty-acid ligase, 3-hydroxyacyl-CoA dehydrogenase, COG0183 Acetyl-CoA acetyltransferase, COG1960 Acyl-CoA dehydrogenase, COG1024 Enoyl-CoA hydratase/carnithine racemase, COG1960 Acyl-CoA dehydrogenase and COG1024 Enoyl-CoA hydratase/carnithine racemase (Figure 36). *LysR* transcriptional activators regulate genes involved in many different processes including, metabolism, cell division, quorum sensing, virulence, motility, nitrogen fixation, oxidative stress responses, toxin production, attachment and secretion (Kovacikova & Skorupski, 1999; Deghmane et al. , 2000, 2002; Cao et al. , 2001; Kim et al. , 2004; Russell et al. , 2004; Byrne et al. , 2007; Lu et al. , 2007; Sperandio et al. , 2007; Maddocks et al., 2008). Whether or not this *lysR* regulator is involved in the regulation of the nitrilase enzyme and/or of the downstream acetyl-coA related genes is unclear at the present time. In addition, it is unknown whether all the downstream acetyl-CoA related genes participate in a similar metabolic process.

Each of the remaining seven nitrilase family genes is flanked by genes encoding different proteins (Figure 33). Two of these genes, encoding nitrilase proteins AFY20214.1 and AFY21723.1, are linked to an AraC -type transcriptional regulator as has been reported for the nitrilases of *Rhodococcus rhodochrous* J1, *Bacillus sp.* OxB, *Pseudomonas syringae* B728a and DC3000. However, none of the eight *P. putida* UW4 nitrilase superfamily genes are associated with a phenylacetaldoxime dehydratase gene as is the case for *Bacillus sp.* OxB-1, *Pseudomonas syringae* B728a and DC

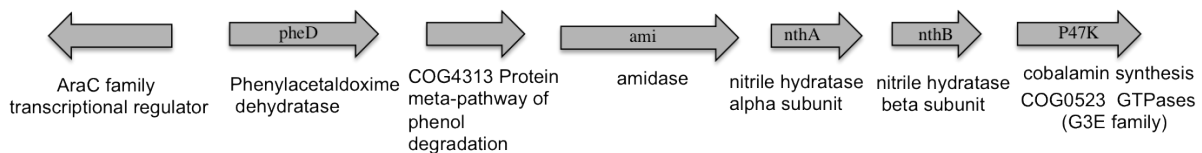


Figure 35. Genetic organization of the nitrile hydratase gene cluster of *P. putida* UW4.

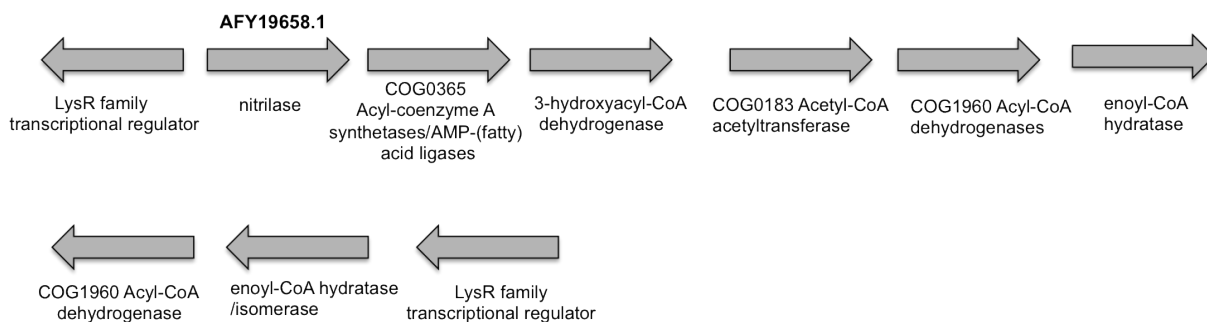


Figure 36. Genetic organization of the characterized nitrilase gene of *P. putida* UW4

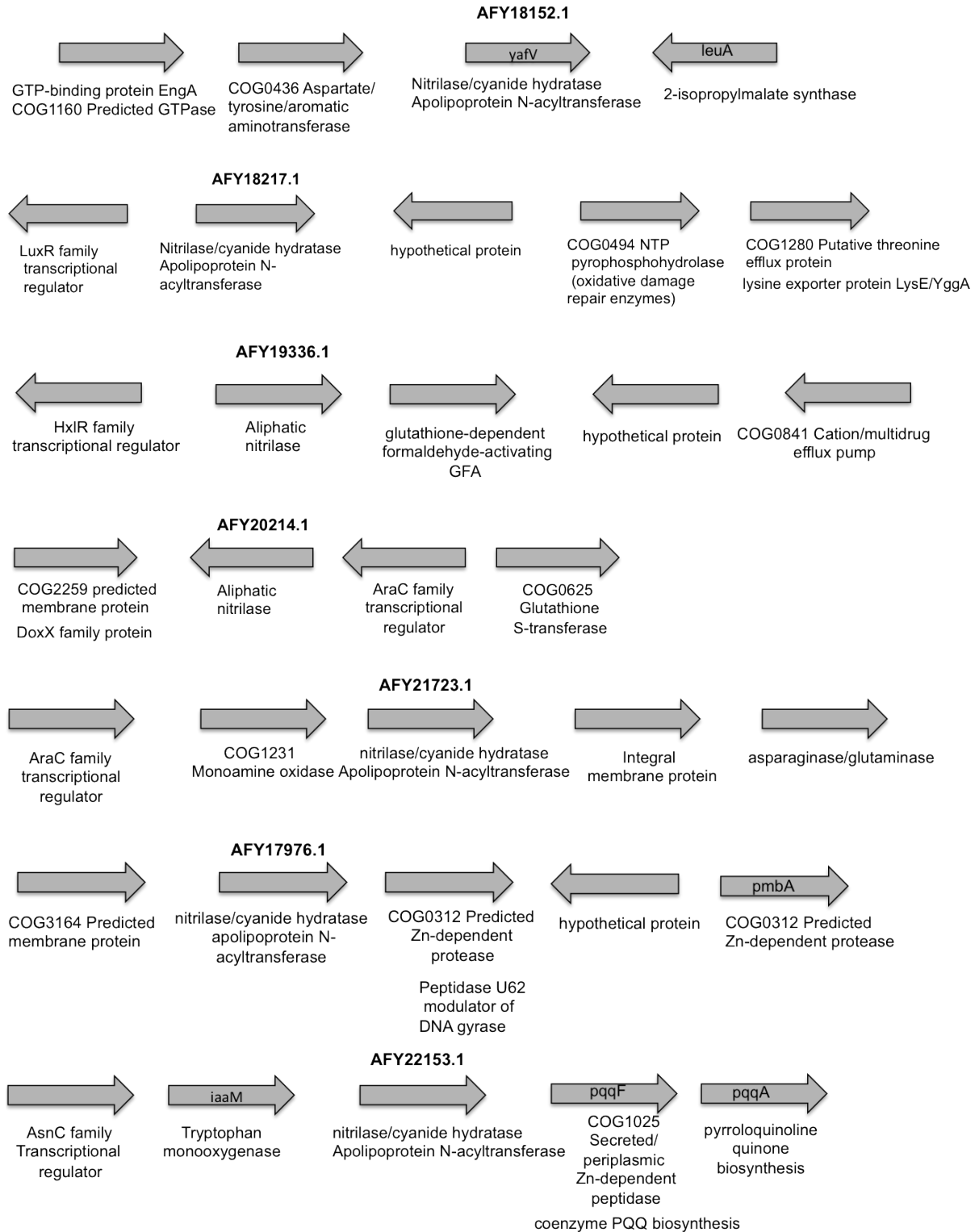


Figure 37. Genetic organization of the seven putative nitrilase superfamily genes of *P. putida* UW4

SEQUENCE ALIGNMENTS

Nitrilase

The nitrilase superfamily is composed of smaller subfamilies with distinct enzymatic properties. These subfamilies have likely undergone functional diversification to carry out the specific biological roles necessitated by different environmental conditions. An ecological niche imparts certain selection pressures upon the genomes of the bacteria living there. This promotes the formation of gene clusters, which encode enzymes that have linked metabolic activities (Podar et al., 2005).

Many bacterial genomes encode multiple nitrilase proteins from various branches of the superfamily. For example, *Pseudomonas*, *Klebsiella* and *Burkholderia* each harbor two nitrilases from different subfamilies (Podar et al., 2005). *P. putida* UW4 harbors eight nitrilase-like genes, some of which may belong to different subfamilies. These multiple copies may come from gene duplications over the course of evolution or horizontal gene transfer. *Klebsiella pneumonia* was found to harbor a nitrilase gene on a plasmid, which supports the possibility of horizontal gene transfer to other bacteria (Podar et al., 2005).

Pace and Brenner (2001), aligned 176 nitrilase members belonging to a single branch of the superfamily based on E-values. The Expect (E) value is a parameter that describes the number of hits in a BLAST search expected to arise by chance. The lower the E-value, the more "significant" the match is (NCBI). Pace and Brenner (2001) suggest that within most nitrilase branches, there is a cutoff such that sequences with E-

values greater than 1×10^{-25} can be assumed to belong to another branch of the superfamily. In our study, a multiple sequence alignment was constructed from a protein Blast search against the *P. putida* UW4 nitrilase gene. Only Blast hits that shared at least 50% identity with the nitrilase gene of *P. putida* UW4 were included in the alignment. The E-values in this alignment ranged from $0-3 \times 10^{-159}$ and were considered significant. Most of the nitrilase sequences ranged from 300- 400 amino acids in length, however the alignment spanned 307 positions after manual refinement and removing sites that could not be reliably aligned. The catalytic triad (E-K-C) was conserved in all sequences in alignment positions Glu44, Lys131, and Cys165. Based on previously aligned nitrilase sequences, the reported consensus sequences flanking the invariant catalytic triad residues are: f P E a f | h R K l _ p T l l _ C W E n _ _ p | upper case letters indicate 90% or greater consensus levels within a branch, whereas lower case are 50% or greater, the underscore (_) represent residues with less than 50% consensus (Pace and Brenner, 2001). In this study the consensus sequences flanking the catalytic triad of the UW4 nitrilase are: m P E A l | H R K L M P T | a i C W E N _ M P. Of the 307 positions in the nitrilase alignment, 44 had 100% consensus, 128 had at least 90% consensus and 253 had at least 50% consensus.

The regions around the catalytic triad were further examined for conservation, taking into account only sites with at least 90% consensus. The region surrounding the catalytic glutamate (E44) has a sequence of LVV_ PEA _ LGGYPKG. The region surrounding the catalytic lysine (K131) has a sequence of: HRKLMPT _ _ ERLIWG _ GDGST. Lastly, the region surrounding the catalytic cysteine (C165) has a sequence

of : **CWEN** _ **MPLLR** _ **AMY**. The residues highlighted in grey were 100% conserved over all of the nitrilase sequences, residues that are not highlighted have at least 90% consensus, while the underscore (_) represents residues with < 90% consensus.

Most nitrilases have a **CWE** motif starting with the catalytic cysteine, however, nitrilases that have been experimentally confirmed to act upon larger substrates such as 2-phenylvaleronitrile, mandelonitrile, and bromoxynil (3,5-dibromo-4-hydroxybenonitrile) have a **CAE** motif (McBride et al., 1986; Robertson et al., 2004; Kiziak et al., 2005; Seffernick, et al., 2009). In the present study, the **CWE** motif was 100% conserved in all the sequences analyzed, including the *P. putida* UW4 nitrilase. Perhaps the UW4 nitrilase cannot utilize such large substrates, although it can utilize indole-3-acetonitrile, which has a similar molecular weight and aromatic structure as phenylvaleronitrile and mandelonitrile.

Sharma and Bhalla (2012), suggest that aromatic nitrilases can be differentiated from aliphatic nitrilases based on four conserved motifs. These motifs were identified in the UW4 nitrilase as being representative of aromatic-type nitrilases (Table 9). Moreover, aliphatic and aromatic nitrilases can be differentiated based on their physicochemical properties. Sharma et al. 2009, report different physicochemical average parameter values for aliphatic vs aromatic nitrilases. When the physicochemical properties of *P. putida* UW4 nitrilase (Nit) were analyzed, for every parameter considered, they best fit to those reported for aromatic nitrilases (Table 10).

Nitrile Hydratase

Multiple sequence alignments were constructed from protein Blast searches against the *P. putida* UW4 nitrile hydratase α -subunit and β -subunit amino acid sequences. Only hits that shared at least 50% identity with the nitrile hydratase of *P. putida* UW4 were included in the alignments. The E-values in the alignments ranged from 10^{-58} - 10^{-142} for the α -subunit and 10^{-34} - 10^{-159} for the β -subunit and were considered significant.

Most of the α -subunit sequences ranged between 177-210 amino acids in length, however the alignment spanned 194 positions after manual refinement and removing sites that could not be reliably aligned. The β -subunit sequences ranged from 175-233 amino acids and the alignment spanned 217 positions.

Nitrile hydratases have a highly conserved CXLCSC motif, where X corresponds to a T (threonine) residue for cobalt-type or S (serine) residue for iron-type nitrile hydratases. This motif encompasses the metal binding site and exists within the sequence of the α -subunit (Precigou et al., 2001). Analysis of the multiple sequence alignment reveals that this metal binding motif was conserved in all α -subunit sequences in positions 98-103. Both cobalt and iron-type nitrile hydratases were included in this alignment. Of the 194 positions in the α -subunit alignment, 32 had 100% consensus, 65 had at least 90% consensus and 146 had at least 50% consensus. Of the 217 positions in the β -subunit alignment, 44 had 100% consensus, 110 had at least 90% consensus and 199 had at least 50% consensus. There is more conservation between the different β -

subunits analyzed than the α -subunits.

P47K Putative Activator Protein

Multiple sequence alignments were constructed from protein Blast searches against the *P. putida* UW4 P47K amino acid sequence. Only hits that shared at least 50% identity with the putative activator protein of *P. putida* UW4 were included in the alignments. The E-values in the alignments ranged from 0- 10^{-155} and were considered significant.

Most of the P47K homologs ranged between 396- 430 amino acids in length, however the alignment spanned 409 positions after manual refinement. Members of the nitrile hydratase activator proteins contain a highly conserved CXCC motif (Lu et al., 2003). Analysis of the multiple sequence alignment reveals a cysteine-rich motif CICC at positions 71-74, which was conserved in all the amino acid sequences analyzed including *P. putida* UW4 P47K. Studies suggest that this motif may be involved in metal trafficking for nitrile hydratase (Lu et al., 2003). Of the 409 positions, 112 had 100% consensus, 168 had at least 90% consensus and 311 had at least 50% consensus.

The P47K protein of *P. putida* UW4 is a member of the COG0523 proteins. This protein family comprises of cobalamin biosynthesis proteins, nitrile hydratase activators and zinc-transport proteins. It is an example of systematic, homology-based mis-annotation, as members are assigned to one of these three functions based only on

homology to a few family members. The COG0523 proteins belong to the G3E family of GTPases. They are characterized by the Walker A (GxxGxGK), Walker B (hhhExxG) and NKxD motifs. Only the two Walker motifs were identified in the amino acid sequence of the UW4 P47K protein, however the Walker B motif did not have the “hhh” stretch but instead had LLI which was 100% conserved in all sequences. Characterized members of the G3E family either help incorporate a co-factor into the target protein’s catalytic site or store/deliver a metal cofactor to a target metalloprotein. These metallochaperones are characterized by a histidine stretch. COG0523 members generally have a well-conserved N-terminal region and a variable C-terminal region. This was evident in our multiple sequence alignment of the P47K putative activator. Moreover, COG0523 genes have been labeled as "segmentally variable genes" (SVGs)," because they code for proteins that have highly variable regions interspersed with well-conserved regions (Zheng et al., 2004; Haas et al., 2009).

The UW4 P47K putative activator protein shares 58-98% sequence identity with proteins that have been annotated as 4-hydroxytetrahydrobiopterin dehydratases and 56-74% identity with cobalamin synthesis proteins in the NCBI database. Most bacteria produce enzymes that require cobalamin (vitamin B12) as a cofactor and thus have the ability to synthesize it. Cobalamin has a centrally chelated metal ion such as cobalt, which is delivered by ATP-dependent cobalt chelatases (Rodionov et al., 2003). Since the UW4 P47K is annotated as a cobalamin synthesis protein (Duan et al., 2012), the amino acid sequence was compared to those of the cobalt chelatases CobN, CobS, and CobT of *P. denitrificans*, CbiK from *S. typhimurium* and CbiX from *B. megaterium*. There is no

significant sequence similarity with any of these proteins. Although the *P. putida* UW4 P47K protein is annotated as a "cobalamin biosynthesis protein" based on sequence similarity, it is not necessarily a true labeling of function. Haas et al., (2009) performed comparative genomic and phylogenetic analysis of COG0523 protein members and reports that true cobalamin synthesis proteins (CobW) represent only 12.5% of the COG0523 family. Moreover, cobW genes in Proteobacteria are located within the cobalamin biosynthesis gene clusters and all CobW proteins analyzed contain a histidine-stretch of 4 – 15 residues (Haas et al., 2009). Neither of these criteria hold true for the P47K protein of UW4. There are no histidine-rich motifs and the gene is not located near other cobalamin-related genes.

On the other hand, UW4 P47K does share significant sequence identity with some experimentally confirmed nitrile hydratase activators. For example, it shares 46% identity with the P47K activator of *Rhodococcus* sp. N-771, 46% with P47K of *Rhodococcus* sp. N-774, 74% with P47K of *Pseudomonas chlororaphis* B23 and 59% identity with the P44K activator of *Rhodococcus erythropolis* AJ270. These proteins have been shown to be involved in the functional expression of iron-nitrile hydratase (Hashimoto et al. 1994; Nojiri et al. 1999; Goda et al. 2002; Lu et al., 2003). UW4 P47K does not share any significant identity with the *Rhodococcus rhodochrous* J1 nitrile hydratase activator P14K that mediates cobalt trafficking and is essential for activity of cobalt-type nitrile hydratase (Zhou et al., 2009). Likewise, there is no significant homology with the AnhE activator of *Rhodococcus jostii* RHA1, which is required for the in vivo production of functional cobalt-nitrile hydratase (Okamoto et al., 2010). The sequence similarities suggest that UW4 P47K is specifically an iron-type nitrile hydratase activator, perhaps

playing a role in the incorporation of iron into the active site. Haas et al., (2009), report that nitrile hydratase activators represent less than 1% of the COG0523 protein family. Moreover, these authors report that these activators are found clustered exclusively with the genes encoding the two subunits of the iron-type nitrile hydratase (Haas, et al., 2009). This holds true for the *P47K* gene of UW4, as it is located directly downstream of the β -subunit of the nitrile hydratase (Figure 35).

PHYLOGENETIC TREES

Maximum-likelihood (ML), neighbor-joining (NJ) and maximum parsimony (MP) trees were constructed to infer the phylogeny of nitrilase, nitrile hydratase α and β subunits and the P47K activator protein. The topology between the three different types of trees was nearly identical for each data set.

Nitrilase Phylogeny

The nitrilase phylogenetic analysis included microbial, yeast and plant enzymes (Figure 31). The pseudomonad nitrilases (including UW4 Nit) form a well-supported monophyletic group (Figure 31). It was expected that the UW4 nitrilase is most closely related to other nitrilases from the same bacterial species. *Serratia* sp. M24T3 is a sister taxa to the pseudomonad clade. This bacterium was isolated from pinewood nematode trails and is suspected to have bionematocide action on nematodes that cause pine wilt disease (Proenca et al., 2012). The *Achromobacter* genus forms a distinct clade, with *Acidovorax* sp. CF316 grouping within. *Achromobacter* species are isolated from water environments and are known to cause bacteremia in humans (Duggan et al., 1996). The

Burkholderia genus also forms a well-supported monophyletic clade with most species (*B. gladioli*, *B. glumae*, *B. cepacia*, *B. cenocepacia*) being plant pathogens and some (*B. multivorans*, *B. ambifaria*) being associated with human diseases such as cystic fibrosis (Vandamme et al., 1997; Coenye et al. 2001). *Dickeya* and *Pantoea*, both phytopathogens are sister taxa. *Acidovorax avenae* ATCC 19860 and *Frateuria aurantia* DSM 622, both plant-associated bacteria (Schaad et al., 2008) form a monophyletic clade with two *P. putida* strains. Interestingly these two pseudomonad strains did not group with the rest of the pseudomonad clade. All of the yeast nitrilases analyzed formed a well-supported monophyletic clade. The yeasts share a common ancestor with a monophyletic clade of marine-associated bacteria as well as with most of the other bacterial nitrilases suggesting horizontal gene transfer. *Glaciacola polaris* LMG 21857 was isolated from arctic seawater and is sister taxa to *Glaciacola mesophila* KMM 241 isolated from marine invertebrates and *Pseudoalteromonas atlantica* T6c isolated from marine algae (Guo et al., 2009; Costa-Ramos and Rowley, 2004; Trappen et al., 2004).

Within the plant kingdom, nitrilases are ubiquitously distributed from mosses to higher plants. The plant nitrilases from *Arabidopsis*, rice and tobacco group into a well-supported monophyletic clade. *Arabidopsis* has four nitrilases (NIT 1-4), the first three share high sequence similarity (84–90%), but are less similar to NIT4 (66–68%) (Jenrich et al., 2007). The *Arabidopsis* NIT 1-3 seems to have evolved from the NIT4 progenitor, which in this phylogenetic analysis is a sister taxa to the rice and tobacco NIT4 clade. *A. thaliana* NIT 1-3 have been shown to act on a broad range of aliphatic and aromatic nitriles as substrates, reflecting neofunctionalization during the evolution of the flowering

plants (Jenrich et al., 2007). Members of the NIT4 family of nitrilases have cyanoalanine hydratase activity and are involved in cyanide detoxification in plants. Species from the grass family contain two NIT4 homologs (called NIT4A and NIT4B) that must form heterocomplexes to gain b-cyanoalanine hydrolyzing activity (Jenrich et al., 2007; Kriechbaumer et al., 2007; Park et al., 2003). This is a likely result of an early gene duplication event via paleopolyploidization during evolution of the grass family (Jenrich et al., 2007). *Sorghum bicolor* possesses two isoforms of NIT4B, one of which has undergone neofunctionalization and gained the ability to use different nitrile substrates including the indole-3-acetonitrile (IAN) precursor of IAA (Jenrich et al., 2007). Most flowering plants produce the defense compound glucobrassicin, from which IAN can be released. Hydrolysis of IAN by nitrilases leads to the production of IAA. However, these glucobrassicin producing plants contain NIT1-3 homologs that have low activity on IAN (Agerbirk et al., 2008; Ishikawa et al., 2007; Osswald et al., 2002; Vorwerk et al., 2001). This is because since the IAN substrate is plentiful in these plants, nitrilases with greater IAN-hydrolyzing activity would severely disturb IAA homeostasis. On the other hand, plants that do not contain glucobrassicin and therefore have limited amounts of IAN precursor, evolve highly active IAN-nitrilases. An example of such a plant is *Sorghum*, in which the NIT4B2 isoform has very high activity on IAN (Jenrich et al., 2007). *Capsella rubella*, a close relative of *Arabidopsis*, produces two long-chain glucosinolates and one short-chain glucosinolate. As a result, it has evolved two NIT1 homologs, one that acts on short-chain nitriles and the other on long-chain nitriles (Janowitz et al., 2009). Altogether, these findings suggest that the nitrilase homologs have evolved to accommodate the substrates most available to them and to carry out the biological

function best suited for that particular plant (Janowitz et al., 2009).

An intriguing finding from our nitrilase phylogeny analysis, is that two bacterial nitrilases (*Rhizobium etli* and *Bradyrhizobium japonicum* USDA 110) cluster with the plant nitrilases rather than the bacterial nitrilases (Figure 31). They form a well-supported monophyletic group with the *Arabidopsis*, rice and tobacco nitrilases. Both of these bacteria are nitrogen-fixing plant-symbionts that colonize plant roots and live inside root nodules (Morris et al., 2005; Liu et al., 2007). Since bacteria evolved before plants and these rhizobia form such intimate relationships with their host plant, perhaps the plant nitrilase genes were acquired from these bacteria via a lateral gene transfer at some point throughout evolution.

The phylogenetic tree (Figure 31). shows that nitrilases exist in different bacterial species, inhabiting diverse environments from soil to water. These microbial nitrilases have evolved to carry out a specific biological role. Podar et al., (2005) analyzed microbial nitrilases and identified several residues under strong positive selection in one of two nitrilase lineages analyzed. It is likely that advantageous mutations were fixed at specific sites in these enzymes. They also found that purifying selection has a dominant role across one of the nitrilase sub-families analyzed, indicated by the large number of conserved amino acids. They hypothesize that a group of microbial nitrilases diverged functionally and became associated with other metabolic enzymes and this is reflected by their diverse biochemical activities (Podar et al., 2005).

Nitrile Hydratase Phylogeny

The phylogenetic analyses of the nitrile hydratase α and β subunits included only microbial enzymes. The maximum-likelihood (ML) tree generated for the α -subunit (Figure 32) clusters all the pseudomonads (including NthA of *P. putida* UW4) into a well-supported monophyletic clade. We would expect that UW4 nitrilase is most closely related to nitrile hydratase α -subunits from the same species. Unfortunately, none of the *Pseudomonas* nitrile hydratases within this clade have been experimentally characterized. However, their conserved metal co-factor binding motif identifies them as iron-type nitrile hydratases. This pseudomonad clade is sister to a well-supported iron-type nitrile hydratase *Burkholderia* clade, with the exception of *Burkholderia terrae* BS001, *Burkholderia* sp. BT03 and *Burkholderia phytofirmans* PsJN. These three latter strains are cobalt-type and form a separate clade that shares the most recent common ancestor with the cobalt-type enzymes of *Rhodopseudomonas* and *Bradyrhizobium* clades. Therefore, it appears that bacteria of the same genera (*Burkholderia*) will cluster separately based on the type of metal co-factor they associate with. There is also a distinct *Rhodococcus* clade that has *Microbacterium* sp. SS1-15, *Microbacterium* sp. AJ115 and *Bacillus* sp. SW2-21 nested within. The rhodococci clade forms a polytomy, with several immediate descendants coming off the same node. Brandao et al., (2003), report that strains of *R. erythropolis* from diverse geographical areas possess highly variable enzymatic activities. The variation of nitrile hydratases within a single species suggests a link between environmental/geographic factors and the speciation of microorganisms (Brandao et al., 2003). Some *R. erythropolis* strains possess identical

nitrile hydratase gene sequences, even though they inhabit incredibly different habitats. However, the activities of these enzymes have been shown to be different, reflecting a possible functional diversification to accommodate their environment (Brandao et al., 2003).

The tree topology (Figure 32.) showed a clear separation between the iron-type and the cobalt-type α -subunits. All of the iron-type nitrile hydratase descendants cluster into a monophyletic clade in the upper half of the tree (shown in red box), while the cobalt-type enzymes cluster into a separate monophyletic clade in the bottom half of the tree (shown in blue box).

The maximum-likelihood (ML) tree generated for the β -subunit (Figure 33.) also clusters all the pseudomonads (including NthB of *P. putida* UW4) into a well-supported monophyletic clade as was expected. The UW4 β -subunit is most closely related to other β -subunits from the same species. This pseudomonad clade is sister to the *Burkholderia* clade, a similar tree topology as for the α -subunit. The rhodococci fall into a cluster in the upper half of the tree and form a polytomy. This cluster is not well supported by bootstrap analysis. Perhaps the relatedness of these lineages cannot be well deciphered or all the descendants are very closely related to one another, as their sequence similarity is very high (~80-90%).

Looking at the overall topology of the β -subunit tree, it is separated into two clusters, one that makes up the upper-half of the tree and the other the bottom-half of the tree. This general tree topology was the same as the α -subunit tree. However in the case of the β -subunits, the separation of the two clades was not correlated with the type of metal that that nitrile hydratase associates with. For example, our UW4 nitrile hydratase is an iron-type and the β -subunit clusters in the bottom half of the tree along with other iron-type pseudomonad β -subunits. However, the *Rhodococcus* sp. 312, N-771 and AJ270 are also iron-type β -subunits and these cluster in the clade comprising the upper half of the tree.

P47K Putative Activator Protein Phylogeny

The phylogenetic analysis of the P47K putative activator proteins only includes bacteria. The maximum-likelihood (ML) tree (Figure 34) has multiple clusters of *Pseudomonas* proteins dispersed throughout the tree (pink boxes). The cluster consisting of *Pseudomonas* sp. PAMC 26793 to *P. putida* ND6 forms a well-supported monophyletic clade that includes proteins that have the NKXD motif. All the other pseudomonads in the analysis do not have this motif. This is a conserved motif of the G3E family of P-loop GTPases, so perhaps these *Pseudomonas* proteins belong to this family, while the others belong to a different GTPase class and thus cluster separately. The *P. putida* UW4 P47K protein forms a small cluster with other *Pseudomonas* spp. as was expected. The *Burkholderia* clade (orange box) is sister to the *Herbaspirillum* clade (grey box). When looking back at the multiple sequence alignment, there are blocks of

residues representing possible motifs that are conserved in some of the pseudomonads and not in others. One such block occurs at residues #89-92, where some of the *Pseudomonas* strains have a conserved KEGR sequence, while others have an RQQR sequence. The *Pseudomonas* strains that share the conserved KEGR block, cluster together in the upper region of the phylogenetic tree, while the strains that have the latter block cluster together in the lower region of the tree (*P. putida* UW4 included). Perhaps these protein sequence motifs are signatures of different protein families and are associated with different catalytic functions or protein structures (Bork and Coonin, 1996). The rhodococci form a well-supported monophyletic clade (purple box) that shares a common ancestor with some of the pseudomonads and the *Azotobacter* spp. (beige box) in the upper half of the tree. From the multiple sequence alignment, it was observed that only the *Rhodococcus* strains have an amino acid residue change from a “T” to an “S” in the Walker B motif (ESTG→ESSG). Sometimes even a single residue change in a protein sequence is enough to confer a new function, thus perhaps these rhodococci proteins cluster together based on the effect that the T to S residue change has on the overall protein.

Many of the proteins included in the tree are “hypothetical” proteins that have not been characterized but share sequence similarity with the P47K of UW4. Others are arbitrarily annotated as COG0523 family proteins, which can have various biological functions including zinc transport and cobalamin biosynthesis. The only proteins in the tree that have been experimentally characterized as iron-type nitrile hydratase activators are those of *Rhodococcus* sp. AJ270 and *P. chlororaphis*. While the P47K of UW4 shares sequence identity with these two activators and is related to them, the three of them do

not form a closely related clade together. The function of the UW4 P47K cannot be inferred from the tree topology (Figure 34).

CONCLUSION

IAA is a fundamental phytohormone with the capability of controlling many aspects of plant growth and development. *Pseudomonas putida* UW4 is a rhizospheric plant-growth-promoting bacterium that produces and secretes IAA. However, the biosynthesis pathways leading to the production of this phytohormone are not known. Throughout this study directed towards better understanding the biosynthesis of IAA in strain UW4, the functioning of two enzymes, nitrilase (Nit) and nitrile hydratase (NthAB), both of which mediate the IAN pathway, were investigated. Using enzyme assays, it was shown that both Nit and NthAB can act on the IAN substrate, producing the IAM intermediate, and IAA. NthAB has higher activity than Nit and the two enzymes have very different temperature and pH profiles. Based on multiple sequence alignments and motif analysis, physicochemical properties and enzyme assays, it is concluded that *P. putida* UW4 Nit has aromatic substrate specificity. The NthAB enzyme is identified as an iron-type metalloenzyme that does not require the help of the P47K activator protein to be active. Multiple sequence alignments and homology to other characterized proteins, suggest that the P47K protein of *P. putida* UW4 is an activator specific for iron-type nitrile hydratases, however its biological role must be further explored.

REFERENCES

- Abascal, Federico, Rafael Zardoya, and David Posada. "ProtTest: Selection of Best-Fit Models of Protein Evolution." *Bioinformatics* 21.9 (2005): 2104-5. Print
- Acharya, B. R., and S. M. Assmann. "Hormone Interactions in Stomatal Function." *Plant molecular biology* 69.4 (2009): 451-62. Print.
- Agerbirk, Niels, et al. "Phylogeny and Evolution of Glucosinolates and Specific Nitrile Degrading Enzymes." *Phytochemistry* 69.17 (2008): 2937-49. Print.
- Ahmed, Nazeer, et al. "Effect of Indole-3-Acetic Acid on Fruit Drop and Quality of Date Palm Cultivars." *Int.J.Agric.Appl.Sci.Vol* 4.2 (2012)Print.
- Ahmed, A., and S. Hasnain. "Auxin-Producing Bacillus Sp.: Auxin Quantification and Effect on the Growth of Solanum Tuberosum." *Pure and Applied Chemistry* 82.1 (2010): 313-9. Print.
- Ali, B., A. N. Sabri, and S. Hasnain. "Rhizobacterial Potential to Alter Auxin Content and Growth of Vigna Radiata (L.)." *World Journal of Microbiology and Biotechnology* 26.8 (2010): 1379-84. Print.
- Altschul, Stephen F., et al. "Basic Local Alignment Search Tool." *Journal of Molecular Biology* 215.3 (1990): 403-10. Print.
- Apine, O. A., and J. P. Jadhav. "Optimization of Medium for Indole-3-Acetic Acid Production using Pantoea Agglomerans Strain PVM." *Journal of applied microbiology* 110.5 (2011): 1235-44. Print.
- Artimo, Panu, et al. "ExpASY: SIB Bioinformatics Resource Portal." *Nucleic acids research* 40.W1 (2012): W597-603. Print.
- Atsushi, IKAI. "Thermostability and Aliphatic Index of Globular Proteins." *Journal of Biochemistry* 88.6 (1980): 1895-8. Print.
- Bandyopadhyay, A. K., T. Nagasawa, and Y. Asano. "Purification and Characterization of Benzonitrilase from Arthrobacter Sp. Strain J-1." *Applied and Environmental Microbiology* 51.2 (1986): 302-6. Print.
- Banerjee, A., R. Sharma, and U. Banerjee. "The Nitrile-Degrading Enzymes: Current Status and Future Prospects." *Applied Microbiology and Biotechnology* 60.1-2 (2002): 33-44. Print.
- Bartel, Bonnie, and Gerald R. Fink. "Differential Regulation of an Auxin-Producing Nitrilase Gene Family in Arabidopsis Thaliana." *Proceedings of the National Academy of Sciences* 91.14 (1994): 6649-53. Print.

- Bartling, Dieter, et al. "Cloning and Expression of an Arabidopsis Nitrilase which can Convert indole-3-acetonitrile to the Plant Hormone, indole-3-acetic Acid." *European journal of biochemistry* 205.1 (1992): 417-24. Print.
- Bartling, Dieter, et al. "Molecular Characterization of Two Cloned Nitrilases from Arabidopsis Thaliana: Key Enzymes in Biosynthesis of the Plant Hormone Indole-3-Acetic Acid." *Proceedings of the National Academy of Sciences* 91.13 (1994): 6021-5. Print.
- Benson, Dennis A., et al. "Genbank." *Nucleic acids research* 38.suppl 1 (2010): D46-51. Print.
- Beyeler, M., et al. "Effect of Enhanced Production of Indole-3-Acetic Acid by the Biological Control Agent Pseudomonas Fluorescens CHA0 on Plant Growth." *Plant Growth-Promoting Rhizobacteria: Present Status and Future Prospects. Organization for Economic Cooperation and Development, Paris* (1997): 310-1. Print.
- Bhalla, TC, et al. "The Molecular Cloning and Sequencing of the Nitrilase Gene of Rhodococcus Rhodochrous PA-34." *Acta Biotechnologica* 15.3 (1995): 297-306. Print.
- Bhalla, Tek Chand, and Harish Kumar. "Nocardia Globerula NHB-2: A Versatile Nitrile-Degrading Organism." *Canadian journal of microbiology* 51.8 (2005): 705-8. Print.
- Bhalla, Tek Chand, et al. "Asymmetric Hydrolysis of α -Aminonitriles to Optically Active Amino Acids by a Nitrilase of Rhodococcus Rhodochrous PA-34." *Applied Microbiology and Biotechnology* 37.2 (1992): 184-90. Print.
- Bianco, C., et al. "Indole-3-Acetic Acid Improves Escherichia Coli's Defences to Stress." *Archives of Microbiology* 185.5 (2006): 373-82. Print.
- Bianco, C., E. Imperlini, and R. Defez. "Legumes Like More IAA." *Plant Signaling and Behavior* 4.8 (2009): 763-5. Print.
- Bischoff, M., Low, R., Grsic, S., Rausch, T., Hilgenberg, W., and Ludwig-Müller. "Infection with the Obligate biotroph Plasmodiophora Brassicae, the Causal Agent of the Club Root Disease, does Not Affect Expression of NIT12-Related Nitrilases in roots of Chinese Cabbage." *Plant Physiol.* 147 (1995): 341-345. Print.
- Blakesley, D., GD Weston, and JF Hall. "The Role of Endogenous Auxin in Root Initiation." *Plant Growth Regulation* 10.4 (1991): 341-53. Print.
- Blakey, Alan J., et al. "Regio- and stereo-specific Nitrile Hydrolysis by the Nitrile Hydratase from Rhodococcus AJ270." *FEMS microbiology letters* 129.1 (1995): 57-61. Print.
- Booth, Ian R. "Regulation of Cytoplasmic pH in Bacteria." *Microbiological reviews* 49.4

- (1985): 359. Print.
- Bork, Peer, and Eugene V. Koonin. "Protein Sequence Motifs." *Current opinion in structural biology* 6.3 (1996): 366-76. Print.
- Brandão, Pedro FB, Justin P. Clapp, and Alan T. Bull. "Diversity of Nitrile Hydratase and Amidase Enzyme Genes in *Rhodococcus Erythropolis* Recovered from Geographically Distinct Habitats." *Applied and Environmental Microbiology* 69.10 (2003): 5754-66. Print.
- Brandl, M., E. M. Clark, and S. E. Lindow. "Characterization of the Indole-3-Acetic Acid (IAA) Biosynthetic Pathway in an Epiphytic Strain of *Erwinia Herbicola* and IAA Production in Vitro." *Canadian journal of microbiology* 42.6 (1996): 586-92. Print.
- Brandl, M. T., and S. E. Lindow. "Cloning and Characterization of a Locus Encoding an Indolepyruvate Decarboxylase Involved in Indole-3-Acetic Acid Synthesis in *Erwinia Herbicola*." *Applied and Environmental Microbiology* 62.11 (1996): 4121-8. Print.
- Brandl, M. T., B. Quiñones, and S. E. Lindow. "Heterogeneous Transcription of an Indoleacetic Acid Biosynthetic Gene in *Erwinia Herbicola* on Plant Surfaces." *Proceedings of the National Academy of Sciences of the United States of America* 98.6 (2001): 3454-9. Print.
- Brown, Nigel L., et al. "The MerR Family of Transcriptional Regulators." *FEMS microbiology reviews* 27.2-3 (2003): 145-63. Print.
- Brummell, David A., Coralie C. Lashbrook, and Alan B. Bennett. "Plant Endo-1, 4-Beta-D-Glucanases: Structure, Properties, and Physiological Function". *ACS symposium series*. 1994. Print.
- Busenlehner, Laura S., Mario A. Pennella, and David P. Giedroc. "The SmtB/ArsR Family of Metalloregulatory Transcriptional Repressors: Structural Insights into Prokaryotic Metal Resistance." *FEMS microbiology reviews* 27.2-3 (2003): 131-43. Print.
- Byrne, Gavin A., et al. "Transcriptional Regulation of the virR Operon of the Intracellular Pathogen *Rhodococcus Equi*." *Journal of Bacteriology* 189.14 (2007): 5082-9. Print.
- Cao, Hui, et al. "A Quorum Sensing-Associated Virulence Gene of *Pseudomonas Aeruginosa* Encodes a LysR-Like Transcription Regulator with a Unique Self-Regulatory Mechanism." *Proceedings of the National Academy of Sciences* 98.25 (2001): 14613-8. Print.
- Casal, Jorge J. "Photoreceptor Signaling Networks in Plant Responses to Shade." *Annual review of plant biology* 64 (2013): 403-27. Print.

- Catalá, Carmen, Jocelyn KC Rose, and Alan B. Bennett. "Auxin Regulation and Spatial Localization of an endo-1, 4- β -D-glucanase and a Xyloglucan Endotransglycosylase in Expanding Tomato Hypocotyls." *The Plant Journal* 12.2 (1997): 417-26. Print.
- Catalá, Carmen; Rose, Jocelyn KC; Bennett, Alan B "Auxin-Regulated Genes Encoding Cell Wall-Modifying Proteins are Expressed during Early Tomato Fruit Growth." *Plant physiology* 122.2 (2000): 527-34. Print.
- Cernadas, R. A., and C. E. Benedetti. "Role of Auxin and Gibberellin in Citrus Canker Development and in the Transcriptional Control of Cell-Wall Remodeling Genes Modulated by *Xanthomonas Axonopodis* Pv. Citri." *Plant Science* 177.3 (2009): 190-5. Print.
- Cervantes, María, and Francisco J. Murillo. "Role for Vitamin B12 in Light Induction of Gene Expression in the Bacterium *Myxococcus Xanthus*." *Journal of Bacteriology* 184.8 (2002): 2215-24. Print.
- Chen, Z., et al. "Pseudomonas Syringae Type III Effector AvrRpt2 Alters Arabidopsis Thaliana Auxin Physiology." *Proceedings of the National Academy of Sciences of the United States of America* 104.50 (2007): 20131-6. Print.
- Cheng Zhenyu, Park Eunmi and Glick Bernard R. "1-Aminocyclopropane-1-carboxylate deaminase from *Pseudomonas putida* UW4 facilitates the growth of canola in the presence of salt" *Can. J. Microbiol.* 53: (2007): 912–918 . Print
- Clark, Ellen, et al. "Cloning and Characterization of *iaaM* and *iaaH* from *Erwinia Herbicola* Pathovar *Gypsophila*." *Phytopathology* 83.2 (1993): 234-40. Print.
- Coenye, Tom, et al. "*Burkholderia Ambifaria* Sp. Nov., a Novel Member of the *Burkholderia Cepacia* Complex Including Biocontrol and Cystic Fibrosis-Related Isolates." *International Journal of Systematic and Evolutionary Microbiology* 51.4 (2001): 1481-90. Print.
- Coffey, Lee, et al. "Real-Time PCR Detection of Fe-Type Nitrile Hydratase Genes from Environmental Isolates Suggests Horizontal Gene Transfer between Multiple Genera." *Antonie van Leeuwenhoek* 98.4 (2010): 455-63. Print.
- Comai, L., and T. Kosuge. "Cloning and Characterization of *iaaM*, a Virulence Determinant of *Pseudomonas Savastanoi*." *Journal of Bacteriology* 149.1 (1982): 40-6. Print.
- Comai, L., and T. Kosuge. "Involvement of Plasmid Deoxyribonucleic Acid in Indoleacetic Acid Synthesis in *Pseudomonas Savastanoi*." *Journal of Bacteriology* 143.2 (1980): 950-7. Print.
- Costacurta, A., P. Mazzafera, and Y. B. Rosato. "Indole-3-Acetic Acid Biosynthesis by *Xanthomonas Axonopodis* Pv. Citri is Increased in the Presence of Plant Leaf

- Extracts." *FEMS microbiology letters* 159.2 (1998): 215-20. Print.
- Costacurta, A., and J. Vanderleyden. "Synthesis of Phytohormones by Plant-Associated Bacteria." *Critical reviews in microbiology* 21.1 (1995): 1-18. Print.
- Costa-Ramos, Carolina, and Andrew F. Rowley. "Effect of Extracellular Products of *Pseudoalteromonas Atlantica* on the Edible Crab Cancer *Pagurus*." *Applied and Environmental Microbiology* 70.2 (2004): 729-35. Print.
- Cui, Fuhao, et al. "The *Pseudomonas Syringae* Type III Effector AvrRpt2 Promotes Pathogen Virulence Via Stimulating Arabidopsis Auxin/Indole Acetic Acid Protein Turnover." *Plant physiology* 162.2 (2013): 1018-29. Print.
- Davies, Peter J. "The Plant Hormones: Their Nature, Occurrence, and Functions." *Plant Hormones*. Springer, 2010. 1-15. Print.
- Davies, P. J. *Plant Hormones: Physiology, Biochemistry, and Molecular Biology*. Kluwer Academic, 1995. Print.
- Deghmane, Ala-Eddine, et al. "Down-regulation of Pili and Capsule of *Neisseria Meningitidis* upon Contact with Epithelial Cells is Mediated by CrgA Regulatory Protein." *Molecular microbiology* 43.6 (2002): 1555-64. Print.
- Deghmane, Ala-Eddine, et al. "Intimate Adhesion of *Neisseria Meningitidis* to Human Epithelial Cells is Under the Control of the *crgA* Gene, a Novel LysR-Type Transcriptional Regulator." *The EMBO journal* 19.5 (2000): 1068-78. Print.
- Ding, Xinhua, et al. "Activation of the Indole-3-Acetic acid-amido Synthetase GH3-8 Suppresses Expansin Expression and Promotes Salicylate- and Jasmonate-Independent Basal Immunity in Rice." *The Plant Cell Online* 20.1 (2008): 228-40.
- Dobbelaere, S., et al. "Phyto-stimulatory Effect of *Azospirillum Brasilense* Wild Type and Mutant Strains Altered in IAA Production on Wheat." *Plant and Soil* 212.2 (1999): 155-64. Print.
- Doolittle, W. Ford. "Uprooting the Tree of Life." *Scientific American* 282.2 (2000): 90. Print.
- Duan, Jin, et al. "The Complete Genome Sequence of the Plant Growth-Promoting Bacterium *Pseudomonas* Sp. UW4." *PloS one* 8.3 (2013): e58640. Print.
- Duggan, Joan M., et al. "Achromobacter *Xylosoxidans* Bacteremia: Report of Four Cases and Review of the Literature." *Clinical infectious diseases* 23.3 (1996): 569-76. Print.
- Duran, Robert, et al. "Characterization of Nitrile Hydratase Genes Cloned by DNA Screening from *Rhodococcus Erythropolis*." *Bioscience, biotechnology, and biochemistry* 57.8 (1993): 1323-8. Print.

- Effenberger, Franz, and Steffen Oßwald. "Enantioselective Hydrolysis of (< i> RS</i>)-2-Fluoroarylacetonitriles using Nitrilase from< i> Arabidopsis thaliana</i>." *Tetrahedron: Asymmetry* 12.2 (2001): 279-85. Print.
- Efron, Bradley, Elizabeth Halloran, and Susan Holmes. "Bootstrap Confidence Levels for Phylogenetic Trees." *Proceedings of the National Academy of Sciences* 93.23 (1996): 13429-. Print.
- Eklund, D. M., et al. "Homologues of the Arabidopsis Thaliana SHI/STY/LRP1 Genes Control Auxin Biosynthesis and Affect Growth and Development in the Moss Physcomitrella Patens." *Development* 137.8 (2010): 1275-84. Print.
- Endo, Isao, et al. "Fe-Type Nitrile Hydratase." *Journal of inorganic biochemistry* 83.4 (2001): 247-53. Print.
- Endo, Takakazu, and Ichiro Watanabe. "Nitrile Hydratase of< i> Rhodococcus</i> Sp. N-774 Purification and Amino Acid Sequences." *FEBS letters* 243.1 (1989): 61-4. Print.
- Feil, H., et al. "Comparison of the Complete Genome Sequences of Pseudomonas Syringae Pv. Syringae B728a and Pv. Tomato DC3000." *Proceedings of the National Academy of Sciences of the United States of America* 102.31 (2005): 11064-9. Print.
- Fernandes, Bruno, et al. "Nitrile Hydratase Activity of a Recombinant Nitrilase." *Advanced Synthesis & Catalysis* 348.18 (2006): 2597-603. Print.
- Ferrari, S., et al. "Transgenic Expression of a Fungal Endo-Polygalacturonase Increases Plant Resistance to Pathogens and Reduces Auxin Sensitivity." *Plant physiology* 146.2 (2008): 669-81. Print.
- Fry, SC, et al. "Xyloglucan Endotransglycosylase, a New Wall-Loosening Enzyme Activity from Plants." *Biochem.j* 282 (1992): 821-8. Print.
- Fu, J., et al. "Manipulating Broad-Spectrum Disease Resistance by Suppressing Pathogen-Induced Auxin Accumulation in Rice." *Plant physiology* 155.1 (2011): 589-602. Print.
- Gaffney, T. D., et al. "Indoleacetic Acid Operon of Pseudomonas Syringae Subsp. Savastanoi: Transcription Analysis and Promoter Identification." *Journal of Bacteriology* 172.10 (1990): 5593-601. Print.
- Gaudin, Valérie, and Lise Jouanin. "Expression of Agrobacterium Rhizogenes Auxin Biosynthesis Genes in Transgenic Tobacco Plants." *Plant molecular biology* 28.1 (1995): 123-36. Print.
- Gasteiger, Elisabeth, et al. "Protein Identification and Analysis Tools on the ExPASy Server." *The Proteomics Protocols Handbook*.Springer, 2005. 571-607. Print.

- Glick, Bernard R. "The Enhancement of Plant Growth by Free-Living Bacteria." *Canadian journal of microbiology* 41.2 (1995): 109-17. Print.
- Glickmann, E., and Y. Dessaux. "A Critical Examination of the Specificity of the Salkowski Reagent for Indolic Compounds Produced by Phytopathogenic Bacteria." *Applied and Environmental Microbiology* 61.2 (1995): 793-6. Print.
- Goda, Masahiko, et al. "Isonitrile Hydratase from *Pseudomonas putida* N19-2 cloning, sequencing, gene expression, and identification of its active amino acid residue." *Journal of Biological Chemistry* 277.48 (2002): 45860-5. Print.
- Goldlust, Arie, and Z. Bohak. "Induction, Purification, and Characterization of the Nitrilase of *Fusarium Oxysporum* f. Sp. *Melonis*." *Biotechnology and applied biochemistry* 11.6 (1989): 581-601. Print.
- Gong, Jin-Song, et al. "Nitrilases in Nitrile Biocatalysis: Recent Progress and Forthcoming Research." *Microbial cell factories* 11.1 (2012): 1-18. Print.
- González-Lamothe, Rocío, et al. "The Conjugated Auxin Indole-3-Acetic Acid–Aspartic Acid Promotes Plant Disease Development." *The Plant Cell Online* 24.2 (2012): 762-77. Print.
- Gordon, Solon A., and Robert P. Weber. "Colorimetric Estimation of Indoleacetic Acid." *Plant physiology* 26.1 (1951): 192. Print.
- Grossmann, K. "Auxin Herbicides: Current Status of Mechanism and Mode of Action." *Pest management science* 66.2 (2010): 113-20. Print.
- Guilfoyle, Tom J., and Gretchen Hagen. "Auxin Response Factors." *Current opinion in plant biology* 10.5 (2007): 453-60. Print.
- Guo, Bing, et al. "Gene Cloning, Expression and Characterization of a New Cold-Active and Salt-Tolerant Endo- β -1, 4-Xylanase from Marine Glaciocola *Mesophila* KMM 241." *Applied Microbiology and Biotechnology* 84.6 (2009): 1107-15. Print.
- Guruprasad, Kunchur, BV Bhasker Reddy, and Madhusudan W. Pandit. "Correlation between Stability of a Protein and its Dipeptide Composition: A Novel Approach for Predicting in Vivo Stability of a Protein from its Primary Sequence." *Protein engineering* 4.2 (1990): 155-61. Print.
- Haas, Crysten, et al. "A Subset of the Diverse COG0523 Family of Putative Metal Chaperones is Linked to Zinc Homeostasis in all Kingdoms of Life." *BMC genomics* 10.1 (2009): 470. Print.
- Halliday, K. J., J. F. Martínez-García, and E. M. Josse. "Integration of Light and Auxin Signaling." *Cold Spring Harbor perspectives in biology* 1.6 (2009)Print.

- Hann, Eugenia C., et al. "5-Cyanovaleramide Production using Immobilized *Pseudomonas chlororaphis* B23." *Bioorganic & medicinal chemistry* 7.10 (1999): 2239-45. Print.
- Harari, Amalia, J. Kigel, and Y. Okon. *Involvement of IAA in the Interaction between *Azospirillum Brasilense* and *Panicum Miliaceum* Roots*. 110 Vol. Springer Netherlands, 1988. Print.
- Harper, David B. "Characterization of a Nitrilase from *Nocardia* Sp. Rhodochrous Group NCIB 11215, using p-Hydroxybenzonnitrile as Sole Carbon Source." *International Journal of Biochemistry* 17.6 (1985): 677-83. Print.
- Harper, D. B. "Microbial Metabolism of Aromatic Nitriles. Enzymology of C-N Cleavage by *Nocardia* Sp. (Rhodochrous Group) N.C.I.B. 11216." *Biochemical Journal* 165.2 (1977): 309-19. Print.
- Hashimoto, Yoshihiro, et al. "Nitrile Hydratase Gene from *Rhodococcus* Sp. N-774 Requirement for its Downstream Region for Efficient Expression." *Bioscience, biotechnology, and biochemistry* 58.10 (1994): 1859-65. Print.
- Hayashi, K. -I, et al. "Small-Molecule Agonists and Antagonists of F-Box Protein-Substrate Interactions in Auxin Perception and Signaling." *Proceedings of the National Academy of Sciences of the United States of America* 105.14 (2008): 5632-7. Print.
- Hillebrand, H., et al. "Structure of the Gene Encoding Nitrilase 1 from *Arabidopsis thaliana*." *Gene* 170.2 (1996): 197-200. Print.
- Hook, Robert H., and William G. Robinson. "Ricinine Nitrilase II. Purification and Properties." *Journal of Biological Chemistry* 239.12 (1964): 4263-7. Print.
- Howden, A. J. M., et al. "*Pseudomonas Syringae* Pv. *Syringae* B728a Hydrolyses Indole-3-Acetonitrile to the Plant Hormone Indole-3-Acetic Acid." *Molecular Plant Pathology* 10.6 (2009): 857-65. Print.
- Hull, A. K., R. Vij, and J. L. Celenza. "Arabidopsis Cytochrome P450s that Catalyze the First Step of Tryptophan-Dependent Indole-3-Acetic Acid Biosynthesis." *Proceedings of the National Academy of Sciences of the United States of America* 97.5 (2000): 2379-84. Print.
- Hurvich, Clifford M., and Chih-Ling Tsai. "Bias of the Corrected AIC Criterion for Underfitted Regression and Time Series Models." *Biometrika* 78.3 (1991): 499-509. Print.
- Ikehata, Osamu, et al. "Primary Structure of Nitrile Hydratase Deduced from the Nucleotide Sequence of a *Rhodococcus* Species and its Expression in *Escherichia*

- Coli." *European Journal of Biochemistry* 181.3 (1989): 563-70. Print.
- Imperlini, E., et al. "Effects of Indole-3-Acetic Acid on Sinorhizobium Meliloti Survival and on Symbiotic Nitrogen Fixation and Stem Dry Weight Production." *Applied Microbiology and Biotechnology* 83.4 (2009): 727-38. Print.
- Ishikawa, Toshiki, et al. "Molecular Cloning of Brassica Rapa Nitrilases and their Expression during Clubroot Development." *Molecular plant pathology* 8.5 (2007): 623-37. Print.
- Janowitz, Tim, Inga Trompetter, and Markus Piotrowski. "Evolution of Nitrilases in Glucosinolate-Containing Plants." *Phytochemistry* 70.15 (2009): 1680-6. Print.
- Jenrich, Roland, et al. "Evolution of Heteromeric Nitrilase Complexes in Poaceae with New Functions in Nitrile Metabolism." *Proceedings of the National Academy of Sciences* 104.47 (2007): 18848-53. Print.
- Kato, Y., et al. "Novel Heme-Containing Lyase, Phenylacetaldoxime Dehydratase from Bacillus Sp. Strain OxB-1: Purification, Characterization, and Molecular Cloning of the Gene." *Biochemistry* 39.4 (2000): 800-9. Print.
- Kazan, K., and J. M. Manners. "Linking Development to Defense: Auxin in Plant-Pathogen Interactions." *Trends in plant science* 14.7 (2009): 373-82. Print.
- Kim, Jinwoo, et al. "Quorum Sensing and the LysR-type Transcriptional Activator ToxR Regulate Toxoflavin Biosynthesis and Transport in Burkholderia Glumae." *Molecular microbiology* 54.4 (2004): 921-34. Print.
- Kim, Sang-Hoon, and Patrick Oriol. "Cloning and Expression of the Nitrile Hydratase and Amidase Genes from Bacillus Sp. BR449 into Escherichia coli." *Enzyme and microbial technology* 27.7 (2000): 492-501. Print.
- Kim, YJ, YJ Oh, and WJ Park. "HPLC-Based Quantification of Indole-3-Acetic Acid in the Primary Root Tip of Maize." *J Nano Bio Tech* 3 (2006): 40-5. Print.
- Kim, J. I., et al. "YUCCA6 Over-Expression Demonstrates Auxin Function in Delaying Leaf Senescence in Arabidopsis Thaliana." *Journal of experimental botany* 62.11 (2011): 3981-92. Print.
- Kim, Y. C., et al. "The Multifactorial Basis for Plant Health Promotion by Plant-Associated Bacteria." *Applied and Environmental Microbiology* 77.5 (2011): 1548-55. Print.
- Kittell, B. L., D. R. Helinski, and G. S. Ditta. "Aromatic Aminotransferase Activity and Indoleacetic Acid Production in Rhizobium Meliloti." *Journal of Bacteriology* 171.10 (1989): 5458-66. Print.
- Kiziak, C., et al. "Nitrilase from Pseudomonas Fluorescens EBC191: Cloning and

- Heterologous Expression of the Gene and Biochemical Characterization of the Recombinant Enzyme." *Microbiology* 151.11 (2005): 3639-48. Print.
- Kobayashi, Michihiko, et al. "Nitrilase in Biosynthesis of the Plant Hormone Indole-3-Acetic Acid from Indole-3-Acetonitrile: Cloning of the *Alcaligenes* Gene and Site-Directed Mutagenesis of Cysteine Residues." *Proceedings of the National Academy of Sciences* 90.1 (1993): 247-51. Print.
- Kobayashi, Michihiko, and Sakayu Shimizu. "Metalloenzyme Nitrile Hydratase: Structure, Regulation, and Application to Biotechnology." *Nature biotechnology* 16.8 (1998): 733-6. Print.
- Kobayashi, Michihiko, and Sakayu Shimizu. "Nitrile Hydrolases." *Current opinion in chemical biology* 4.1 (2000): 95-102. Print.
- Kobayashi, Michihiko, et al. "Purification and Characterization of a Novel Nitrilase of *Rhodococcus Rhodochrous* K22 that Acts on Aliphatic Nitriles." *Journal of Bacteriology* 172.9 (1990): 4807-15. Print.
- Kobayashi, M., et al. "Nitrilase in Biosynthesis of the Plant Hormone Indole-3-Acetic Acid from Indole-3-Acetonitrile: Cloning of the *Alcaligenes* Gene and Site-Directed Mutagenesis of Cysteine Residues." *Proceedings of the National Academy of Sciences of the United States of America* 90.1 (1993): 247-51. Print.
- Kobayashi, M., and S. Shimizu. "Versatile Nitrilases: Nitrile-Hydrolysing Enzymes." *FEMS microbiology letters* 120.3 (1994): 217-24. Print.
- Kochar, M., A. Upadhyay, and S. Srivastava. "Indole-3-Acetic Acid Biosynthesis in the Biocontrol Strain *Pseudomonas Fluorescens* Psd and Plant Growth Regulation by Hormone Overexpression." *Research in microbiology* 162.4 (2011): 426-35. Print.
- Koga, Jinichiro. "Structure and Function of Indolepyruvate Decarboxylase, a Key Enzyme in Indole-3-Acetic Acid Biosynthesis." *Biochimica et Biophysica Acta (BBA)-Protein Structure and Molecular Enzymology* 1249.1 (1995): 1-13. Print.
- Koga, J., T. Adachi, and H. Hidaka. "Molecular Cloning of the Gene for Indolepyruvate Decarboxylase from *Enterobacter Cloacae*." *Molecular and General Genetics* 226.1-2 (1991): 10-6. Print.
- Koga, Jinichiro, et al. "Involvement of l-Tryptophan Aminotransferase in Indole-3-Acetic Acid Biosynthesis in *Enterobacter Cloacae*." *Biochimica et Biophysica Acta (BBA) - Protein Structure and Molecular Enzymology* 1209.2 (1994): 241-7. Print.
- Komeda, Hidenobu, Michihiko Kobayashi, and Sakayu Shimizu. "Characterization of the Gene Cluster of High-Molecular-Mass Nitrile Hydratase (H-NHase) Induced by its Reaction Product in *Rhodococcus Rhodochrous* J1." *Proceedings of the National Academy of Sciences* 93.9 (1996): 4267-72. Print.

- Komeda, Hidenobu, Michihiko Kobayashi, and Sakayu Shimizu. "A Novel Gene Cluster Including the Rhodococcus Rhodochrous J1 nhlBA Genes Encoding a Low Molecular Mass Nitrile Hydratase (L-NHase) Induced by its Reaction Product." *Journal of Biological Chemistry* 271.26 (1996): 15796-802. Print.
- Komeda, Hidenobu, Michihiko Kobayashi, and Sakayu Shimizu. "A Novel Transporter Involved in Cobalt Uptake." *Proceedings of the National Academy of Sciences* 94.1 (1997): 36-41. Print.
- Komeda, H., et al. "Transcriptional Regulation of the Rhodococcus Rhodochrous J1 nitA Gene Encoding a Nitrilase." *Proceedings of the National Academy of Sciences of the United States of America* 93.20 (1996): 10572-7. Print.
- Kovacikova, Gabriela, and Karen Skorupski. "A Vibrio Cholerae LysR Homolog, AphB, Cooperates with AphA at the tcpPH Promoter to Activate Expression of the ToxR Virulence Cascade." *Journal of Bacteriology* 181.14 (1999): 4250-6. Print.
- Kriechbaumer, Verena, et al. "Maize Nitrilases have a Dual Role in Auxin Homeostasis and β -Cyanoalanine Hydrolysis." *Journal of experimental botany* 58.15-16 (2007): 4225-33. Print.
- Kyte, Jack, and Russell F. Doolittle. "A Simple Method for Displaying the Hydrophobic Character of a Protein." *Journal of Molecular Biology* 157.1 (1982): 105-32. Print.
- Latifi, A., et al. "A Hierarchical Quorum-Sensing Cascade in Pseudomonas Aeruginosa Links the Transcriptional Activators LasR and RhIR (VsmR) to Expression of the Stationary-Phase Sigma Factor RpoS." *Molecular microbiology* 21.6 (1996): 1137-46. Print.
- Layh, Norman, Julian Parratt, and Andrew Willetts. "Characterization and Partial Purification of an Enantioselective Arylacetonitrilase from Pseudomonas fluorescens DSM 7155." *Journal of Molecular Catalysis B: Enzymatic* 5.5 (1998): 467-74. Print.
- Lehmann, T., et al. "Indole-3-Acetamide-Dependent Auxin Biosynthesis: A Widely Distributed Way of Indole-3-Acetic Acid Production?" *European journal of cell biology* 89.12 (2010): 895-905. Print.
- Lin, Lan, and Xudong Xu. "Indole-3-Acetic Acid Production by Endophytic Streptomyces Sp. En-1 Isolated from Medicinal Plants." *Current microbiology* (2013): 1-9. Print.
- Linton, Eleanor A., and Christopher J. Knowles. "Utilization of Aliphatic Amides and Nitriles by Nocardia Rhodochrous LL100-21." *Journal of general microbiology* 132.6 (1986): 1493-501. Print.

- Liu, Yi, et al. "Strategy for Successful Expression of the Pseudomonas Putida Nitrile Hydratase Activator P14K in Escherichia Coli." *BMC biotechnology* 13.1 (2013): 48. Print.
- Liu, S. T., et al. "Agrobacterium Ti Plasmid Indoleacetic Acid Gene is Required for Crown Gall Oncogenesis." *Proceedings of the National Academy of Sciences of the United States of America* 79.9 I (1982): 2812-6. Print.
- Liu, Xiao Yun, et al. "Diverse Bacteria Isolated from Root Nodules of Trifolium, Crotalaria and Mimosa Grown in the Subtropical Regions of China." *Archives of Microbiology* 188.1 (2007): 1-14. Print.
- Loper, J.E, and M.N Scroth. "Influence of Bacterial Sources of Indole-3-Acetic-Acid on Root Elongation of Sugar-Beet." *Phytopathology* 76.4 (1986): 386-9. Print.
- Lu, Jun, et al. "Motif CXCC in Nitrile Hydratase Activator is Critical for NHase Biogenesis in Vivo." *FEBS letters* 553.3 (2003): 391-6. Print.
- Lu, Zuolei, Michio Takeuchi, and Tsutomu Sato. "The LysR-Type Transcriptional Regulator YofA Controls Cell Division through the Regulation of Expression of ftsW in Bacillus Subtilis." *Journal of Bacteriology* 189.15 (2007): 5642-51. Print.
- Maddocks, Sarah E., and Petra CF Oyston. "Structure and Function of the LysR-Type Transcriptional Regulator (LTTR) Family Proteins." *Microbiology* 154.12 (2008): 3609-23. Print.
- Maldiney, R., et al. "Endogenous Levels of Abscisic Acid, indole-3-acetic Acid, Zeatin and zeatin-riboside during the Course of Adventitious Root Formation in Cuttings of Craigella and Craigella Lateral Suppressor Tomatoes." *Physiologia plantarum* 68.3 (1986): 426-30. Print.
- Malhotra, M., and S. Srivastava. "An ipdC Gene Knock-Out of Azospirillum Brasilense Strain SM and its Implications on Indole-3-Acetic Acid Biosynthesis and Plant Growth Promotion." *Antonie van Leeuwenhoek, International Journal of General and Molecular Microbiology* 93.4 (2008): 425-33. Print.
- Malhotra, M., and S. Srivastava. "Stress-Responsive Indole-3-Acetic Acid Biosynthesis by Azospirillum Brasilense SM and its Ability to Modulate Plant Growth." *European Journal of Soil Biology* 45.1 (2009): 73-80. Print.
- Manulis, S., et al. "Differential Involvement of Indole-3-Acetic Acid Biosynthetic Pathways in Pathogenicity and Epiphytic Fitness of Erwinia Herbicola Pv. Gypsophilae." *Molecular Plant-Microbe Interactions* 11.7 (1998): 634-42. Print.
- Martínková, Ludmila, and Vladimír Křen. "Biotransformations with Nitrilases." *Current opinion in chemical biology* 14.2 (2010): 130-7. Print.
- Martinkova, Ludmila, and Vladimír Kren. "Nitrile-and Amide-Converting Microbial

- Enzymes: Stereo-, Regio- and Chemoselectivity." *Biocatalysis and Biotransformation* 20.2 (2002): 73-93. Print.
- Mathew, Caluwadewa Deepal, et al. "Nitrilase-Catalyzed Production of Nicotinic Acid from 3-Cyanopyridine in *Rhodococcus Rhodochrous* J1." *Applied and Environmental Microbiology* 54.4 (1988): 1030-2. Print.
- Mauger, Jacques, Toru Nagasawa, and Hideaki Yamada. "Nitrile Hydratase-Catalyzed Production of Isonicotinamide, Picolinamide and Pyrazinamide from 4-Cyanopyridine, 2-Cyanopyridine and Cyanopyrazine in *Rhodococcus rhodochrous* J1." *Journal of Biotechnology* 8.1 (1988): 87-95. Print.
- Mayaux, Jean-Francois, et al. "Purification, Cloning, and Primary Structure of an Enantiomer-Selective Amidase from *Brevibacterium* Sp. Strain R312: Structural Evidence for Genetic Coupling with Nitrile Hydratase." *Journal of Bacteriology* 172.12 (1990): 6764-73. Print.
- Mazzola, M., and F. F. White. "A Mutation in the Indole-3-Acetic Acid Biosynthesis Pathway of *Pseudomonas Syringae* Pv. *Syringae* Affects Growth in *Phaseolus Vulgaris* and Syringomycin Production." *Journal of Bacteriology* 176.5 (1994): 1374-82. Print.
- McBride, Kevin, E., James W. Kenny, and David M. Stalker. "Metabolism of the Herbicide Bromoxynil by *Klebsiella Pneumoniae* Subsp. *Ozaenae*." *Applied and Environmental Microbiology* 52.2 (1986): 325-30. Print.
- McNear Jr, DH. "The Rhizosphere—Roots, Soil and Everything in between. Nature Education Knowledge 4 (3): 1 Email what is the Rhizosphere and how can Understanding Rhizosphere Processes Help Feed the World and Save the Environment? this Article Will Review the Critical Biogeochemical Processes Occurring at the Plant Root-Soil Interface." *McNear banner* (2013)Print.
- McSteen, P. "Auxin and Monocot Development." *Cold Spring Harbor perspectives in biology* 2.3 (2010)Print.
- Melotto, M., et al. "Plant Stomata Function in Innate Immunity Against Bacterial Invasion." *Cell* 126.5 (2006): 969-80. Print.
- Mikkelsen, M. D., et al. "Cytochrome P450 CYP79B2 from *Arabidopsis* Catalyzes the Conversion of Tryptophan to Indole-3-Acetaldoxime, a Precursor of Indole Glucosinolates and Indole-3-Acetic Acid." *Journal of Biological Chemistry* 275.43 (2000): 33712-7. Print.
- Morgenstern, Ely, and Yaacov Okon. "The Effect of *Azospirillum Brasilense* and Auxin on Root Morphology in Seedlings of *Sorghum Bicolor* × *Sorghum Sudanense*." *Arid Soil Research and Rehabilitation* 1.2 (1987): 115-27. Print.

- Moris, Martine, et al. "Effective Symbiosis between *Rhizobium Etli* and *Phaseolus Vulgaris* Requires the Alarmone ppGpp." *Journal of Bacteriology* 187.15 (2005): 5460-9. Print.
- Nagamune, Teruyuki, et al. "Purification of Inactivated Photoresponsive Nitrile Hydratase." *Biochemical and biophysical research communications* 168.2 (1990): 437-42. Print.
- Nagasawa, Toru, Tetsuji Nakamura, and Hideaki Yamada. "E-Caprolactam, a New Powerful Inducer for the Formation of *Rhodococcus Rhodochrous* J1 Nitrilase." *Archives of Microbiology* 155.1 (1990): 13-7. Print.
- Nagasawa, Toru, et al. "Nitrile Hydratase of *Pseudomonas Chlororaphis* B23." *European Journal of Biochemistry* 162.3 (1987): 691-8. Print.
- Nagasawa, Toru, Koichiro Ryuno, and Hideaki Yamada. "Nitrile Hydratase of *Brevibacterium* R312—purification and Characterization—." *Biochemical and biophysical research communications* 139.3 (1986): 1305-12. Print.
- Nagasawa, Toru, Koji Takeuchi, and Hideaki Yamada. "Characterization of a new cobalt-containing Nitrile Hydratase Purified from urea-induced Cells of *Rhodococcus Rhodochrous* J1." *European journal of biochemistry* 196.3 (1991): 581-9. Print.
- Nagasawa, Toru, and Hideaki Yamada. "Nitrile Hydratase is a Quinoprotein a Possible New Function of Pyrroloquinoline Quinone: Activation of H₂O in an Enzymatic Hydration Reaction." *Biochemical and biophysical research communications* 147.2 (1987): 701-9. Print.
- Nakamura, Nobuhumi, et al. "Biosynthesis of Topa Quinone Cofactor in Bacterial Amine Oxidases Solvent origin of C-2 oxygen determined by Raman Spectroscopy." *Journal of Biological Chemistry* 271.9 (1996): 4718-24. Print.
- Navarro, L., et al. "A Plant miRNA Contributes to Antibacterial Resistance by Repressing Auxin Signaling." *Science* 312.5772 (2006): 436-9. Print.
- Nei, Masatoshi, and Sudhir Kumar. *Molecular Evolution and Phylogenetics*. Oxford University Press, 2000. Print.
- Nishiyama, Makoto, et al. "Cloning and Characterization of Genes Responsible for Metabolism of Nitrile Compounds from *Pseudomonas Chlororaphis* B23." *Journal of Bacteriology* 173.8 (1991): 2465-72. Print.
- Noguchi, Takumi, et al. "Photosensitive Nitrile Hydratase Intrinsically Possesses Nitric Oxide Bound to the Non-Heme Iron Center: Evidence by Fourier Transform Infrared Spectroscopy." *FEBS letters* 358.1 (1995): 9-12. Print.
- Noguchi, Takumi, et al. "Resonance Raman Evidence that Photodissociation of Nitric Oxide from the Non-Heme Iron Center Activates Nitrile Hydratase from

- Rhodococcus Sp. N-771." *Biochemistry* 35.51 (1996): 16777-81. Print.
- Nojiri, Masaki, et al. "Functional Expression of Nitrile Hydratase in Escherichia Coli: Requirement of a Nitrile Hydratase Activator and Post-Translational Modification of a Ligand Cysteine." *Journal of Biochemistry* 125.4 (1999): 696-704. Print.
- Normanly, Jennifer, et al. "Arabidopsis Mutants Resistant to the Auxin Effects of Indole-3-Acetonitrile are Defective in the Nitrilase Encoded by the NIT1 Gene." *The Plant Cell Online* 9.10 (1997): 1781-90. Print.
- Normanly, J. "Approaching Cellular and Molecular Resolution of Auxin Biosynthesis and Metabolism." *Cold Spring Harbor perspectives in biology* 2.1 (2010)Print.
- O'Mahony, Rebecca, et al. "Characterisation of the Nitrile Hydratase Gene Clusters of Rhodococcus Erythropolis Strains AJ270 and AJ300 and Microbacterium Sp. AJ115 Indicates Horizontal Gene Transfer and Reveals an Insertion of IS1166." *Antonie van Leeuwenhoek* 87.3 (2005): 221-32. Print.
- Oberhänsli, Thomas, Geneviève Défago, and Dieter Haas. "Indole-3-Acetic Acid (IAA) Synthesis in the Biocontrol Strain CHA0 of Pseudomonas Fluorescens: Role of Tryptophan Side Chain Oxidase." *Journal of general microbiology* 137.10 (1991): 2273-9. Print.
- Odaka, Masafumi, et al. "Activity Regulation of Photoreactive Nitrile Hydratase by Nitric Oxide." *Journal of the American Chemical Society* 119.16 (1997): 3785-91. Print.
- Okamoto, Sachi, et al. "AnhE, a Metallochaperone Involved in the Maturation of a Cobalt-Dependent Nitrile Hydratase." *Journal of Biological Chemistry* 285.33 (2010): 25126-33. Print.
- O'Reilly, C., and P. D. Turner. "The Nitrilase Family of CN Hydrolysing Enzymes - A Comparative Study." *Journal of applied microbiology* 95.6 (2003): 1161-74. Print.
- Osswald, Steffen, Harald Wajant, and Franz Effenberger. "Characterization and Synthetic Applications of Recombinant AtNIT1 from Arabidopsis Thaliana." *European Journal of Biochemistry* 269.2 (2002): 680-7. Print.
- Pace, H. C., and C. Brenner. "The Nitrilase Superfamily: Classification, Structure and Function." *Genome biology* 2.1 (2001)Print.
- Patek, M., et al. "Organization, Regulation and Expression of Nitrile Degradation Genes of Rhodococcus erythropolis." *New Biotechnology* 25 (2009): S104. Print.
- Patten, Cheryl L., and Bernard R. Glick. "Bacterial Biosynthesis of Indole-3-Acetic Acid." *Canadian journal of microbiology* 42.3 (1996): 207-20. Print.

- Patten, Cheryl L., and Bernard R. Glick. "Regulation of Indoleacetic Acid Production in *Pseudomonas Putida* GR12-2 by Tryptophan and the Stationary-Phase Sigma Factor RpoS." *Canadian journal of microbiology* 48.7 (2002): 635-42. Print.
- Patten, Cheryl L., Andrew J. C. Blakney, and Thomas J. D. Coulson. "Activity, Distribution and Function of Indole-3-Acetic Acid Biosynthetic Pathways in Bacteria." *Critical reviews in microbiology* (2012): 1-21. Print.
- Park, Woong June, et al. "The Nitrilase ZmNIT2 Converts Indole-3-Acetonitrile to Indole-3-Acetic Acid." *Plant physiology* 133.2 (2003): 794-802. Print.
- Payne, Mark S., et al. "A Stereoselective Cobalt-Containing Nitrile Hydratase." *Biochemistry* 36.18 (1997): 5447-54. Print.
- Pedraza, R. O., et al. "Aromatic Amino Acid Aminotransferase Activity and Indole-3-Acetic Acid Production by Associative Nitrogen-Fixing Bacteria." *FEMS microbiology letters* 233.1 (2004): 15-21. Print.
- Pereira, Rui A., et al. "A Novel Thermostable Nitrile Hydratase." *Extremophiles* 2.3 (1998): 347-57. Print.
- Persello-Cartieaux, F., L. Nussaume, and C. Robaglia. "Tales from the Underground: Molecular." *Plant, Cell & Environment* 26.2 (2003): 189-99. Print.
- Phillips, K. A., et al. "Vanishing tassell2 Encodes a Grass-Specific Tryptophan Aminotransferase Required for Vegetative and Reproductive Development in Maize." *Plant Cell* 23.2 (2011): 550-66. Print.
- Pilet, P. E., M. C. Elliott, and M. M. Moloney. "Endogenous and Exogenous Auxin in the Control of Root Growth." *Planta* 146.4 (1979): 405-8. Print.
- Pilet, P. -E, and M. Saugy. "Effect of Applied and Endogenous Indol-3-Yl-Acetic Acid on Maize Root Growth." *Planta* 164.2 (1985): 254-8. Print.
- Piotrowski, Markus, Sabine Schönfelder, and Elmar W. Weiler. "The Arabidopsis Thaliana Isogene NIT4 and its Orthologs in Tobacco Encode β -Cyano-L-Alanine hydratase/nitrilase." *Journal of Biological Chemistry* 276.4 (2001): 2616-21. Print.
- Podar, Mircea, Jonathan R. Eads, and Toby H. Richardson. "Evolution of a Microbial Nitrilase Gene Family: A Comparative and Environmental Genomics Study." *BMC evolutionary biology* 5.1 (2005): 42. Print.
- Pollmann, S., A. Müller, and E. W. Weiler. "Many Roads Lead to "Auxin": Of Nitrilases, Synthases, and Amidases." *Plant Biology* 8.3 (2006): 326-33. Print.
- Posada, David, and Thomas R. Buckley. "Model Selection and Model Averaging in Phylogenetics: Advantages of Akaike Information Criterion and Bayesian Approaches Over Likelihood Ratio Tests." *Systematic Biology* 53.5 (2004): 793-

808. Print.

- Prasad, S., J. Raj, and TC Bhalla. "Purification of a Hyperactive Nitrile Hydratase from Resting Cells of *Rhodococcus Rhodochrous* PA-34." *Indian Journal of Microbiology* 49.3 (2009): 237-42. Print.
- Prasad, Shreenath, and Tek Chand Bhalla. "Nitrile Hydratases (NHases): At the Interface of Academia and Industry." *Biotechnology Advances* 28.6 (2010): 725-41. Print.
- Prasad, Shreenath, et al. "A Propionitrile-Induced Nitrilase of *Rhodococcus* Sp. NDB 1165 and its Application in Nicotinic Acid Synthesis." *World Journal of Microbiology and Biotechnology* 23.3 (2007): 345-53. Print.
- Prasad, Shreenath, Deep Raj Sharma, and Tek Chand Bhalla. "Nitrile-and Amide-Hydrolysing Activity in *Kluyveromyces Thermotolerans* MGBY 37." *World Journal of Microbiology and Biotechnology* 21.8-9 (2005): 1447-50. Print.
- Precigou, Sylvain, Philippe Goulas, and Robert Duran. "Rapid and Specific Identification of Nitrile Hydratase (NHase)-encoding Genes in Soil Samples by Polymerase Chain Reaction." *FEMS microbiology letters* 204.1 (2001): 155-61. Print.
- Prinsen, E., et al. "Azospirillum Brasilense Indole-3-Acetic Acid Biosynthesis: Evidence for a Non-Tryptophan Dependent Pathway." *Mol.Plant-Microbe Interact.* 6 (1993): 609-15. Print.
- Prinsen, E., et al. "HPLC Linked Electrospray Tandem Mass Spectrometry: A Rapid and Reliable Method to Analyse Indole-3-Acetic Acid Metabolism in Bacteria." *Journal of Mass Spectrometry* 32.1 (1997): 12-22. Print.
- Prinsen, Els, et al. "Stimulation of Indole-3-Acetic Acid Production in *Rhizobium* by Flavonoids." *FEBS letters* 282.1 (1991): 53-5. Print.
- Proença, Diogo Neves, et al. "Draft Genome Sequence of *Serratia* Sp. Strain M24T3, Isolated from Pinewood Disease Nematode *Bursaphelenchus Xylophilus*." *Journal of Bacteriology* 194.14 (2012): 3764-. Print.
- Radojčić Redovniković, Ivana, et al. "Glucosinolates and their Potential Role in Plant." *Periodicum Biologorum* 110.4 (2008): 297-309. Print.
- Reeves, Jaxk H. "Heterogeneity in the Substitution Process of Amino Acid Sites of Proteins Coded for by Mitochondrial DNA." *Journal of Molecular Evolution* 35.1 (1992): 17-31. Print.
- Reid, A. E., et al. "Radiosynthesis of C-11 Labeled Auxin (3-Indolyl[1-11C]Acetic Acid) and its Derivatives from Gramine." *Journal of Labelled Compounds and Radiopharmaceuticals* 54.8 (2011): 433-7. Print.
- Reid, J. B., S. E. Davidson, and J. J. Ross. "Auxin Acts Independently of DELLA

- Proteins in Regulating Gibberellin Levels." *Plant Signaling and Behavior* 6.3 (2011): 406-8. Print.
- Revelles, Olga, et al. "Multiple and Interconnected Pathways for L-Lysine Catabolism in *Pseudomonas Putida* KT2440." *Journal of Bacteriology* 187.21 (2005): 7500-10. Print.
- Robertson, Dan E., et al. "Exploring Nitrilase Sequence Space for Enantioselective Catalysis." *Applied and Environmental Microbiology* 70.4 (2004): 2429-36. Print.
- Robinson, William G., and Robert H. Hook. "Ricinine Nitrilase I. Reaction Product and Substrate Specificity." *Journal of Biological Chemistry* 239.12 (1964): 4257-62. Print.
- Rodionov, Dmitry A., et al. "Comparative Genomics of the Vitamin B12 Metabolism and Regulation in Prokaryotes." *Journal of Biological Chemistry* 278.42 (2003): 41148-59. Print.
- Russell, Dean A., et al. "The LysR-Type Transcriptional Regulator VirR is Required for Expression of the Virulence Gene *vapA* of *Rhodococcus Equi* ATCC 33701." *Journal of Bacteriology* 186.17 (2004): 5576-84. Print.
- Saleh, S. S., and B. R. Glick. "Involvement of *gacS* and *rpoS* in Enhancement of the Plant Growth-Promoting Capabilities of *Enterobacter Cloacae* CAL2 and UW4." *Canadian journal of microbiology* 47.8 (2001): 698-705. Print.
- Sambrook, Joseph, David W. Russell, and David W. Russell. "Molecular Cloning: A Laboratory Manual (3-Volume Set)." (2001)Print.
- Sayers, EW, et al. "Database Resources of the National Center for Biotechnology Information (2008) Nucl." *Acids Res* 36: 13-21. Print.
- Schaad, Norman W., et al. "Reclassification of Subspecies of *Acidovorax avenae* as *A. Avenae* (Manns 1905) emend., *A. cattleyae* (Pavarino, 1911) comb. Nov., *A. citrulli* (Schaad Et Al., 1978) comb. Nov., and Proposal of *A. oryzae* Sp. Nov." *Systematic and applied microbiology* 31.6 (2008): 434-46. Print.
- Scheppler, Judith A., Patricia E. Cassin, and Rosa M. Gambier. *Biotechnology Explorations: Applying the Fundamentals*. Am Soc Microbiol, 2000. Print.
- Schröder, G., et al. "The T-Region of Ti Plasmids Codes for an Enzyme Synthesizing Indole-3-Acetic Acid." *European Journal of Biochemistry* 138.2 (1984): 387-91. Print.
- Schwarz, Gideon. "Estimating the Dimension of a Model." *The annals of statistics* 6.2 (1978): 461-4. Print.
- Seffernick, Jennifer L., et al. "Investigative Mining of Sequence Data for Novel

- Enzymes: A Case Study with Nitrilases." *Journal of Biotechnology* 143.1 (2009): 17-26. Print.
- Sergeeva, E., D. L. M. Hirkala, and L. M. Nelson. "Production of Indole-3-Acetic Acid, Aromatic Amino Acid Aminotransferase Activities and Plant Growth Promotion by *Pantoea Agglomerans* Rhizosphere Isolates." *Plant and Soil* 297.1-2 (2007): 1-13. Print.
- Sharma, N., and TC Bhalla. "Motif Design for Nitrilases." *J Data Mining Genomics Proteomics* 3.119 (2012): 2153,0602.1000119. Print.
- Sharma, Nikhil, et al. "In Silico Analysis of Amino Acid Sequences in Relation to Specificity and Physicochemical Properties of some Microbial Nitrilases." *J Proteomics Bioinform* 2 (2009): 185-92. Print.
- Shokri, D., and G. Emtiazi. "Indole-3-Acetic Acid (IAA) Production in Symbiotic and Non-Symbiotic Nitrogen-Fixing Bacteria and its Optimization by Taguchi Design." *Current microbiology* 61.3 (2010): 217-25. Print.
- Sitbon, F., et al. "Transgenic Tobacco Plants Coexpressing the *Agrobacterium Tumefaciens* *iaaM* and *iaaH* Genes Display Altered Growth and Indoleacetic Acid Metabolism." *Plant physiology* 99.3 (1992): 1062-9. Print.
- Sitbon, F., et al. "Free and Conjugated Indoleacetic Acid (IAA) Contents in Transgenic Tobacco Plants Expressing the *iaaM* and *iaaH* IAA Biosynthesis Genes from *Agrobacterium Tumefaciens*." *Plant physiology* 95.2 (1991): 480-5. Print.
- Smidt, M., and T. Kosuge. "The Rôle of Indole-3-Acetic Acid Accumulation by Alpha Methyl Tryptophan-Resistant Mutants of *Pseudomonas Savastanoi* in Gall Formation on Oleanders." *Physiological Plant Pathology* 13.2 (1978): 203,210,IN17,211-213. Print.
- Soeno, K., et al. "Auxin Biosynthesis Inhibitors, Identified by a Genomics-Based Approach, Provide Insights into Auxin Biosynthesis." *Plant and Cell Physiology* 51.4 (2010): 524-36. Print.
- Song, Liya, et al. "Efficient Expression in *E. Coli* of an Enantioselective Nitrile Hydratase from *Rhodococcus Erythropolis*." *Biotechnology Letters* 30.4 (2008): 755-62. Print.
- Spaepen, S., et al. "Effects of *Azospirillum Brasilense* Indole-3-Acetic Acid Production on Inoculated Wheat Plants." *Plant and Soil* 312.1-2 (2008): 15-23. Print.
- Spaepen, S., J. Vanderleyden, and R. Remans. "Indole-3-Acetic Acid in Microbial and Microorganism-Plant Signaling." *FEMS microbiology reviews* 31.4 (2007): 425-48. Print.

- Sperandio, Brice, et al. "Control of Methionine Synthesis and Uptake by MetR and Homocysteine in Streptococcus Mutans." *Journal of Bacteriology* 189.19 (2007): 7032-44. Print.
- Stevenson, DE, et al. "Mechanistic and Structural Studies on Rhodococcus ATCC 39484 Nitrilase." *Biotechnology and applied biochemistry* 15.3 (1992): 283-302. Print.
- Sugawara, S., et al. "Biochemical Analyses of Indole-3-Acetaldoximedependent Auxin Biosynthesis in Arabidopsis." *Proceedings of the National Academy of Sciences of the United States of America* 106.13 (2009): 5430-5. Print.
- Sun, Yili, Zhenyu Cheng, and Bernard R. Glick. "The Presence of a 1-aminocyclopropane-1-carboxylate (ACC) Deaminase Deletion Mutation Alters the Physiology of the Endophytic Plant growth-promoting Bacterium Burkholderia Phytofirmans PsJN." *FEMS microbiology letters* 296.1 (2009): 131-6. Print.
- Surico, G., N. S. Iacobellis, and A. Sisto. "Studies on the Role of Indole-3-Acetic Acid and Cytokinins in the Formation of Knots on Olive and Oleander Plants by Pseudomonas Syringae Pv. Savastanoi." *Physiological Plant Pathology* 26.3 (1985): 309-20. Print.
- Taiz, L., and E. Zeiger. *Plant Physiology*. Benjamin/Cummings, 1991. Print.
- Tamura, Koichiro, et al. "MEGA5: Molecular Evolutionary Genetics Analysis using Maximum Likelihood, Evolutionary Distance, and Maximum Parsimony Methods." *Molecular biology and evolution* 28.10 (2011): 2731-9. Print.
- Tao, Y., et al. "Rapid Synthesis of Auxin Via a New Tryptophan-Dependent Pathway is Required for Shade Avoidance in Plants." *Cell* 133.1 (2008): 164-76. Print.
- Teale, William D., Ivan A. Paponov, and Klaus Palme. "Auxin in Action: Signalling, Transport and the Control of Plant Growth and Development." *Nature Reviews Molecular Cell Biology* 7.11 (2006): 847-59. Print.
- Theunis, M., et al. "Flavonoids, NodD1, NodD2, and Nod-Box NB15 Modulate Expression of the y4wEFG Locus that is Required for Indole-3-Acetic Acid Synthesis in Rhizobium Sp. Strain NGR234." *Molecular Plant-Microbe Interactions* 17.10 (2004): 1153-61. Print.
- Thimann, Kenneth Vivian. *Hormone Action in the Whole Life of Plants*. Univ of Massachusetts Press, 1977. Print.
- Thomashow, L. S., S. Reeves, and M. F. Thomashow. "Crown Gall Oncogenesis: Evidence that a T-DNA Gene from the Agrobacterium Ti Plasmid pTiA6 Encodes an Enzyme that Catalyzes Synthesis of Indoleacetic Acid." *Proceedings of the National Academy of Sciences* 81.16 (1984): 5071-5. Print.
- Thuku, RN, et al. "Microbial Nitrilases: Versatile, Spiral Forming, Industrial Enzymes."

- Journal of applied microbiology* 106.3 (2009): 703-27. Print.
- Tien, TM, MH Gaskins, and DH Hubbell. "Plant Growth Substances Produced by *Azospirillum Brasilense* and their Effect on the Growth of Pearl Millet (*Pennisetum Americanum* L.)." *Applied and Environmental Microbiology* 37.5 (1979): 1016-24. Print.
- Tromas, A., and C. Perrot-Rechenmann. "Recent Progress in Auxin Biology." *Comptes Rendus - Biologies* 333.4 (2010): 297-306. Print.
- Tsunoda, H., and Yamaguchi, K. "the cDNA Sequence of an auxin-Producing Nitrilase Homologue in Tobacco ." *Plant Physiol.* 109: 339. Print.
- Uggla, C., et al. "Auxin as a Positional Signal in Pattern Formation in Plants." *Proceedings of the National Academy of Sciences of the United States of America* 93.17 (1996): 9282-6. Print.
- Van Onckelen, Harry, et al. "< i> Agrobacterium</i> T-DNA Gene< i> 1</i> Codes for Tryptophan 2-Monooxygenase Activity in Tobacco Crown Gall Cells." *FEBS letters* 198.2 (1986): 357-60. Print.
- Vandamme, Peter, et al. "Occurrence of Multiple Genomovars of Burkholderia Cepacia in Cystic Fibrosis Patients and Proposal of Burkholderia Multivorans Sp. Nov." *International Journal of Systematic Bacteriology* 47.4 (1997): 1188-200. Print.
- Vande Broek, A., et al. "Auxins Upregulate Expression of the Indole-3-Pyruvate Decarboxylase Gene in *Azospirillum Brasilense*." *Journal of Bacteriology* 181.4 (1999): 1338-42. Print.
- Van Trappen, Stefanie, et al. "Glaciecola Polaris Sp. Nov., a Novel Budding and Prosthecate Bacterium from the Arctic Ocean, and Emended Description of the Genus Glaciecola." *International Journal of Systematic and Evolutionary Microbiology* 54.5 (2004): 1765-71. Print.
- Vega-Hernández, M. C., M. León-Barrios, and R. Pérez-Galdona. "Indole-3-Acetic Acid Production from Indole-3-Acetonitrile in Bradyrhizobium." *Soil Biology and Biochemistry* 34.5 (2002): 665-8. Print.
- Vorwerk, Sonja, et al. "Enzymatic Characterization of the Recombinant Arabidopsis Thaliana Nitrilase Subfamily Encoded by the NIT2/NIT1/NIT3-Gene Cluster." *Planta* 212.4 (2001): 508-16. Print.
- Wang, D., et al. "Salicylic Acid Inhibits Pathogen Growth in Plants through Repression of the Auxin Signaling Pathway." *Current Biology* 17.20 (2007): 1784-90. Print.
- Whelan, Simon, and Nick Goldman. "A General Empirical Model of Protein Evolution Derived from Multiple Protein Families using a Maximum-Likelihood Approach." *Molecular biology and evolution* 18.5 (2001): 691-9. Print.

- Wilson, Stuart A., and Robert E. Drew. "Transcriptional Analysis of the Amidase Operon from *Pseudomonas Aeruginosa*." *Journal of Bacteriology* 177.11 (1995): 3052-7. Print.
- Wilson, Stuart, and Robert Drew. "Cloning and DNA Sequence of *amiC*, a New Gene Regulating Expression of the *Pseudomonas Aeruginosa* Aliphatic Amidase, and Purification of the *amiC* Product." *Journal of Bacteriology* 173.16 (1991): 4914-21. Print.
- Wu, S., RD Fallon, and MS Payne. "Over-Production of Stereoselective Nitrile Hydratase from *Pseudomonas Putida* 5B in *Escherichia Coli*: Activity Requires a Novel Downstream Protein." *Applied Microbiology and Biotechnology* 48.6 (1997): 704-8. Print.
- Xie, Hong, JJ Pasternak, and Bernard R. Glick. "Isolation and Characterization of Mutants of the Plant Growth-Promoting Rhizobacterium *Pseudomonas Putida* GR12-2 that Overproduce Indoleacetic Acid." *Current microbiology* 32.2 (1996): 67-71. Print.
- Xie, Sheng-Xue, et al. "A Gene Cluster Responsible for Alkylaldoxime Metabolism Coexisting with Nitrile Hydratase and Amidase in *Rhodococcus Globerulus* A-4." *Biochemistry* 42.41 (2003): 12056-66. Print.
- Yamada, T., et al. "Nucleotide Sequences of the *Pseudomonas Savastanoi* Indoleacetic Acid Genes show Homology with *Agrobacterium Tumefaciens* T-DNA." *Proceedings of the National Academy of Sciences of the United States of America* 82.19 (1985): 6522-6. Print.
- Yamaki, Toshifumi, et al. "Cloning and Sequencing of a Nitrile Hydratase Gene from *Pseudonocardia thermophila* JCM3095." *Journal of Fermentation and Bioengineering* 83.5 (1997): 474-7. Print.
- Yang, Shihui, et al. "Global Effect of Indole-3-Acetic Acid Biosynthesis on Multiple Virulence Factors of *Erwinia Chrysanthemii* 3937." *Applied and Environmental Microbiology* 73.4 (2007): 1079-88. Print.
- Yang, Ziheng. "Maximum-Likelihood Estimation of Phylogeny from DNA Sequences when Substitution Rates Differ Over Sites." *Molecular biology and evolution* 10.6 (1993): 1396-401. Print.
- Zhao, Yunde, et al. "Trp-Dependent Auxin Biosynthesis in *Arabidopsis*: Involvement of Cytochrome P450s CYP79B2 and CYP79B3." *Genes & development* 16.23 (2002): 3100-12. Print.
- Zhao, Yunde. "Auxin Biosynthesis: A Simple Two-Step Pathway Converts Tryptophan to Indole-3-Acetic Acid in Plants." *Molecular plant* 5.2 (2012): 334-8. Print.
- Zhao, M., et al. "Expansins are Involved in Cell Growth Mediated by Abscisic Acid and

- Indole-3-Acetic Acid Under Drought Stress in Wheat." *Plant Cell Reports* 31.4 (2012): 671-85. Print.
- Zhao, Y. Auxin Biosynthesis and its Role in Plant Development. *Annu. Rev. Plant Biol.* 61 (2010): 49-64
- Zhao, Y. "Auxin Biosynthesis: A Simple Two-Step Pathway Converts Tryptophan to Indole-3-Acetic Acid in Plants." *Molecular Plant* 5.2 (2012): 334-8. Print.
- Zheng, Yu, Richard J. Roberts, and Simon Kasif. "Segmentally Variable Genes: A New Perspective on Adaptation." *PLoS biology* 2.4 (2004): e81. Print.
- Zhou, L., Bartel, B., and Thornburg, R. "Nucleotide sequence of a Pathogen-Induced Nitrilase Gene from Arabidopsis Thaliana: Nit2." *Plant physiology* 110 (1996): 1048. Print.
- Zhou, L., Bartel, B., and Thornburg, R. "Nucleotide sequence of the Arabidopsis Thaliana Nitrilase 1 Gene ." *Plant physiology* 110 (1996): 337. Print.
- Zhou, L., Bartel, B., and Thornburg, R. "Plant Gene Register PGR96-006." Print.
- Zhou, Zhemin, Yoshiteru Hashimoto, and Michihiko Kobayashi. "Self-Subunit Swapping Chaperone Needed for the Maturation of Multimeric Metalloenzyme Nitrile Hydratase by a Subunit Exchange Mechanism also Carries Out the Oxidation of the Metal Ligand Cysteine Residues and Insertion of Cobalt." *Journal of Biological Chemistry* 284.22 (2009): 14930-8. Print.
- Zhou, Zhemin, et al. "Discovery of Posttranslational Maturation by Self-Subunit Swapping." *Proceedings of the National Academy of Sciences* 105.39 (2008): 14849-54. Print.
- Zimmer, W., M. Wesche, and L. Timmermans. "Identification and Isolation of the Indole-3-Pyruvate Decarboxylase Gene from Azospirillum Brasilense Sp7: Sequencing and Functional Analysis of the Gene Locus." *Current microbiology* 36.6 (1998): 327-31. Print.